ABSTRACT

BACHMANN, ADAM LEE. Unconventional Laser Fabrication of Electronic Devices. (Under the direction of Dr. Michael Dickey).

This dissertation addresses the use of lasers to pattern and manipulate metals and polymers. Specifically, the careful control of laser settings allows conventional materials, like flexible printed circuit boards, to be cut and folded to produce 3D structures while the directed energy of a focused laser also promotes the localized transformation of insulating polymers into conductive carbon traces. Chapter 1 begins as a brief introduction to the history of lasers and provides a high-level view of multiple technologies and techniques that have been enabled by the development of lasers with select highlights from analytical techniques, medicine, and laser manufacturing. The use of lasers in rapid prototyping is then explored further in chapter 2 with a particular emphasis on laser forming, the folding of materials in response to localized stresses generated by laser heating. Chapter 3 presents an application of laser forming in electronics manufacturing by demonstrating the successful laser cutting and laser bending of a flexible printed circuit board. Chapter 4 demonstrates the laser carbonization of SU-8 patterns and progress toward functional micromolding and soft lithography. Chapter 5 then provides a brief outlook for the future of lasers in rapid prototyping and manufacturing.

Unconventional Laser Fabrication of Electronic Devices

by
Adam Lee Bachmann

A dissertation submitted to the Graduate Faculty of
North Carolina State University
in partial fulfillment of the
requirements for the degree of
Doctor of Philosophy

Chemical Engineering

Raleigh, North Carolina
2022

APPROVED BY:

_____	_____
Dr. Michael D. Dickey Committee Chair	Dr. Nathan Lazarus
_____	_____
Dr. Jan Genzer	Dr. Brendan O'Connor
_____	
Dr. Wei Gao	

DEDICATION

Deo optimo maximo

BIOGRAPHY

Adam Bachmann was born in Florida before the US Air Force moved him and his family all over the place, from Colorado and Maryland and even to South Korea before landing him back in Florida. He then attended the University of Florida on scholarship and graduated with a B.S in Chemical Engineering in 2017. Not knowing exactly what he wanted to do, but wanting to avoid the “real world,” Adam enrolled at NC State University to pursue his PhD in Chemical Engineering. While there, he learned how to play water polo and even did some science. Part-way through graduate school, Adam went to the Army Research Labs to conduct research in the middle of a pandemic. After graduation, he will pursue a post-doc with no plans beyond that, but thinks a cushy, tenured faculty position might be nice.

ACKNOWLEDGMENTS

This PhD would not have happened without the support of numerous people with their order being a function of my ability to recall their assistance and not a judgement on the level of their help. To Evan and Rebecca North for welcoming me into their lives since I first met them at Lifepointe Church. THE® real Tommy Rudibaugh, you have been a great roommate these many years. To my fellow graduate students, like Rachel Nye, Zach Campbell, Chris Estridge, Emily Krzystowczyk, Seif Yusef, Cathryn Connor, and many others, for being there with kind words or silence, depending on the need. The various students of the Dickey group have been there through the entire process, and the liquid metal has been as well. Nik and Paige Bravo, Josh Horner, Harry Schrickx, and the many other water polo coaches and players I have had the privilege to play under or with during my time at NC State have been a tremendous blessing. To the students I have been fortunate to TA over the years, teaching y'all has been a bright spot; I hope that you learned something. Despite the pandemic, my time at the Army Research Labs was wonderful thanks to the hospitality of the Klavers, the Pews, and the entire FBC Laurel congregation that welcomed me, knowing fully my transience. Alan Ferris, it has been wonderful working with you throughout the years and I cannot wait to see what you accomplish. Last, to my family for helping remind me why I decided to pursue this degree and keeping me grounded despite having no clue what the path to a Ph.D entailed. To anyone else not named, know that it is purely the result of my faulty memory and reflects only on me and not you.

TABLE OF CONTENTS

LIST OF TABLES

LIST OF FIGURES

CHAPTER 1 A Brief History of Lasers

1.1 Laser Theory

Lasers are devices that can emit highly-focused, monochromatic light which has led to their rapid adoption in many areas of science and technology.[1] The term laser is an acronym that stands for "*light amplification by stimulated emission of radiation*" which operate by the principle of stimulated emission which was first proposed by Einstein and demonstrated to be thermodynamically consistent in 1917.[2] In this pioneering work, Einstein considered how light can interact with matter in one of three ways (**Figure 1.1**).

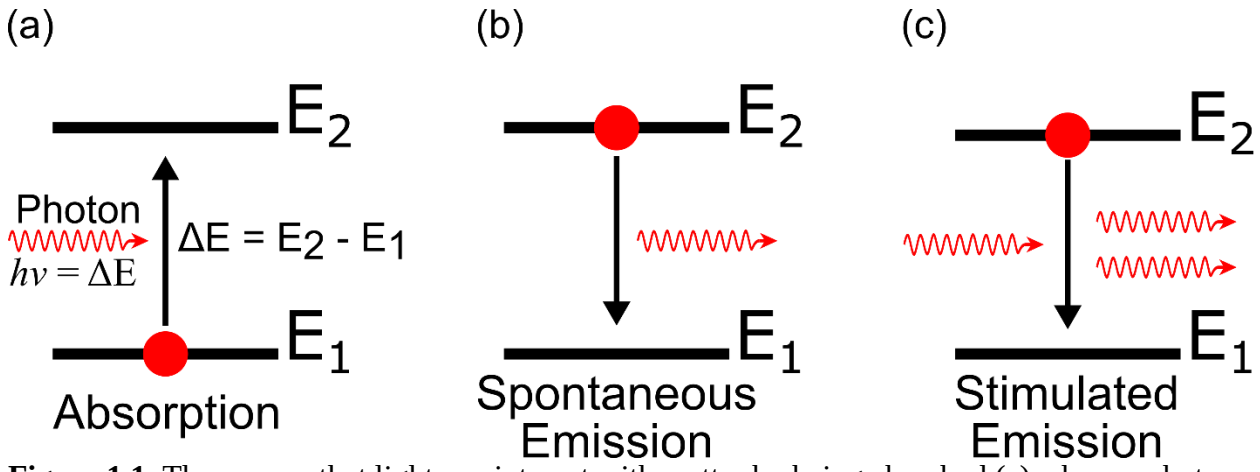

Figure 1.1. Three ways that light can interact with matter by being absorbed (a) where a photon with energy equal to the difference between two level excites the system from state 1 to state 2. State 2 is higher in energy and so the system can drop back to state one by spontaneously emitting a photon (b) with the energy of this photon equal to the energy difference between the two states. When the system is in state 2, an incoming photon can stimulate the system (c) to drop back to state 1 and emit a photon that is in-phase with the incident photon. This stimulated emission process is essential to the successful operation of a laser.

The first process is absorption (**Figure 1.1a**) in which the energy of an incoming photon is used to promote the system from one energy state to another, higher energy state. This process only happens if the energy of the incoming photon is equal to the energy difference between the two states; otherwise, absorption does not occur. Once in the higher energy state (E_2), two processes are possible, and both involve the system returning to the lower energy state (E_1). First, the system can spontaneously emit a photon (**Figure 1.1b**), dropping from E_2 down to E_1,

releasing a photon with the same energy as the difference between the two states in a random direction in a random phase. The other option is for an incident photon to interact with the system in E_2, stimulating the system to emit a photon (**Figure 1.1c**) and drop back to E_1.

Of central importance to stimulated emission is that the stimulated photon has the same phase and direction as the incident photon. Since the photon energy is dictated by the difference in energy levels, the wavelength of laser light is very narrow. Taken together, these properties of stimulated emission allow lasers to be focused to a very narrow beam that does not diverge greatly over long distances.

In order to sustain lasing action, a population inversion needs to be established, that is, the number of species in the higher energy state, E_2, needs to be larger than the population in the lower energy state, E_1. In a simple two energy-level system, such inversion is impossible under thermal equilibrium because, at best, the population in each level can equalize, but only in the extreme limit as the temperature goes to infinity. Thus, sustained laser action requires at least a 3 energy-level system, though many of the common laser systems are 4 level systems.

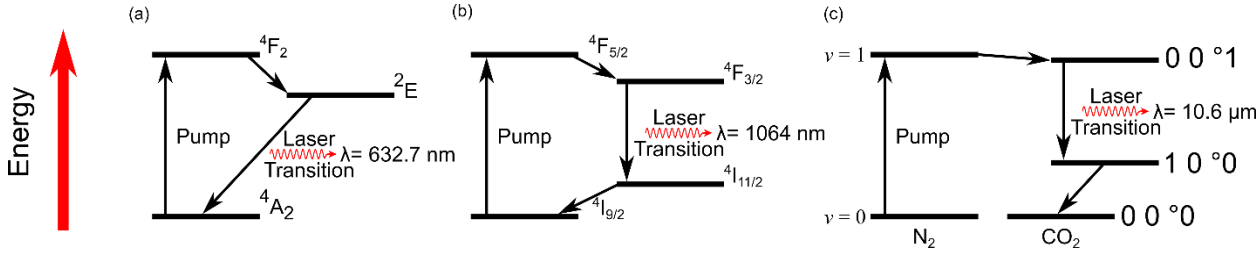

Figure 1.2. The energy level diagram showing the transitions for the ruby laser, the Nd:YAG laser, and the CO_2 laser. The ruby laser (a) is a three energy-level system and relies on electronic transitions of the Cr^{3+} dopant in the α-alumina matrix to provide sustained lasing action in the visible region. The Nd:YAG laser (b) is similar to the ruby laser, relying on the electronic transitions of a dopant, Nd^{3+}, in a solid matrix of YAG, yttrium aluminum garnet. The Nd:YAG laser, however, is a four energy-level system emitting in the near infrared. Another four energy-level system laser is the CO_2 laser (c) which relies on vibrational, rather than electronic, transitions between the asymmetric stretch (0 0 °1) and the symmetric stretch (1 0 °0) to sustain lasing action. As vibrational transitions are much lower in energy than electronic transitions, the CO_2 laser emits in the mid infrared.

The first laser was built in 1960[3] and relied on a three energy-level system (**Figure 1.2a**) using ruby, chromium-doped aluminum oxide, as the gain medium, the material that undergoes stimulated emission leading to a gain in the number of photons leaving the laser cavity. Sufficient energy is supplied to the ruby crystal to pump the system from the $^4A_2$ electronic ground state to the excited $^4F_2$ state. The system then undergoes a non-radiative decay down to the ^2E state. Since the ground state can be continuously pumped to the $^4F_2$ excited state without impacting the ^2E state, a population inversion between the ^2E excited state and the $^4A_2$ ground state. The energy of this transition is 694.3 nm, the wavelength of the ruby laser.

With this demonstration, the development of new lasers took off with two more lasers being demonstrated in 1960, the uranium-doped calcium fluoride[4] and the samarium-doped calcium fluoride,[5] but both required cryogenic cooling so they soon were abandoned as more lasers were demonstrated. The first continuous-wave laser was reported in 1961[6] with multiple laser lines being observed in the near-infrared region. Soon after, the first laser diode in was reported in 1962.[7] Two years later, in 1964, saw the report of two of the most common lasers in use today, the Nd:YAG[8] (neodymium-doped yttrium aluminum garnet) and the CO_2 laser.[9]

Like the ruby laser, the Nd:YAG laser relies on electronic transitions to generate a population inversion, but is a four-level laser system (**Figure 1.2b**). An electron is excited from the ground state, $^4I_{9/2}$, to the top excited state $^4F_{5/2}$. This top excited state then decays to the $^4F_{3/2}$ state, establishing a population inversion relative to the $^4I_{11/2}$. The fundamental laser transition of the Nd:YAG laser is between the $^4F_{3/2}$ state and the $^4I_{11/2}$, emitting at 1064 nm.

The other common four-level laser system is the CO_2 laser, but unlike the Nd:YAG laser, the CO_2 laser relies on vibrational transitions, causing the laser to emit in the mid-infrared region at 10.6 μm. Despite being called a CO_2 laser, modern lasers use a gain medium consisting of a

gas mixture of CO_2, N_2, and He.[10] The helium is used to dissipate heat in the system from non-radiative transitions while the nitrogen is used to improve the efficiency of establishing a population inversion (**Figure 1.2c**). The nitrogen is excited from its ground vibrational state $\nu=0$ to the excited $\nu=1$ state. This vibrational mode is close in energy to the asymmetric stretch of CO_2 so when the excited N_2 molecule collides with a CO_2 molecule, the energy can be transferred to the CO_2 molecule. The population inversion is then established between the asymmetric stretch and the symmetric stretch which is the main transition for the CO_2 laser. The CO_2 molecules are then returned to the ground vibrational state by colliding with helium. The CO_2-N_2-He system enabled high-power continuous-wave laser output which has made the CO_2 laser exceedingly popular.

Efficient laser processing requires the laser light to overlap with absorption bands in the materials being processed. This need for more laser wavelengths led to rapid development of new laser systems in the 1960s with each emitting at their own wavelength. New laser systems, however, were not the only way to produce new laser wavelengths. The large electric fields generated by the lasers enabled scientists to study very-weak, non-linear optical effects. In 1961 scientists used a ruby laser to demonstrate second-harmonic generation.[11] Second-harmonic generation (SHG) is a special case of sum-frequency generation in which two incident photons combine to form a single photon with a frequency that is the sum of the two incident photons. By shining the intense light of a ruby laser (λ =694 nm) through a quartz crystal, they were able to produce a laser beam at half the wavelength of the incident beam, λ = 347 nm.

As a second-order effect, SHG is not observed in every material as it requires some anisotropy, usually a lack of an inversion center in the crystal structure.[12] Furthermore, to produce a strong SHG signal, the frequency doubled light should be phase-matched to the

incident light to prevent destructive interference. This phase-matching criteria is essentially the conservation of momentum applied to the optical process and provides further restrictions on the SHG crystal. The refractive index of a material is generally dispersive, that is, a function of the wavelength of the light. The phase-matching condition says that the refractive index of the SHG crystal must be the same for the both the frequency-doubled laser and the fundamental laser.[13] Once satisfied, SHG enables new laser wavelengths using an existing gain medium, such as green (λ = 532 nm) laser pointers from frequency-doubled Nd:YAG lasers (λ = 1064 nm). As SHG does not occur with 100% efficiency, it is important to isolate the frequency-doubled beam from the fundamental beam to avoid potential laser exposure, especially when frequency-doubling invisible (IR) lasers.[14]

The rapid development and proliferation of laser technology has led to numerous fundamental discoveries culminating in Nobel Prizes.[15] Lasers have also enabled advances in analytical techniques, medicine, and manufacturing with the ability to focus the high-intensity radiation of a laser critical to these advances.

1.2 Laser-Based Analytical Techniques

Numerous laser-based analytical techniques have been developed with many of them being spectroscopic techniques. Raman spectroscopy, and its many variations, uses a laser to probe molecular vibrations that are often not seen, or very weak in infrared spectroscopy.[16–18] Laser-induced breakdown spectroscopy (LIBS) uses a highly-focused, short-pulse laser to generate a plasma near the surface of a material, providing elemental information of the sample being studied.[19] Depending on the wavelength, lasers can induce fluorescence[20] which is useful for quantifying pollutants[21] and studying biological systems using confocal microscopy.[22] Lasers are also used in mass spectrometry in a technique called MALDI, matrix-assisted laser

desorption/ionization, which is used to generate ions in the gas-phase with minimal fragmentation.[23] The MALDI technique enables large molecules and proteins to be analyzed using mass spectrometry, even from aqueous solutions.[24]

1.3 Laser Medicine

All these laser-based techniques require appropriate safety precautions because the laser is also capable of interacting with the various tissues of the human body, causing severe damage. This laser-tissue interaction is the basis for many useful applications of lasers in medicine,[25] with one of the most known applications being corrective eye surgery.[26] While not as well-known in the public, lasers have been used in surgery[27] and to treat tumors[28] almost since the first demonstration of the laser. Continued development has expanded the use of lasers in both these areas.[29,30] Lasers have seen use in cosmetic procedures such as laser tattoo removal[31] and laser hair removal.[32]

1.4 Lasers in Manufacturing

Of present interest is the use of lasers to synthesize, modify, and pattern hard and soft materials to produce structural, optical, electrical, and opto-electrical devices. The unique features of lasers enable many techniques to accomplish this goal, as summarized in **Table 1.1**.

Table 1.1 Summary of Laser Manufacturing Techniques

Technique	Materials	Process Summary	Limitations
Photolithography	Light-sensitive polymers and photomasks	Short-wavelength light changes polymer solubility to selectively expose the substrate to further processing.	Small (nm) features require expensive short wavelength lasers and cleanrooms.
Laser Chemical Vapor Deposition (LCVD)	Gaseous precursors of metals and ceramics	Lasers locally heat a substrate, enhancing the deposition reaction.	Precursors tend to be hazardous and require high-vacuum techniques. Not compatible with soft substrates.
Laser-Induced Forward Transfer (LIFT)	Metals and semiconductors on sacrificial layers	Laser ablation propels the material from the sacrificial substrate to the receiving one	Complex oxides and materials show reduced quality. Deposited films tend to be porous. Microscale resolution.

Table 1.1 (continued).

Selective Laser Sintering (SLS)	Powdered metals, polymers and ceramics	A laser is scanned over the powder bed, merging the particles. A new powder layer is then deposited, and 3D structures are built layer-by-layer.	Control of microstructure remains challenging. Parts often have reduced mechanical properties compared to bulk materials.
Two-Photon Polymerization (2PP)	Photopolymerizable resin transparent to fundamental laser wavelength	Two photons are simultaneously absorbed to polymerize a small volume (voxel). Scanning the laser builds 3D structures	Highly focused, ultra-short (fs) pulse lasers are needed since the two-photon absorption cross-section is exceedingly small (~10^{-50} cm^4 s $photon^{-1}$)
Laser Cutting/Drilling	Metals, ceramics, polymers, and glass	High-power lasers ablate (polymers) or vaporize (metals, glass, and ceramics) material.	Process gasses need to remove melted materials with high boiling points. Caution should be taken when working with kW lasers.

Table 1.1 (continued).

Laser Forming	Metals, ceramics, polymers, and glass	Laser absorption generates localized heating to produce out-of-plane folding. Bidirectional folding is possible.	Niche technique so limited experimental studies. Thin substrates cut easily. Sensitive to clamping conditions and edge effects.

Modern electronic devices rely on integrated circuits (ICs) that are commonly patterned using photolithography.[33] Photolithography is the use of light to pattern thin films of photoresists to selectively expose areas to further processing. Current industrial production of ICs relies on exciplex, which stands for excited complex, lasers such as krypton fluoride or argon fluoride which emit at 248 nm and 193 nm, respectively. The use of shorter wavelength lasers enables smaller features to be patterned and has helped contribute to the near doubling of transistor density every couple of years—a phenomenon known as Moore's law. Continued progress relies on switching to extreme ultraviolet (EUV) lithography which uses lasers to produce plasmas that emit light at 13.5 nm.[33] The fine features in the photoresist are then used to control where the metals or semiconductors are deposited in one step while another photolithography step can selectively expose a different region to etching allowing complex circuits to be designed with nearly nanometer feature sizes.

Another method to pattern these semiconductors is to directly deposit them where desired in a series of techniques known as direct writing.[34] The tight focusing of a laser beam enables a variety of techniques such as laser chemical vapor deposition (LCVD),[35] laser-induced forward transfer (LIFT),[36,37] and even 3D printing[38,39], among others. During normal CVD, a heated

substrate is exposed to a gaseous precursor which decomposes when it contacts the substrate. LCVD uses a laser to induce localized heating, so the decomposition reaction only occurs locally, and a thin film is deposited. As the laser is scanned over the substrate, a patterned film can be deposited over a large area. This process works well for substrates that can withstand high temperatures, such as silicon wafers or sapphire. As the desire for flexible electronics has grown, the preferred substrates are more susceptible to thermal damage so new techniques need to be used.

Laser-induced forward transfer (LIFT) separates the thin film formation from the laser patterning step allowing high-quality materials and films to be prepared using standard techniques on conventional substrates. The unpatterned film is then exposed to a pulsed laser beam which generates enough force locally to propel the film onto a receiving substrate. LIFT has generally been used for the submicron patterning of simple metal films, but modifications to the procedure have expanded the films that have been patterned on the receiving substrate,[37] though improvements still need to be made to match the films produced by lithographic processes. The LIFT process can be repeated to build up 3D features, though the thickness of a given layer is small compared to other additive manufacturing techniques.

Lasers are receiving the spotlight in additive manufacturing as the directed energy is capable of manufacturing 3D objects from both hard and soft materials. Metals and other hard materials are 3D printed using a technique called selective laser sintering[39] that scans a laser over a bed of powdered material. The laser-induced heating locally merges the particles to produce a single layer. Fresh power is deposited over the sintered layer, at which point the process is repeated to build up a 3D object, layer by layer. Selective laser sintering is principally used for 3D printing metals, but control of laser settings also allows 3D printing of more thermally

sensitive powders such as powdered medicines.[40] The photothermal sintering of particles is not the only use of lasers in additive manufacturing as short wavelength light is capable of directly inducing photopolymerization.

Photopolymerization in 3D printing uses light, typically UV, to excite a photoinitiator that causes the exposed area to rapidly polymerize, but the low penetration depth of UV photons results in slow printing speeds.[41] Micrometer scale resolution is easily achievable using standard light sources, but lasers enable a pronounced reduction in feature size by taking advantage of two-photon polymerization. As the name implies, two-photon polymerization (2PP) requires two photons, each at least half the energy required for the photoinitiation, to interact with the 3D printing resin at the same time.[42] Successful 2PP uses a highly-focused femtosecond laser to generate sufficient photon density in the polymerizable resin.[38] When the two photons interact with the resin, they rapidly polymerize a voxel (the 3D *volumetric* pixel) that is an order of magnitude smaller than the fundamental laser wavelength, producing structures with sub-100 nm resolution which are useful in optical devices.[43]

There remain many advanced laser-based patterning or processing techniques such as optical tweezers[44] or holography,[45,46] but lasers find much utility in more industrial settings as a valuable tool in manufacturing. Lasers are often used as extremely precise tools capable of drilling and cutting a wide variety of materials, like metals[47–49] and polymers.[50] The high-power laser is absorbed by the material and rapidly heated. Soft materials like polymers tend to ablate while hard materials like metals will melt and the molten material is removed via plasma formation or a jet of compressed gas.[48] At lower powers, laser ablation is minimized, so the same laser systems can be used for cladding,[51,52] laser welding,[53] and laser marking.[54,55] The ability to induce surface coloration by laser-induced oxidation[56,57] suggests that lasers can also be used as a

post-processing tool in a manufacturing environment. All these processes rely on photothermal conversion of the laser light to produce the desired effect, allowing the laser to be thought of as a highly focused heat source. This observation led to people speculating that lasers could be used to replace oxyacetylene torches.

One niche application of oxyacetylene torches is line heating which uses brief, localized heating to produce bending in metal sheets and was embraced by the shipbuilding industry as a flexible manufacturing technique for the production of ship hulls.[58] Line heating normally requires skilled craftsmen to carefully deliver the correct amount of heat in the correct location to produce the desired bend. Replacing the oxyacetylene torch with a laser enables more precise delivery of heat and automated control. This new technique, laser forming, has attracted recent attention as a new rapid prototyping technology[59,60] because the controlled bending produces 3D structures from metal sheets. This technique will be discussed in more detail in chapter 2.

1.5 Motivation for Thesis

The goal of this this thesis is to expand the use of lasers, specifically for fabricating electronic devices. This goal is accomplished in two ways: by using lasers to compliment conventional fabrication techniques and extend them for prototyping 3D electronics and using lasers to locally carbonize polymers for direct-writing circuits in insulators.

More specifically, flexible printed circuit boards were identified as a potential substrate for laser forming. Printed circuit board technology is industrially mature but is limited to two dimensions. Laser forming uses photothermal stresses from a scanned laser beam to fold materials out-of-plane. By combining flexible printed circuit boards with laser forming, 3D electronics could be rapidly prototyped, especially thin shell structures such as antennas which would be difficult to produce with any other technology.

Recent reports demonstrated that lasers can carbonize the surface layers of certain polymers to produce a porous graphene film called laser-induced graphene (LIG).[61,62] SU-8 was identified as a new candidate for LIG owing to its high thermal stability and its extensive use in microelectromechanical systems (MEMS)[63] and micromolding.[64] The LIG process on SU-8 was studied and the carbonized films were successfully transferred to silicone elastomers demonstrating functional micromolding—conductive elements and microchannels produced in elastomers in a single step.

1.6 References

(1) Hecht, J. Short History of Laser Development. *OE* **2010**, *49* (9), 091002. https://doi.org/10.1117/1.3483597.

(2) Einstein, A. Zur Quantentheorie Der Strahlung. *Physikalische Zeitschrift* **1917**, *18*, 121–128.

(3) Maiman, T. H. Stimulated Optical Radiation in Ruby. *Nature* **1960**, *187* (4736), 493–494. https://doi.org/10.1038/187493a0.

(4) Sorokin, P. P.; Stevenson, M. J. Stimulated Infrared Emission from Trivalent Uranium. *Phys. Rev. Lett.* **1960**, *5* (12), 557–559. https://doi.org/10.1103/PhysRevLett.5.557.

(5) Sorokin, P. P.; Stevenson, M. J. Solid-State Optical Maser Using Divalent Samarium in Calcium Fluoride [Letter to the Editor]. *IBM Journal of Research and Development* **1961**, *5* (1), 56–58. https://doi.org/10.1147/rd.51.0056.

(6) Javan, A.; Bennett, W. R.; Herriott, D. R. Population Inversion and Continuous Optical Maser Oscillation in a Gas Discharge Containing a He-Ne Mixture. *Phys. Rev. Lett.* **1961**, *6* (3), 106–110. https://doi.org/10.1103/PhysRevLett.6.106.

(7) Hall, R. N.; Fenner, G. E.; Kingsley, J. D.; Soltys, T. J.; Carlson, R. O. Coherent Light Emission From GaAs Junctions. *Phys. Rev. Lett.* **1962**, *9* (9), 366–368. https://doi.org/10.1103/PhysRevLett.9.366.

(8) Geusic, J. E.; Marcos, H. M.; Van Uitert, L. G. LASER OSCILLATIONS IN Nd-DOPED YTTRIUM ALUMINUM, YTTRIUM GALLIUM AND GADOLINIUM GARNETS. *Appl. Phys. Lett.* **1964**, *4* (10), 182–184. https://doi.org/10.1063/1.1753928.

(9) Patel, C. K. N. Continuous-Wave Laser Action on Vibrational-Rotational Transitions of C${\mathrm{O}}_{2}$. *Phys. Rev.* **1964**, *136* (5A), A1187–A1193. https://doi.org/10.1103/PhysRev.136.A1187.

(10) Patel, C. K. N.; Tien, P. K.; McFee, J. H. CW HIGH-POWER CO2–N2–He LASER. *Appl. Phys. Lett.* **1965**, *7* (11), 290–292. https://doi.org/10.1063/1.1754264.

(11) Franken, P. A.; Hill, A. E.; Peters, C. W.; Weinreich, G. Generation of Optical Harmonics. *Phys. Rev. Lett.* **1961**, *7* (4), 118–119. https://doi.org/10.1103/PhysRevLett.7.118.

(12) Kleinman, D. A. Theory of Second Harmonic Generation of Light. *Phys. Rev.* **1962**, *128* (4), 1761–1775. https://doi.org/10.1103/PhysRev.128.1761.

(13) Laud, B. B. *Lasers and Non-Linear Optics*, 3rd ed.; New Delhi : New Age International Publishers, 2011.: New Delhi, 2010.

(14) Galang, J.; Restelli, A.; Hagley, E. W.; Clark, C. W. A Green Laser Pointer Hazard. **2010**.

(15) Dudley, J. M. Light, Lasers, and the Nobel Prize. *AP* **2020**, *2* (5), 050501. https://doi.org/10.1117/1.AP.2.5.050501.

(16) Long, D. A. (Derek A. *Raman Spectroscopy*; New York : McGraw-Hill, [1977]: New York, 1977.

(17) Das, R. S.; Agrawal, Y. K. Raman Spectroscopy: Recent Advancements, Techniques and Applications. *Vibrational Spectroscopy* **2011**, *57* (2), 163–176. https://doi.org/10.1016/j.vibspec.2011.08.003.

(18) Stiles, P. L.; Dieringer, J. A.; Shah, N. C.; Van Duyne, R. P. Surface-Enhanced Raman Spectroscopy. *Annual Review of Analytical Chemistry* **2008**, *1* (1), 601–626. https://doi.org/10.1146/annurev.anchem.1.031207.112814.

(19) Rusak, D. A.; Castle, B. C.; Smith, B. W.; Winefordner, J. D. Fundamentals and Applications of Laser-Induced Breakdown Spectroscopy. *Critical Reviews in Analytical Chemistry* **1997**, *27* (4), 257–290. https://doi.org/10.1080/10408349708050587.

(20) Wehry, E. L., 1941-. *Modern Fluorescence Spectroscopy*; New York : Plenum Press, c1976- : New York, 1976.

(21) Baumann, T.; Haaszio, S.; Niessner, R. Applications of a Laser-Induced Fluorescence Spectroscopy Sensor in Aquatic Systems. *Water Research* **2000**, *34* (4), 1318–1326. https://doi.org/10.1016/S0043-1354(99)00260-2.

(22) Paddock, S. W. Principles and Practices of Laser Scanning Confocal Microscopy. *Mol Biotechnol* **2000**, *16* (2), 127–149. https://doi.org/10.1385/MB:16:2:127.

(23) Dreisewerd, K. The Desorption Process in MALDI. *Chem. Rev.* **2003**, *103* (2), 395–426. https://doi.org/10.1021/cr010375i.

(24) Charvat, A.; Abel, B. How to Make Big Molecules Fly out of Liquid Water: Applications, Features and Physics of Laser Assisted Liquid Phase Dispersion Mass Spectrometry. *Phys. Chem. Chem. Phys.* **2007**, *9* (26), 3335–3360. https://doi.org/10.1039/B615114K.

(25) Peng, Q.; Juzeniene, A.; Chen, J.; Svaasand, L. O.; Warloe, T.; Giercksky, K.-E.; Moan, J. Lasers in Medicine. *Rep. Prog. Phys.* **2008**, *71* (5), 056701. https://doi.org/10.1088/0034-4885/71/5/056701.

(26) Sakimoto, T.; Rosenblatt, M. I.; Azar, D. T. Laser Eye Surgery for Refractive Errors. *The Lancet* **2006**, *367* (9520), 1432–1447. https://doi.org/10.1016/S0140-6736(06)68275-5.

(27) Jako, G. J. Laser Surgery of the Vocal CordsAn Experimental Study with Carbon Dioxide Lasers on Dogs. *The Laryngoscope* **1972**, *82* (12), 2204–2216. https://doi.org/10.1288/00005537-197212000-00009.

(28) Zweng, H. C.; Flocks, M.; Kapany, N. S.; Silbertrust, N.; Peppers, N. A. Experimental Laser Photocoagulation. *American Journal of Ophthalmology* **1964**, *58* (3), 353–362. https://doi.org/10.1016/0002-9394(64)91213-9.

(29) Ossoff, R. H.; Coleman, J. A.; Courey, M. S.; Duncavage, J. A.; Werkhaven, J. A.; Reinisch, L. Clinical Applications of Lasers in Otolaryngology—Head and Neck Surgery. *Lasers in Surgery and Medicine* **1994**, *15* (3), 217–248. https://doi.org/10.1002/lsm.1900150302.

(30) Stafford, R. J.; Fuentes, D.; Elliott, A. A.; Weinberg, J. S.; Ahrar, K. Laser-Induced Thermal Therapy for Tumor Ablation. *CRB* **2010**, *38* (1). https://doi.org/10.1615/CritRevBiomedEng.v38.i1.70.

(31) Kent, K. M.; Graber, E. M. Laser Tattoo Removal: A Review. *Dermatologic Surgery* **2012**, *38* (1), 1–13. https://doi.org/10.1111/j.1524-4725.2011.02187.x.

(32) Gan, S. D.; Graber, E. M. Laser Hair Removal: A Review. *Dermatologic Surgery* **2013**, *39* (6), 823–838. https://doi.org/10.1111/dsu.12116.

(33) Wagner, C.; Harned, N. Lithography Gets Extreme. *Nature Photon* **2010**, *4* (1), 24–26. https://doi.org/10.1038/nphoton.2009.251.

(34) Balani, S. B.; Ghaffar, S. H.; Chougan, M.; Pei, E.; Şahin, E. Processes and Materials Used for Direct Writing Technologies: A Review. *Results in Engineering* **2021**, *11*, 100257. https://doi.org/10.1016/j.rineng.2021.100257.

(35) Allen, S. d. Laser Chemical Vapor Deposition: A Technique for Selective Area Deposition. *Journal of Applied Physics* **1981**, *52* (11), 6501–6505. https://doi.org/10.1063/1.328600.

(36) Serra, P.; Piqué, A. Laser-Induced Forward Transfer: Fundamentals and Applications. *Advanced Materials Technologies* **2019**, *4* (1), 1800099. https://doi.org/10.1002/admt.201800099.

(37) Arnold, C. B.; Serra, P.; Piqué, A. Laser Direct-Write Techniques for Printing of Complex Materials. *MRS Bulletin* **2007**, *32* (1), 23–31. https://doi.org/10.1557/mrs2007.11.

(38) Zhang, Y.-L.; Chen, Q.-D.; Xia, H.; Sun, H.-B. Designable 3D Nanofabrication by Femtosecond Laser Direct Writing. *Nano Today* **2010**, *5* (5), 435–448. https://doi.org/10.1016/j.nantod.2010.08.007.

(39) Das, S.; Bourell, D. L.; Babu, S. S. Metallic Materials for 3D Printing. *MRS Bulletin* **2016**, *41* (10), 729–741. https://doi.org/10.1557/mrs.2016.217.

(40) Fina, F.; Goyanes, A.; Gaisford, S.; Basit, A. W. Selective Laser Sintering (SLS) 3D Printing of Medicines. *International Journal of Pharmaceutics* **2017**, *529* (1), 285–293. https://doi.org/10.1016/j.ijpharm.2017.06.082.

(41) Bagheri, A.; Jin, J. Photopolymerization in 3D Printing. *ACS Appl. Polym. Mater.* **2019**, *1* (4), 593–611. https://doi.org/10.1021/acsapm.8b00165.

(42) Farsari, M.; Chichkov, B. N. Two-Photon Fabrication. *Nature Photon* **2009**, *3* (8), 450–452. https://doi.org/10.1038/nphoton.2009.131.

(43) Deubel, M.; von Freymann, G.; Wegener, M.; Pereira, S.; Busch, K.; Soukoulis, C. M. Direct Laser Writing of Three-Dimensional Photonic-Crystal Templates for Telecommunications. *Nature Mater* **2004**, *3* (7), 444–447. https://doi.org/10.1038/nmat1155.

(44) Ashkin, A. Acceleration and Trapping of Particles by Radiation Pressure. *Phys. Rev. Lett.* **1970**, *24* (4), 156–159. https://doi.org/10.1103/PhysRevLett.24.156.

(45) Katz, J.; Sheng, J. Applications of Holography in Fluid Mechanics and Particle Dynamics. *Annual Review of Fluid Mechanics* **2010**, *42* (1), 531–555. https://doi.org/10.1146/annurev-fluid-121108-145508.

(46) Campbell, M.; Sharp, D. N.; Harrison, M. T.; Denning, R. G.; Turberfield, A. J. Fabrication of Photonic Crystals for the Visible Spectrum by Holographic Lithography. *Nature* **2000**, *404* (6773), 53–56. https://doi.org/10.1038/35003523.

(47) Caristan, C. L. *Laser Cutting Guide for Manufacturing*; Dearborn, MI : Society of Manufacturing Engineers, [2004]: Dearborn, MI, 2004.

(48) Mahrle, A.; Beyer, E. Theoretical Aspects of Fibre Laser Cutting. *J. Phys. D: Appl. Phys.* **2009**, *42* (17), 175507. https://doi.org/10.1088/0022-3727/42/17/175507.

(49) Olsen, F. O.; Alting, L. Pulsed Laser Materials Processing, ND-YAG versus CO2 Lasers. *CIRP Annals* **1995**, *44* (1), 141–145. https://doi.org/10.1016/S0007-8506(07)62293-8.

(50) Henry, M.; Harrison, P.; Wendland, J.; Parsons-Karavassilis, D. Cutting Flexible Printed Circuit Board with a 532NM Q-Switched Diode Pumped Solid State Laser. *ICALEO* **2005**, *2005* (1), M804. https://doi.org/10.2351/1.5060568.

(51) Brandt, M.; Scott, D. A.; Emms, S. B.; Yellup, J. M. Laser Cladding with a Pulsed Nd:YAG Laser and Optical Fibers. *Journal of Laser Applications* **1997**, *9* (2), 67–75. https://doi.org/10.2351/1.4745446.

(52) Vilar, R. Laser Cladding. *Journal of Laser Applications* **1999**, *11* (2), 64–79. https://doi.org/10.2351/1.521888.

(53) Stavridis, J.; Papacharalampopoulos, A.; Stavropoulos, P. Quality Assessment in Laser Welding: A Critical Review. *Int J Adv Manuf Technol* **2018**, *94* (5), 1825–1847. https://doi.org/10.1007/s00170-017-0461-4.

(54) Noor, Y. Md.; Tam, S. C.; Lim, L. E. N.; Jana, S. A Review of the Nd: YAG Laser Marking of Plastic and Ceramic IC Packages. *Journal of Materials Processing Technology* **1994**, *42* (1), 95–133. https://doi.org/10.1016/0924-0136(94)90078-7.

(55) Amara, E. H.; Haïd, F.; Noukaz, A. Experimental Investigations on Fiber Laser Color Marking of Steels. *Applied Surface Science* **2015**, *351*, 1–12. https://doi.org/10.1016/j.apsusc.2015.05.095.

(56) Wautelet, M.; Baufay, L. Laser-Induced Oxidation of Thin Cadmium and Copper Films. *Thin Solid Films* **1983**, *100* (1), L9–L12. https://doi.org/10.1016/0040-6090(83)90233-X.

(57) Antończak, A. J.; Stępak, B.; Kozioł, P. E.; Abramski, K. M. The Influence of Process Parameters on the Laser-Induced Coloring of Titanium. *Appl. Phys. A* **2014**, *115* (3), 1003–1013. https://doi.org/10.1007/s00339-013-7932-8.

(58) Scully, Kevin. Laser Line Heating. *Journal of Ship Production* **1987**, *3* (4), 237–246.

(59) Thomson, G.; Pridham, M. S. Controlled Laser Forming for Rapid Prototyping. *Rapid Prototyping Journal* **1997**, *3* (4), 137–143. https://doi.org/10.1108/13552549710191845.

(60) Bachmann, A. L.; Dickey, M. D.; Lazarus, N. Making Light Work of Metal Bending: Laser Forming in Rapid Prototyping. *Quantum Beam Science* **2020**, *4* (4), 44. https://doi.org/10.3390/qubs4040044.

(61) Lin, J.; Peng, Z.; Liu, Y.; Ruiz-Zepeda, F.; Ye, R.; Samuel, E. L. G.; Yacaman, M. J.; Yakobson, B. I.; Tour, J. M. Laser-Induced Porous Graphene Films from Commercial Polymers. *Nature Communications* **2014**, *5*, 5714. https://doi.org/10.1038/ncomms6714.

(62) Chyan, Y.; Ye, R.; Li, Y.; Singh, S. P.; Arnusch, C. J.; Tour, J. M. Laser-Induced Graphene by Multiple Lasing: Toward Electronics on Cloth, Paper, and Food. *ACS Nano* **2018**, *12* (3), 2176–2183. https://doi.org/10.1021/acsnano.7b08539.

(63) Lorenz, H.; Despont, M.; Fahrni, N.; LaBianca, N.; Renaud, P.; Vettiger, P. SU-8: A Low-Cost Negative Resist for MEMS. *J. Micromech. Microeng.* **1997**, *7* (3), 121–124. https://doi.org/10.1088/0960-1317/7/3/010.

(64) Xia, Y.; Whitesides, G. M. Soft Lithography. *Annual Review of Materials Science* **1998**, *28* (1), 153–184. https://doi.org/10.1146/annurev.matsci.28.1.153.

Chapter 2 Making Light Work of Metal Bending: Laser Forming in Rapid Prototyping

Adam L. Bachmann,[1,2] Michael D. Dickey,[2] and Nathan Lazarus[3]

[1]Oak Ridge Associated Universities (ORAU) Fellowship Program at US Army Research Laboratory

[2]Department of Chemical and Biomolecular Engineering, North Carolina State University

[3]Sensors and Electron Devices Directorate, US Army Research Laboratory

This chapter has been published as a manuscript in the journal Quantum Beam Science (2020)

Abstract

Lasers can be used to bend 2D metal sheets into complex 3D objects in a process called ‘laser forming.’ Laser forming bends metal sheets by locally heating the sheets to generate plastic strains and is an established metal bending technology in the shipbuilding industry. Recent studies have investigated the laser forming of thin metal parts as a complementary rapid prototyping technology to metal 3D printing. This review discusses the laser forming process, beginning with the mechanisms before covering various design considerations. Laser forming for the rapid manufacturing of metal parts is then reviewed, including the recent advances in process planning before highlighting promising future research directions.

2.1 Introduction

Fabricating complex 3D structures is a difficult task as many materials and processes are inherently 2D. Flat structures need to be carefully assembled to produce the desired 3D shape, whether a ship, an automobile, or a solar array. One of the oldest ways to produce 3D structures from flat objects is origami, the Japanese art of paper folding.[1,2] Origami principles can apply to other sheets of material, often with the goal of assembling the final 3D structure far from the point of production of the 2D pattern.[3–5]

Researchers have developed algorithms to achieve complex 3D shapes from 2D fold patterns.[6] These algorithms are not limited to paper, although the algorithms typically neglect the effect of substrate thickness and thus work best on materials that are thin and inextensible, like paper. Oftentimes, the desired structures need to be made of materials that have a non-negligible thickness.[7,8] Folding rigid materials is typically done by attaching rigid facets with compliant hinges,[9] but this places restrictions on what can be produced, a term called rigid foldability.[10] One of the most common rigid folding patterns is the Miura-ora pattern (**Figure 2.1a & 2.1b)** as it allows large area structures to be compactly stored before deployment, which is valuable for space applications.[5,7,11,12] In many applications, actuation (folding) is done manually (**Figure 2.1c & 2.1d**);[13] however, researchers are exploring ways to create hinges that fold in response to external stimuli (e.g. light, electricity, heat, moisture), allowing for self-folding (**Figure 2.1e**).[3,14–17]

Origami is not the only means available for manufacturing custom 3D parts and prototypes. Prototyping is critical to the product design cycle, so a slew of technologies have been developed to speed up this process. Rapid prototyping covers a wide range of technologies that allow computer aided design (CAD) files to be translated into objects such as

stereolithography, laminated object manufacturing, and 3D printing, with the latter being one of the most popular.[18] 3D printing is a popular technology that additively builds objects through the layered deposition of material.[19,20] 3D printing allows highly customized metal parts to be fabricated with minimal waste (**Figure 2.1f**), making it an attractive technology for 'mass customization.' [21] Many metal 3D printing methods use a focused energy beam (laser or electron beam) to fuse metal powders together, building the part layer by layer, but the process is long and has a limited build volume[20,22,23] and metal 3D printers are also relatively expensive (on the order of hundreds of thousands of dollars for a commercial printer).[23] The unfused powder acts a support, allowing pieces to be built with moderate overhangs, but sharp bends remain challenging[23] as well as thin shells.[24] Origami folding, which allows rapid and cheap creation of 3D shells of material, is therefore an important complementary technology well-suited for many devices such as antennas, waveguides and other systems that rely on thin layers of metal. Thin metal sheets are easy to bend, and overhangs can be generated with almost any degree of bend angle, enabling the production of complex shapes with simple folds and cuts (**Figure 2.1g**).

Successful metal origami requires precise control over the bending of the sheets of metal. There are multiple ways to bend metal, the most common methods use expensive equipment such as press brakes (**Figure 2.2a**), or roll formers (**Figure 2.2b**).[25–27] Press brakes involves placing the sheet metal over a shaped die and then applying intense mechanical pressure to force the metal into the die. Roll forming involves the gradual bending of the sheet metal by passing through successively narrower rollers. Both processes rely on mechanically deforming the sheet which leads to a spring-back effect that causes the final bend angle to differ from the dies and rollers, as a result of residual elastic strains after the mechanical pressure is removed.[28–31] Proper control for spring-break often involves extensive testing of how the brakes and substrates

interact.[29] A change of design shape or material means this testing would need to be repeated, making this a poor choice for rapid prototyping.

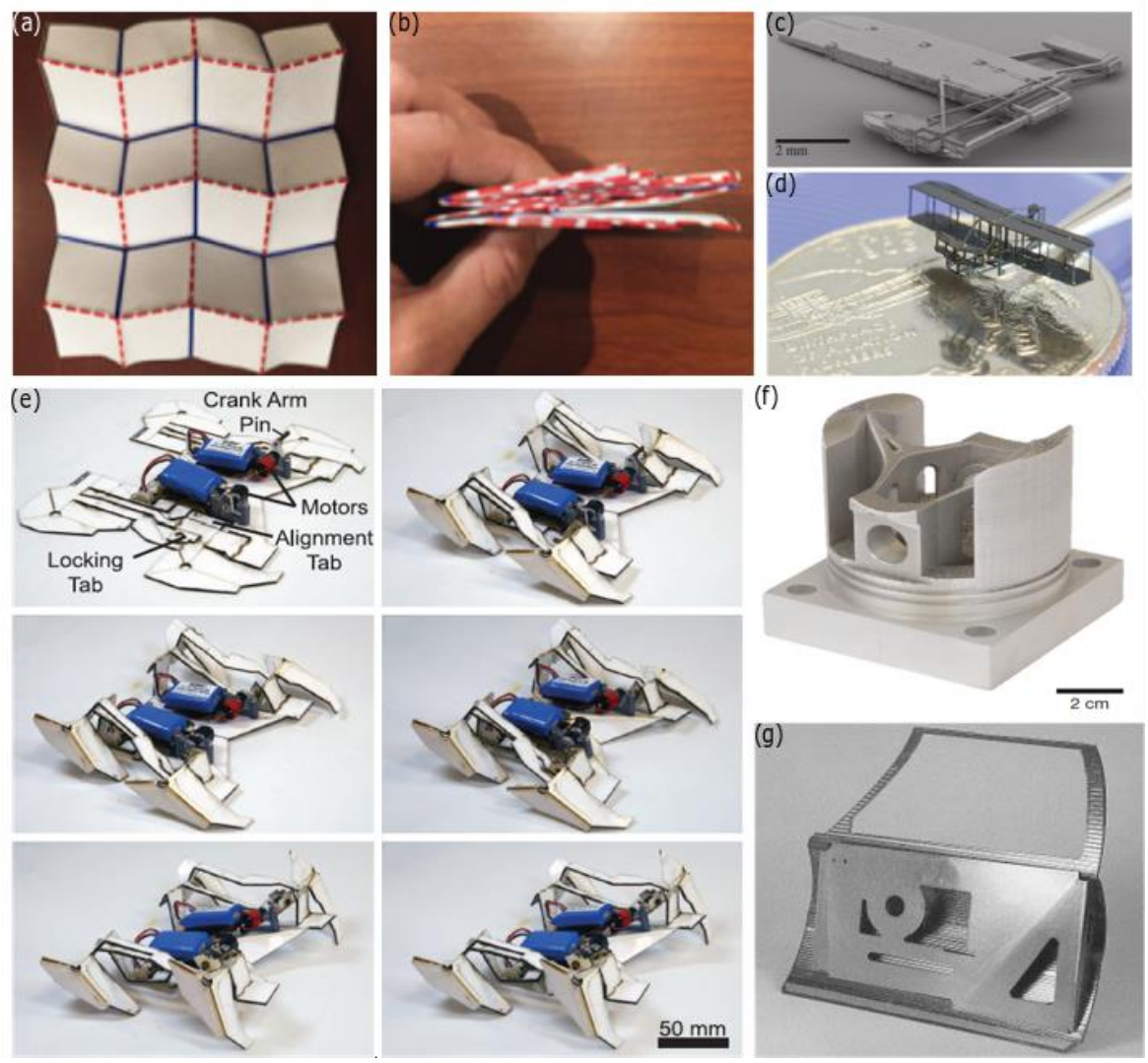

Figure 2.1. Complex 3D origami requires fold patterns such as the Miura-ori which compresses a (a) large sheet in the unfolded sheet into a (b) compact folded state.[1] Copyright SAGE publications, 2016. Origami principles can be used to produce complex structures. A (c) folded MEMS structure becomes a (d) scale replica of the Wright flyer once the unfolding is complete.[13] © IOP Publishing. Reproduced with permission. All rights reserved. Self-folding (e) has been used to produce crawling robots from flat sheets.[3] Reprinted with permission from AAAS. Rapid prototyping of metallic 3D structures can be done with (f) 3D printing[32]. Reprinted with permission from Springer Nature, copyright 2017. Metal products can also be formed by the (g) laser forming of sheet metal.[33]. Reproduced with permission from Emerald Publishing, copyright 1997.

Another method of metal bending involves thermal stress-induced bending called line heating.[34] Line heating uses a gas torch to carefully heat a piece of metal followed by cooling the part rapidly in water to generate plastic strains that bend the metal. This process, unlike press break forming, is highly labor intensive. Line heating also depends on the craftsmanship of the bender since the gas torch is a diffuse heat source, which can lead to large heat-affected zones and degraded material properties.[35] Aiming to automate this process, researchers suggested replacing the skill of a bender and flame torches with the highly controllable heat of a laser.[35] The process is similar to line forming, but uses lasers to localize the heating. Thus, these early researchers called this process 'laser forming'.[36,37]

Laser forming is defined as the use of a laser beam to locally heat and introduce thermal stresses to plastically deform a work piece.[38] The interaction of a laser beam and a substrate generates localized thermal gradients (**Figure 2.2c**)[36,37] that cause unequal material expansions. The thermal expansions generate stresses large enough to cause the heated material to yield, generating plastic response stresses.[39,40] As the piece cools, the scanned area returns to its normal size and stops straining the surrounding material, but the compressive stresses remain leading to a permanent deformation in the substrate without a spring-back effect.[37] Laser forming consists of several related mechanisms, and is most commonly used for bending but can also be used for shortening/adjusting a work piece.[41,42]

While this review uses the term "laser forming" for thermal metal forming processes, as accepted in the related research community, we want to address potential confusion in terminology. Another technique also used for laser bending is laser peen forming (also known as laser shock forming). In laser peen forming (**Figure 2.2d**), a short-pulsed laser is focused on a sacrificial coating on top of the workpiece.[43] When the coating ablates, it generates a plasma

plume that attempts to expand in all directions.[43] The laser peen forming setup confines this expanding plume, usually with a layer of water, and redirects this energy as a shockwave into the workpiece leading to bending.[43] This process is entirely mechanical and thus susceptible to the similar drawbacks of more conventional fabrication. A recent review of the field can be found elsewhere[44] and this approach will not be covered further here. The term 'laser forming' has also been used by researchers in reference to other technologies based on producing (i.e. forming) a material with a laser, including powder bed fusion,[45] or laser metal cladding (**Figure 2.2e**).[46] Both techniques use a laser to selectively heat metal powders, causing them to coalesce, but 'laser forming' is not the preferred terminology in those fields.

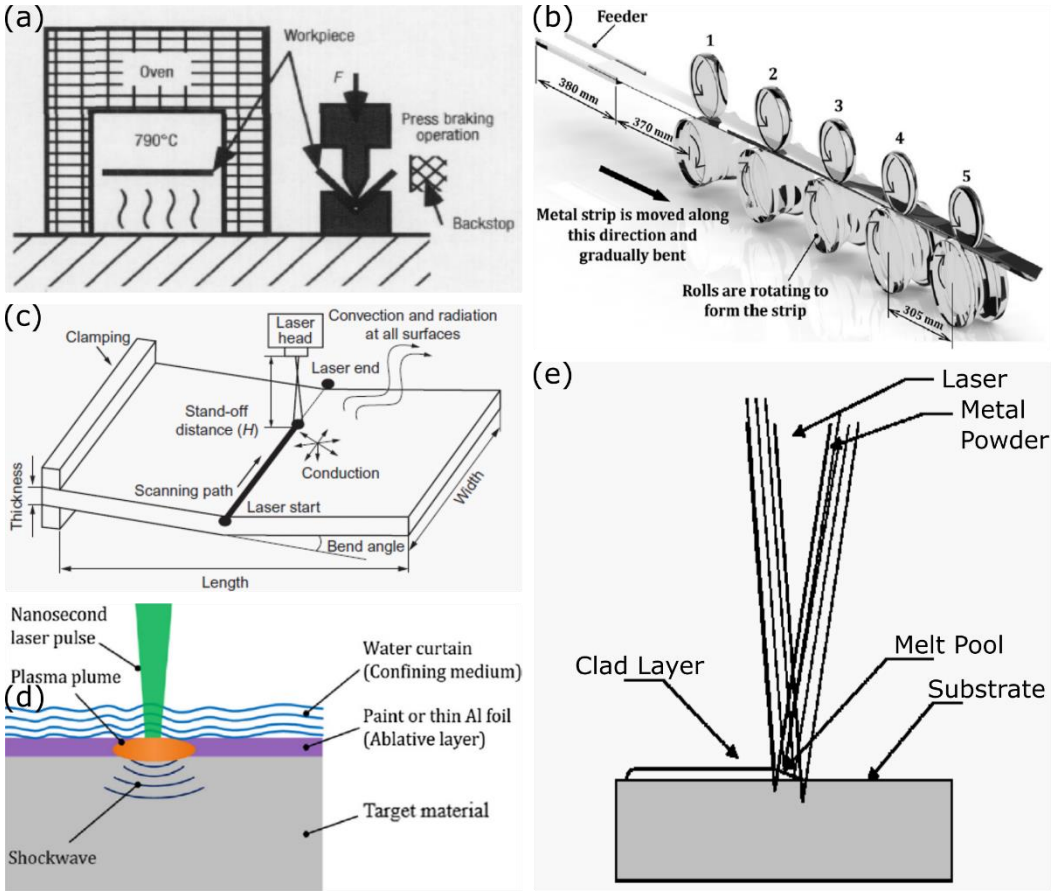

Figure 2.2. Common metal forming techniques include (a) press brake forming[27] over dies to produce sharp bends. Brittle materials, such as titanium, require a preheating step to exceed the ductile-brittle transition temperature so they can be bent without breaking. Reprinted with permission of Elsevier, copyright 2000. Long sheets of metal can be (b) roll formed[31] to generate pieces with a constant cross-section. Reprinted with permission of Elsevier, copyright 2000. Laser forming is term that is commonly used to describe many processes but is used in this review to refer to (c) the process by which a laser-induced thermal gradient generates plastic stresses in a workpiece that leads to a permanent deformation.[47] Reprinted with permission of Elsevier, copyright 2016 Some other process that are sometimes (erroneously) referred to as laser forming include (d) laser peen (shock) forming[44] where a laser-induced shockwave mechanically deforms a workpiece. Reprinted with permission of Elsevier, copyright 2018. Some author have also used laser forming to describe (e) laser metal cladding.[46]. Reprinted with permission of Taylor & Francis, copyright 2000.

Laser forming was first developed in the 1980s,[35] and much of the early research was focused on understanding the complex interaction between the laser and the material properties with a goal of developing formulas that can accurately predict the final bend angle.[37,48,49] A number of studies now exist on modelling of laser forming, including a notable review,[38] so we

refrain from focusing on these research efforts here. Instead, we aim to survey laser forming as a rapid prototyping strategy for developing 3D structures from flat substrates. The most recent review focusing on the manufacturing applications of laser forming is almost two decades old,[50] and there have been many advances in the field since then.

This review of laser forming begins with a discussion of the three dominant sub-mechanisms of laser forming before discussing how to select appropriate process parameters to achieve a desired bend shape. We then survey the application space of laser forming, from larger scale fabrication to smaller scale rapid prototyping and adjustment before providing an outlook on current challenges and unresolved problems in the field.

2.2 Laser Forming Mechanisms

Laser forming is a relatively broad term that refers to the plastic deformation of a workpiece resulting from laser-induced thermal stresses. From experimental studies and finite element modelling of laser forming, three main sub-mechanisms have been identified for understanding laser forming: the temperature gradient mechanism (TGM), the buckling mechanism (BM), and the upsetting (shortening) mechanism, (UM).[36–38] All three mechanisms arise from plastic strains generated in the work piece as a result of the absorbed laser energy, but the dominance of one mechanism over the others depends on how that energy propagates in the work piece.[51] This energy propagation depends on the workpiece geometry and the lasing parameters.

2.2.1 Temperature Gradient Mechanism (TGM)

The temperature gradient mechanism is dominant when a thermal gradient is generated through the thickness of the work piece through laser heating.[37] This vertical gradient is achieved with a higher laser scan speed and a thicker substrate (or a thinner substrate with

relatively poor thermal conductivity).[52] The thickness of the material in the TGM case is typically on the order of the laser beam diameter.[53,54] For example, researcher laser formed sheets between 0.5 mm and 4 mm thick using a laser with beam diameter of 5.2 mm travelling at 1.5 m/min.[52] Once the laser energy is absorbed by the surface of the metal, the temperature rises rapidly (**Figure 2.3a**). In most materials, the hotter areas expand, generating stresses on the cooler sections.[55] As the top of the workpiece is much hotter than the bottom, the top of the workpiece expands more than the bottom, leading to a small counter-bend (**Figure 2.3b**) away from the laser.[38,52] At these high temperatures, the mechanical properties, such as the Young's modulus, drop precipitously.[56] At these elevated temperatures, the thermal expansion stresses exceed the flow stress which means the thermal stresses are large enough to maintain plastic deformation.[36,39,40] The work piece surrounding the thermally expanded portion is stiff and resists the expansion by exerting an equal compressive force.[52,55] Initially, the material bends away from the laser (the counter-bend) and is a consequence of the thermal expansion combined with the decreased yield stress of metals at higher temperatures.[36] Once the piece has time to cool, the material scanned by the laser returns to its normal volume, but the compressive stresses remain in the piece. Consequently, the laser scanned volume is under compression causing the work piece to develop a final bend angle, θ, toward the laser (**Figure 2.3c**).[36,50] At the cooler temperatures, the mechanical properties return to their higher values which prevents the formation of new plastic stresses and so this bend angle is permanent.[38,52,55] The TGM mechanism, therefore, always results in a bend toward the laser source.

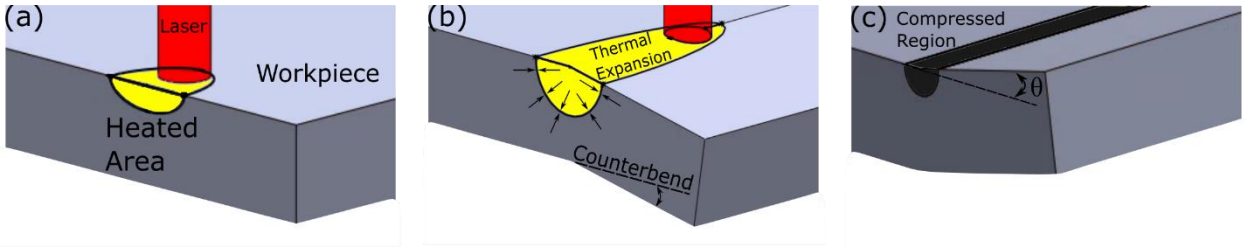

Figure 2.3. Schematic of the temperature gradient mechanism during the immediate laser exposure (a) showing the thermal gradient established through the thickness of the substrate while (b) the thermal expansion causes a counter-bend that also generates plastic, compressive strains. After the laser has passed and the area locally cools (c) the compressive forces remain, causing the substrate the bend toward the laser and generating a bend angle, θ.

2.2.2 Buckling Mechanism (BM)

The buckling mechanism also relies on a thermal gradient, but in this mechanism, the work piece is either thinner or has a high thermal conductivity relative to the laser scan speed.[36] The first report of laser forming using the buckling mechanism used a laser beam with a diameter of .12 mm traveling at 5 mm/s to laser form 0.1 mm thick steel foils. [57] In this case, there is essentially no temperature gradient through the thickness of the substrate, but rather, the thermal gradient spreads outward from the scan line (**Figure 2.4a**).[57] This means the resulting compressive forces are pushing against each other, generating a buckling instability (**Figure 2.4b**).[57] Consequently, the work piece can bend either toward or away from the laser (**Figure 2.4c**).[57] As an instability, the bending direction should be random, but this assumes the sheet has no residual stresses prior to laser forming.[57] Commercially available materials have a complex internal stress state because of the hot and cold working that the sheet experiences during manufacturing, and this stress state determines the buckling direction.[58] Complete knowledge of this stress state would allow the bending direction to be predicted[57,58], though this is usually unknown. Beyond predicting the bending direction, researchers have also developed ways to control the buckling direction. Such methods include pre-bending the metal sheet, [52,59] or through judicious choice of the lasing parameters.[60,61] The ability to generate bidirectional bending

expands the design space for laser forming,[62,63] without the need for human input, i.e. flipping the work piece.[50] As bending with the buckling mechanism can occur both toward and away from the laser, there can be some ambiguity which mechanism is occurring. Downward bending currently remains the best confirmation that buckling is occurring because the TGM only bends the workpiece toward the laser. It has been reported that buckling can lead to larger bend angles per pass,[57,58] which suggests the bend angle can be another way to differentiate the mechanisms, though visual downward bending is the easier method.

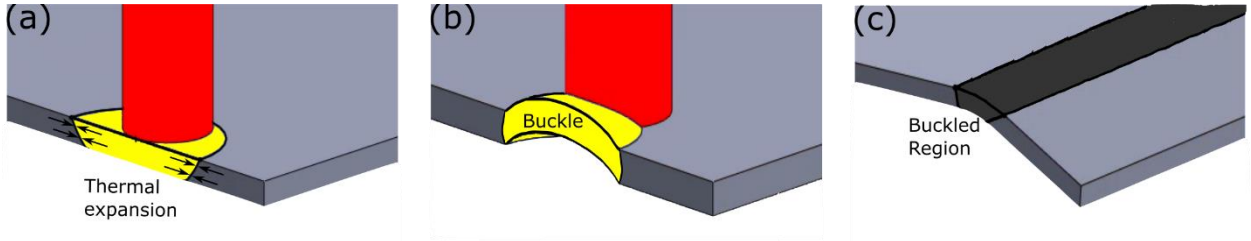

Figure 2.4. When laser forming thinner materials, the thermal gradient is unable to be established through the thickness of the material, so (a) the material expands outward. The compressive forces (b) are pushing opposite of each other, causing the workpiece to buckle. Once the buckling has formed, it (c) propagates and leads to bending in the direction opposite to the buckle. As the buckle is an instability, it can buckle either direction.

2.2.3 Upsetting Mechanism (UM)

The third mechanism of laser forming is the upsetting mechanism.[37,64] The upsetting mechanism begins in a similar manner to the buckling mechanism. The laser scan speed is kept low to prevent a thermal gradient from developing through the thickness of the substrate, generating similar stresses to the buckling mechanism (**Figure 2.5a**).[54] In the upsetting mechanism, however, the substrate is much stiffer along the scan path, preventing an out-of-plane bend.[36,64] This stiffness can be the result of using a thicker workpiece or one where the material has a higher Young's modulus.[50] Since the flow stress has been reached, but the substrate is unable to bend, the laser scan path becomes locally thicker and the substrate becomes, consequently, shorter (**Figure 2.5b**).[42] One of the more comprehensive studies on the

upsetting mechanisms reliably shortened 2 mm thick steel plates using 12 mm laser beams scanning at speeds around 1 mm/s.[51] The upsetting mechanism allows for in-plane substrate adjustments which expands what shapes are laser formable by producing a change in Gaussian curvature.[53,65]

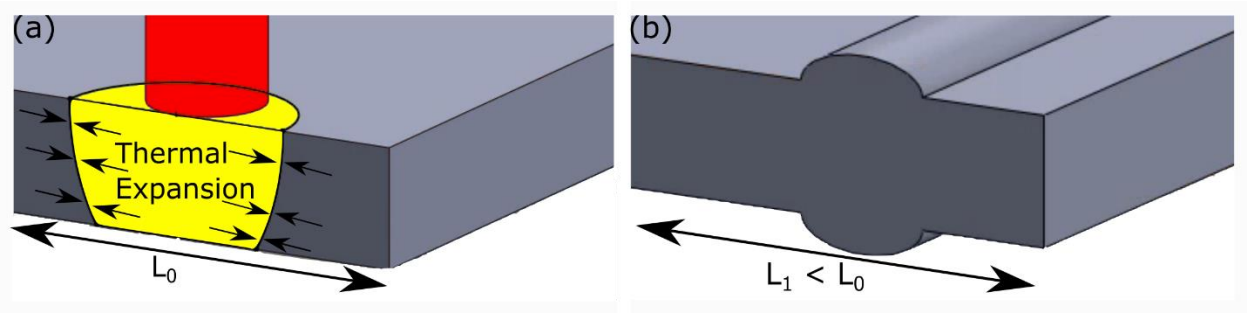

Figure 2.5. A slow laser scan speed (a) is used to minimize the thermal gradient through the thickness of the workpiece. Instead, the thermal gradient is established horizontally. The plastic compressive forces that resist the thermal expansion are insufficient to cause buckling as the bending moment is too large. This results in the (b) scanned area locally thickening. Since volume is conserved, the workpiece shortens and changes its Gaussian curvature.

2.2.4 Coupling Mechanism

Some recent reports have suggested that the three mechanisms described above are not sufficient to capture the full range of experimental results and so they have proposed a coupling mechanism that combines both TGM and the upsetting mechanism. [51,64,66] This combination of forming mechanisms was already discussed[36,57] in early reports but was not considered a separate mechanism. The proposed coupling mechanism is a consequence of the mechanisms above being idealized, limiting cases. As the laser forming parameters are adjusted, it is reasonable that the other mechanisms might start to play an increasingly important role, especially near the transition region between TGM and buckling.[36] For this reason, the proposed coupling mechanism will not be treated as a distinct mechanism of laser forming here, but it is still important to consider when designing a laser forming process and is even useful for laser forming certain structures.[66]

2.3 Design Considerations for Laser Forming

2.3.1 Laser and Substrate Selection

Since its first reports, laser forming has been used to bend sheets of common metals, such as stainless steel[67–69] and aluminum[70–72] out of plane without mechanical inputs.[36,37,67] As the understanding of the process developed, more varied substrates were explored such as titanium,[27,73] and copper alloys,[74,75] hoping to develop new ways to form 3D structures for aerospace and electrical applications. Researchers have also explored laser forming on non-metallic substrates and have bent typically brittle materials such as silicon,[76–78] ceramics,[41,79] and glass.[79,80] More recently, there have also been demonstrations of the laser forming of more complex structures such as metal foams[81,82] and laminates.[83] Despite the success of laser forming non-metals, metal bending has remained the primary application of laser forming due to the use of metals as engineering materials in applications such as ship hulls.[35,54,84] There have also been some reports of laser forming of a limited number of polymers, [85,86] although polymer laser forming remains relatively rare. Laser forming, therefore, is a general process reliant on controlled heating to generate plastic stresses and appears possible for most materials. Large bending angles are more readily realized in metals as their ductility helps avoid crack formation at the bend line,[80,82,82] though experimental results suggest that the maximum bend angle is a strong function of material thickness with thinner samples being able to demonstrate larger bend angles.[79,82,87] Studies of many of the more well-studied substrates have been able to demonstrate deformation by all three mechanisms. Laser forming of the more exotic materials tends to be realized using the TGM,[76,80,82] though BM has been demonstrated in glass[79] and UM in silicon.

Critical to the success of the laser forming process is appropriate coupling of the laser energy to the material being formed. This coupling can be achieved by selecting the appropriate

laser wavelength that corresponds to the absorption maximum of the substrate[75,88], by using a much higher power laser so sufficient energy is absorbed by the substrate even with low absorptivity, or by using an absorbing coating layer that is matched with the laser wavelength being used (**Figure 2.6**).[85,89] Metals thicker than 100 nm are optically opaque[90] and do not transmit light so the metal substrates that have been used in laser forming can either reflect or absorb the laser energy. The percentage of the incoming laser energy that is reflected is called the reflectance and these values have been measured as a function of wavelength.[91] The most common lasers[27] used for laser forming are Nd:YAG lasers that operate at 1.064 μm[57,58,76,78,85,86,92,93] and CO_2 lasers that emit at 10.6 μm.[39,50,54,68,89,94–96] CO_2 lasers are common in industrial setting as they were one of the first gas lasers developed[97] and exhibit a high energy efficiency while operating as a continuous-wave mode at high average powers (>1 kW); however, their absorption into metals is low and an absorbing coating is often required. Nd:YAG lasers are popular in industry as the 1.064 μm output wavelength is better absorbed by metals for cutting and welding and so absorbing coatings are not needed.

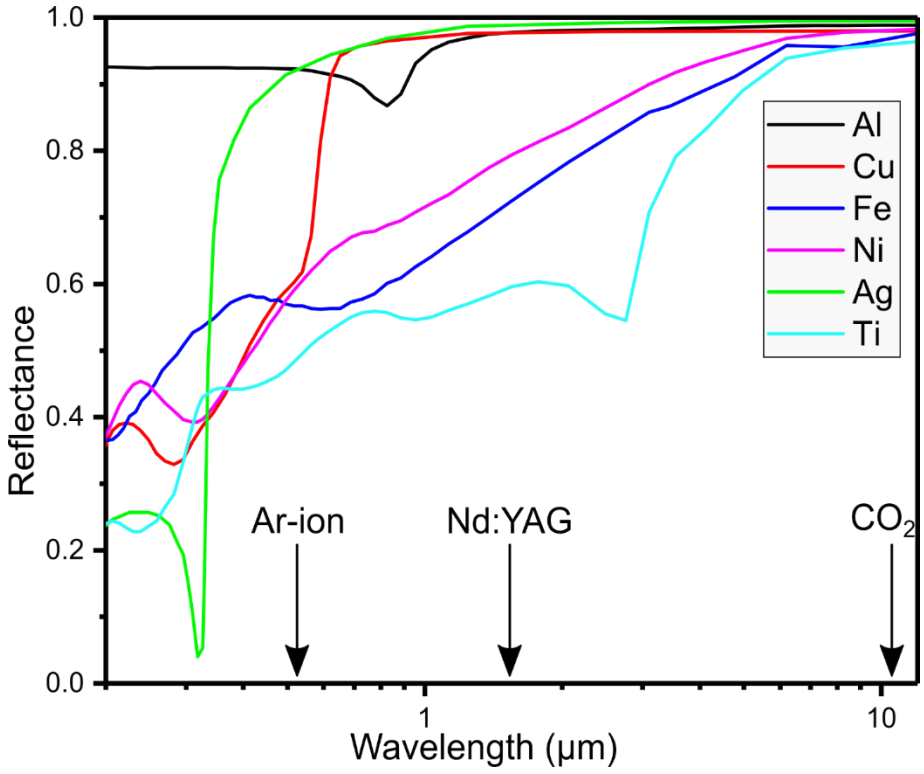

Figure 2.6. The spectral reflectance of metals, plotted from the data in [91], with the wavelength of some common lasers also identified. Almost all metals are entirely reflective to the 10.6 μm light of CO_2 lasers while metals tend to be less reflective to the 1.064 μm light of the Nd:YAG laser, though copper, aluminum, and silver are still fairly reflective. Copper has a much higher absorbance to the 514 nm beam from an Ar-ion laser.

The early reports focused on using high power (>1 kW) lasers[40,60,61,70,71,98–103] as the intent was to bend large sheets as part of the ship building process.[35] Laser forming of thinner substrates enables the use of lower power (<100 W) lasers such as those found in commercial metal marking laser systems.[57,63,67,76,85,88,93,104]

Studies on the laser forming of plastics took advantage of the high transmissivity of high-density polyethylene (HDPE) to the wavelength of the Nd:YAG laser[85,86]. The laser energy was absorbed by a resinous black coating applied to the surface of the plastic. The laser power was kept low and the scan speed high to ensure that the bending occurred through the temperature gradient mechanism, which reliably generates bending toward the laser. As expected, this was observed when the resin was on the side of the plastic exposed to the laser. With the same

process parameters, but the coating placed on the opposite side, the plastic was reliably bent away from the laser. This downward bending should not be possible if using the TGM, but the optical transparency of HDPE to the laser made the system behave as if it was exposed to a laser on the underside and the TGM was causing the plastic to bend that direction. This same technique could be adopted for laser systems with multiple wavelengths as glass absorbs the radiation from a CO_2 laser but is transparent to the light from a Nd:YAG laser. Thus, sealed metal structures could still be bent if there is a glass window for the laser to pass through.[105] As seen in **Figure 2.6,** some metals, such as copper, are highly reflective to the fundamental wavelength of the Nd:YAG laser (1.064 μm). Consequently, laser forming copper with a Nd:YAG laser requires a substantially higher power or the use of a different wavelength. Recently, laser forming was demonstrated with other laser systems that might be commonly found in research environments such as fiber lasers[106], exciplex lasers[74] and even Ar-ion lasers[67] which expands the substrate choice for laser forming.

Once the appropriate laser/substrate matching has been done, judicious selection of process parameters is essential to the laser forming process as the laser power and scan speed control which mechanism is dominant.[37] Typically, laser power is kept low and speeds high to ensure that the substrate is being bent by the TGM, generating reliable bending toward the laser. As the TGM only generates a bend of one or two degrees per pass or less,[38,74,101] many passes are needed to create structures with large bend angles, sometimes taking as many as 150 passes to produce a full 90 degree bend.[88]

2.3.2 Cooling Effects in Laser Forming

To ensure that the same thermal gradient is established with each laser pass, an appropriate cooling time must also be built into the laser forming process. Consistent laser

forming requires that the workpiece be cooled to the same thermal state in between each laser pass. The majority of laser forming setups use free convection with the surrounding air to cool the workpiece, which is relatively slow and leads to a pronounced increase in processing time (**Figure 2.7a**). In fact, cooling can be the longest part of a laser forming process.[52,59,86,107] To reduce the processing time, researchers have proposed multiple methods for forced cooling such as forced convection with compressed gas streams aimed at either side (**Figure 2.7b**),[92,108] passive water cooling with the bottom of the workpiece being placed in a water bath (**Figure 2.7c**),[109–111] and forced liquid cooling, such as a circulated cooling fluid placed in contact with the bottom of the substrate (**Figure 2.7d**),[112–115] All these methods showed a pronounced reduction in the total processing time as the workpieces cooled to room temperature in a matter of seconds, with active water cooling showing the largest reduction in processing time.

Active cooling systems are not typically desirable when designing manufacturing processes as they require pumps that increase both capital and operating costs of the process, but they are acceptable if the active cooling offers a substantial decrease in processing time or improvement in the reliability of a process. Fortunately, passive water cooling has also been demonstrated to provide sufficient reductions in processing time (**Figure 2.7d**) that active cooling may not be needed.[109] Some researchers have reported that forced cooling can lead to an increased bend angle per pass (**Figure 2.7e**) under the same lasing conditions but reports differ on how pronounced this effect is, with some arguing there is no measurable effect. [35,108,109,112,113] Overall, integrated cooling systems offer a way to increase the throughput of laser forming by greatly reducing the time needed to establish thermal equilibrium in between laser passes for multi-pass forming.

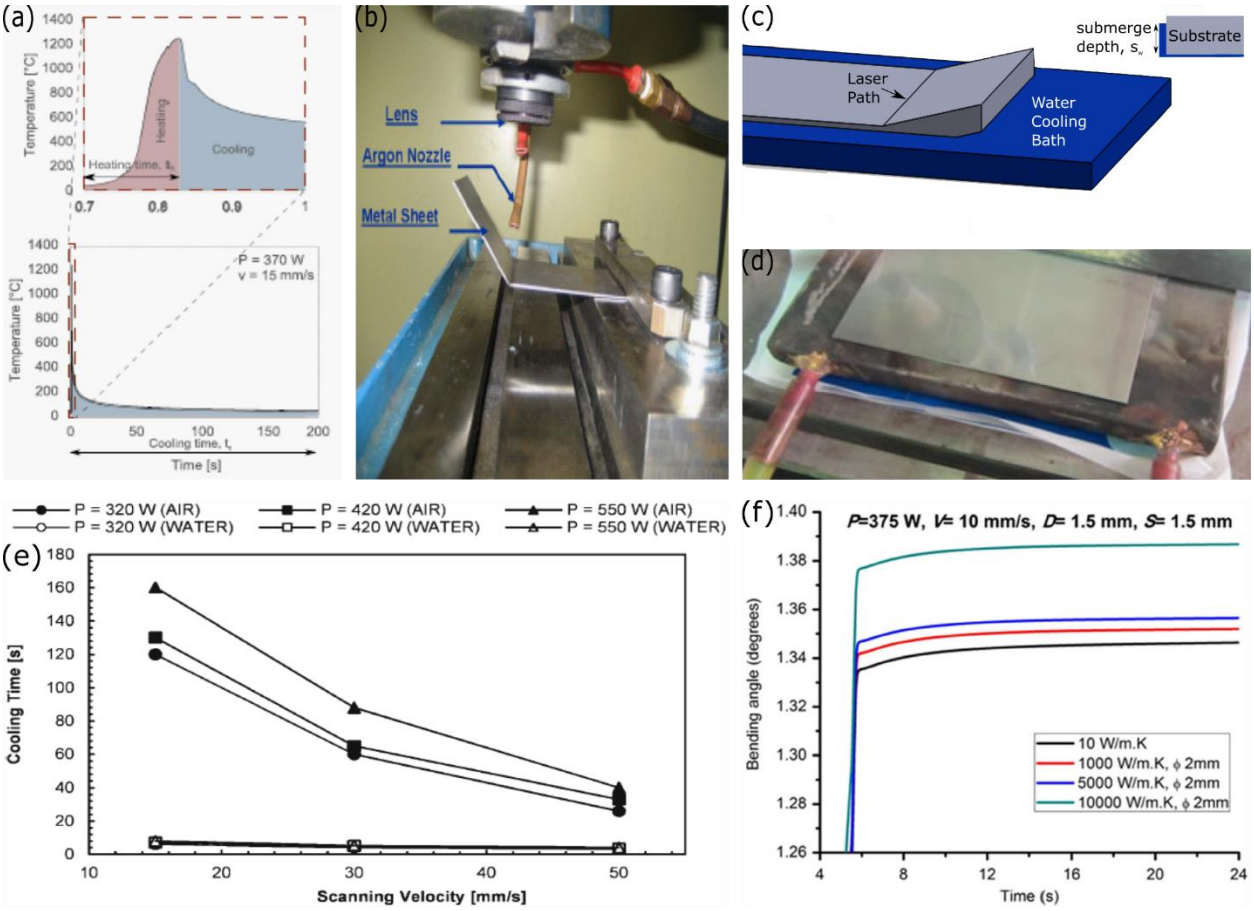

Figure 2.7. Most of the processing time (a) while laser forming is cooling the workpiece back to its initial state after each laser pass which is usually done by free convection.[114] Reprinted with permission from Springer Nature, copyright 2015. This time can be reduced by building in other cooling mechanisms such as (b) forced air cooling[92] (c) passive water cooling, adapted from[109] on the unexposed side or (d) forced liquid cooling.[115] (b) Reprinted with permission from Elsevier, copyright 2013. (d) Reprinted with permission from Cambridge University Press, copyright 2017. Passive water cooling leads to a (e) dramatic reduction in cooling time for most processing conditions.[109] Reprinted with permission from Springer Nature, copyright 2012. Sometimes, cooling offers a small increase (f) in the bending angle achieved per pass.[112]. Reprinted with permission from Springer Nature, copyright 2017.

The processing time can be further decreased by using the buckling mechanism as buckling is capable of generating larger bending angles per pass than the TGM because more energy is put into the workpiece.[56,57] Typically, laser forming using the buckling mechanism is avoided as the mechanism is fundamentally an instability and so the workpiece can bend either toward the laser or away from it.[57] This instability is theoretically random but can be controlled by multiple factors such as external loads,[57,104] or the relaxation of internal stresses that exist

because of the cold-working of common metal sheets.[57] The main reason to use the buckling mechanism is the downward bending which greatly broadens the number of structures that can be laser formed.[59,61]

2.3.3 Macro-scale Laser Forming

Early research efforts were focused on macro-scale laser forming of sheet metals that are millimeters thick.[35,50,103] Among the macro-scale design targets were ship hulls,[35,84] fuselage panels,[70] and car doors (**Figure 2.1g**).[33] These structures highlight different uses for laser forming in a manufacturing environment as ship hulls and fuselage panels are low-volume parts whereas car doors are high-volume components. Laser forming is considered less desirable for manufacturing high-volume metal parts as it cannot compete with the speed of conventional methods because the laser forming process is dominated by the cooling time needed between laser passes.[33,50,52,114]

Both high-volume and low-volume products need to be joined to other parts which is the second use for laser forming in manufacturing of macro-scale objects. Metal parts are often joined via welding which can introduce distortions and lead to misalignment.[35,116] These distortions arise from two main contributions. First, the high heat of welding introduces thermal stresses similar to laser forming.[116] Second, the heat of welding releases stored plastic strains that result from mechanical forming.[35] While the distortions from welding are often small, they still need to be corrected and laser forming offers a way to address these problems in a process known as hybrid laser forming.[50,54,117,118] Accurate manipulation of metals near weld lines is, however, challenging because the local weld distortion is not uniform due to the complex stress state generated during welding.[119]

The ability to shape large 3D objects using only a laser offers promising opportunities such as remote deployment, the production of replacement parts where they are needed rather than at a centralized facility and shipped. In the 1980s, it was proposed that laser forming would be a valuable technology in space.[103] A laser system is more compact than a hydraulic press and the high energy efficiency of CO_2 and diode lasers lowers the energy consumption required for metal bending. Laser systems also offer the potential for cutting the workpiece[59] and joining[120] it with others pieces that traditional press brakes do not, making laser systems valuable for areas with minimal electricity generation or limited space.

2.3.4 Laser Forming Curved Surfaces

Ship hulls are an example of a doubly curved structure and so researchers needed to design methods of introducing curvature into laser formed parts.[53] Currently, there are two main methods for developing curvature in laser formed parts. The first way is to make multiple bend lines close to each other,[33,68,121] approximating a smooth curve as the limit of many bend lines close together (**Figure 2.8d**). By adjusting the distance between the laser passes, bends of varying curvature are able to be produced as the heat affected zone is not limited to the laser pass line.[68] As this curvature is produced by simple bends, the resulting structures are considered developable surfaces.[65] Developable surfaces are the family of surfaces that can be produced by transforming a plane as long as the Gaussian curvature remains unchanged (**Figure 2.8a**).[65] This means bending, rolling, and cutting are permitted, but stretching or compressing a region are forbidden.[65] As developable surfaces are produced from bending and folding, much of the knowledge gained in origami engineering is applicable to producing structures with laser forming.[1,14,26,122,123]

The second method to produce curved structures relies on the upsetting mechanism which produces in-plane strains.[53] These planar strains cause local distance to be distorted, changing the Gaussian curvature of the workpiece[53,124] which simple bending does not. Since the strain changes the Gaussian curvature, the final workpiece is considered a non-developable surface as developable surfaces have zero Gaussian curvature.[65] Non-developable surfaces include hyperbolic paraboloids (**Figure 2.8b**) and hyperboloids which are often called saddles (**Figure 2.8e**)[53,84] and pillows,[53] respectively, in the laser forming literature. The ability to generate these surfaces from flat sheets using laser forming greatly expands the design space of 3D structures that can be rapidly prototyped.

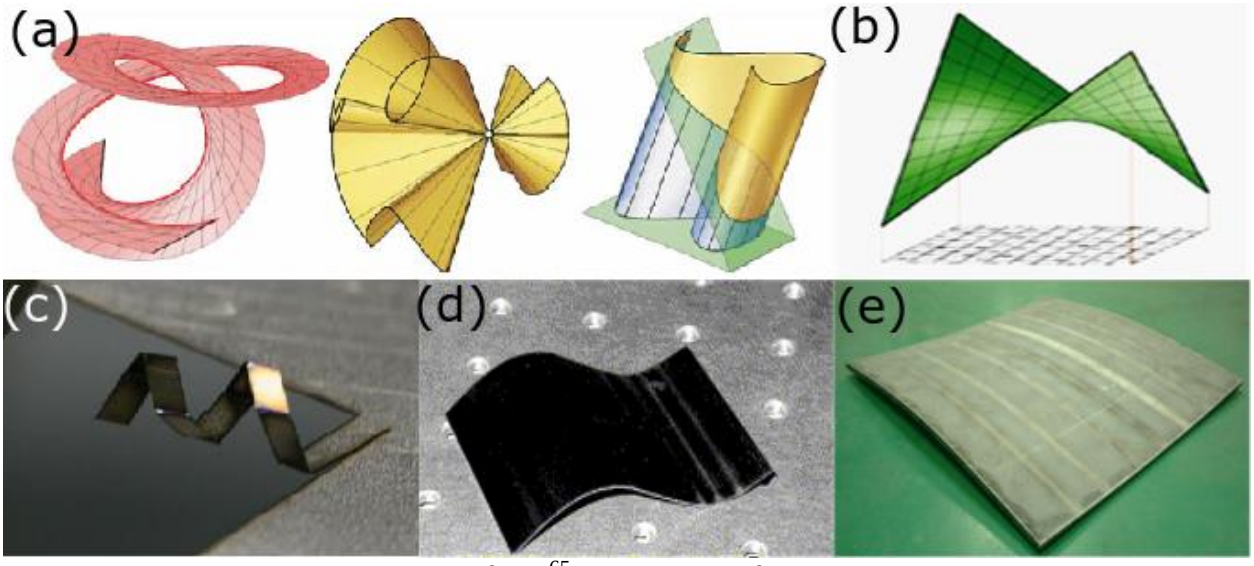

Figure 2.8. Some (a) developable surfaces[65] which are surfaces with zero Gaussian curvature which means they can be produced from flat sheets while non-developable surfaces such as the (b) hyperbolic paraboloid[65] or "saddle shape" cannot be formed by bending and cutting inelastic sheets as they have a non-zero Gaussian curvature. (a,b) Published under a CC BY License. Laser forming with the TGM or buckling mechanisms can produce developable surfaces such as (c) a coil[59] or (d) a cubic spline curve[99] which only require simple bends to produce from a metal sheet. (d) Reproduced with permission from Elsevier, copyright 2003. The upsetting mechanism causes a shortening of the workpiece, which changes the Gaussian curvature, so (e) a doubly curved saddle shape can be successfully laser formed.[84]. Reproduced with permission from Elsevier, copyright 2013.

While the majority of laser forming research has been done on planar substrates, some researchers have investigated laser forming as a means to bend metal tubes for heat exchangers and engines.[40,125–127] Laser formed tubes bend toward the laser though researchers disagree about what mechanism is causing the bending. Some suggest the TGM is causing the bending[126] while others suggest that the stiff nature of metal pipes means that the upsetting mechanism is dominant, leading to a local shortening which causes the tube to bend toward the laser without a spring-back effect.[40,128] Like laser forming of sheets, laser tube bending is a highly flexible method that does not require specially designed dies. This makes laser tube bending valuable for rapid prototyping as well as low volume, customized production.[126] When bending tubes, it is important to consider the distortion of the tube cross-section, or ovalization.[40] Multiple reports have confirmed that laser tube bending tends to produce less ovalization than mechanical bending as the laser induced stresses are less than the mechanical forces used when cold bending the tubes.[40,126]

Matching the optical absorbance of the substrate with the laser output allows the energy to couple more effectively, lowering the laser power required for successful laser forming. As lower powered (<100 W) laser cutting systems proliferated, researchers hoped to use these systems for laser forming as well as laser cutting. Laser cutting requires high laser fluences, so the beam size needs to be small to achieve clean cuts. Since the output power is lower, the fluence is kept high by decreasing the spot size. For successful laser forming, the laser spot size is typically the same order of magnitude as the substrate being bent which has lead researchers to experiment with laser forming of smaller and thinner substrates.[67,72,129]

2.3.5 Micro-laser Forming

Complex, 3D silicon microstructures are difficult to produce because silicon is a brittle material that requires high temperatures and specialized tools to produce the desired shape.[130] Laser forming has been applied to adjusting silicon microstructures.[76] The precise control of heating enables silicon microstructures to be bent out of plane even with more thermally sensitive components, as long as the thermally sensitive components are not located near the laser scan path. Laser forming is not heavily used for the rapid prototyping of MEMS structures, but has been found tremendously successful as a quality control technique called laser micro-adjustment.[64,131] Laser micro-adjustment is a valuable application of laser forming as evidenced by industrial adoption of the technique.[41,131,132]

Laser micro-adjustment uses a laser to make submicron final adjustments to microstructures.[106,133] Any of the mechanisms can be used for this adjustment but the smaller bending angle per pass makes the TGM preferable to the buckling mechanism for out-of-plane bends.[38,64] The upsetting mechanism is useful for shortening the workpiece locally which has been used for aligning actuators.[42,133] The laser forming mechanism can be easily determined by adjusting the lasing parameters,[36] but the size of the sheets being micro-adjusted makes edge effects more common[134] and increases the coupling between the TGM and the upsetting mechanism.[64,101,106,135] This coupling leads to both in-plane shortening and out-of-plane bending that is especially common in actuators. Bridge actuators are micromechanical structures that holds functional components and allows fine adjustments to the final positioning to be made. Bridge actuators are produced by removing most of the structural material in a small area so that they are connected by thin strips called bridges. When laser forming a two-bridge actuator, the scan path effectively creates two hot and two cold sides, the usual irradiated and unirradiated

sides of the work piece as well as a hot bridge and a cold bridge. The usual irradiated sides produce the out of plane bending while the hot bridge causes an in-plane bend.[42,135] While actuators are one of the most common pieces laser micro-adjusted, the process is general and has been applied to multiple devices[136] and companies have filed for patents on using laser adjustments based on these reports. [137–139]

One application of laser micro-adjustment is the precise alignment of optical fibers to ensure optimal coupling with a photonic integrated circuit (PIC).[140] While glass has been successfully laser formed,[81,82] laser forming the optical fiber would only produce bends into the fiber rather than aligning it. To align the optical fiber, the researchers sheathed the fiber into a thin metal tube and the tube was then laser formed.[140,141] The optical fiber is flexible so the bend in the metal tube will cause a deflection in the fiber tip. In effect, the metal tube is being used as an alignment actuator with sub-micron precision owing to the controllability of laser forming.[140,141]

2.3.6 Laser Forming for Rapid Prototyping

The flexibility of laser forming makes it a promising technology for rapid prototyping and researchers have identified rapid prototyping as one of the areas where laser forming is most likely to make meaningful contributions in the industrial product lifecycle.[50] This promise remains largely unfulfilled compared to more conventional 3D printing for various reasons. Despite the many different methods for 3D printing, such as fused filament fabrication[142,143] and stereolithography,[144,145] 3D printing follows the same general workflow to produce a printed object from a computer aided design (CAD) file (**Figure 2.9a**). Once the engineer has designed the object they want to be 3D printed using a CAD software, they need to export it to a format that can be 3D printed.[19] The default file format for the additive manufacturing community is the

STL file format which approximates the surface of the CAD object as a collection of tessellated triangles.[146] Since 3D printers build structures in a layer by layer fashion, the STL file needs to be passed to a slicer which converts the 3D object to the build layers. From this file, the scan path is developed, and support structures are calculated if the object needs them. For modern 3D printing, the conversion of the CAD file to printed object is entirely automated.[19,146] Critical to the broad adoption of laser forming for rapid prototyping is developing a similar software structure which can convert a CAD file into a path planning program that also calculates the appropriate lasing setting to produce the desired 3D object without human intervention. Extensive research efforts have been undertaken to achieve this goal with recent results suggesting that this goal might be realized soon.[62]

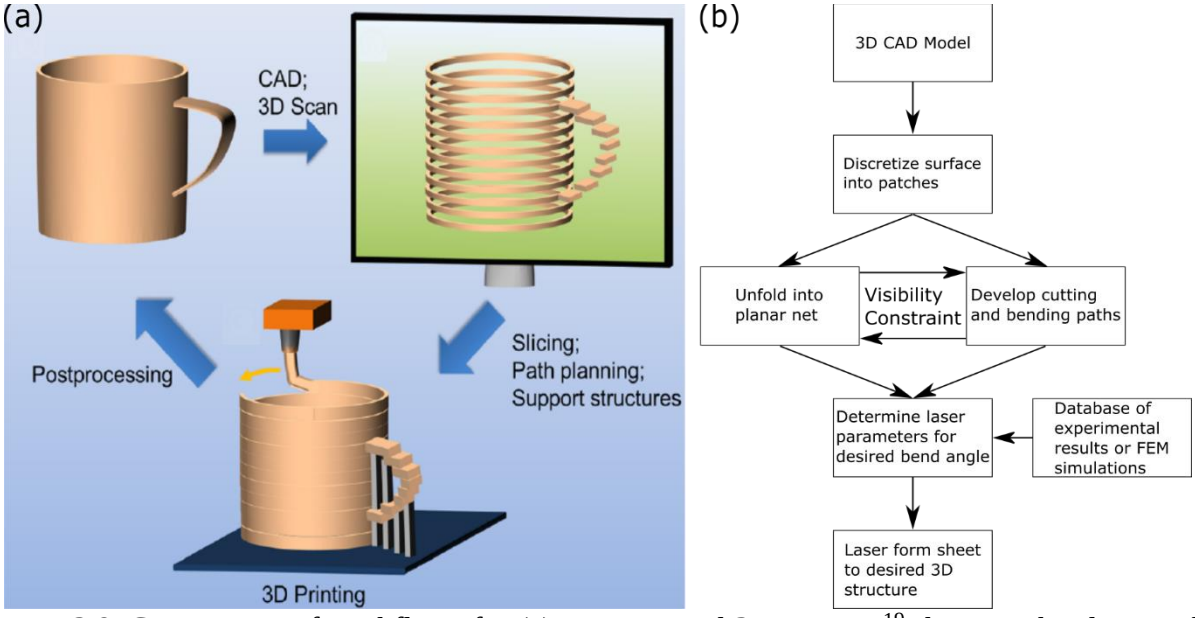

Figure 2.9. Comparison of workflows for (a) conventional 3D printing[19] showing the slicer and path planner compared to (b) proposed workflow for the automated laser forming of arbitrary convex polyhedra. (a) Image originally published under a CC BY license. Unlike 3D printing, path planning for laser forming is strongly dependent on the material being formed which requires a database to determine laser power and speed settings. For more advanced structures, laser forming algorithms need to consider the optical path of the laser beam as this couples the unfolding algorithm and the path planning.

One of the first complex objects successfully prototyped using laser forming was a car door (**Figure 2.1g**).[33] This demonstration is notable for many reasons, chiefly the entire production was done in the laser system. The researchers started from a blank sheet of metal that was laser formed to produce the desired bends and the final structure was cut from the sheet using the same laser. As the buckling mechanism was only recently reported and control strategies were limited, the researchers were laser forming only using TGM. The complex shape of the car door required both concave and convex bending, so the workpiece needed to be manually flipped to produce the bi-directional bending needed for the car panel. While these experiments involved no prediction of laser settings, the researchers introduced a novel feedback system where the scanning speed was adjusted to produce the desired bend angle. Additionally, a car panel might be considered far from an arbitrary design and so the scan pattern was relatively easy to design.

To produce more complex objects via laser forming, it is necessary to know which bend lines are needed to produce a given shape, a classic origami problem.[1] To this end, the inverse design of scan strategies to generate a desired laser formed structure has been a productive research topic.[53,66,84,99,147–150] The design of irradiation paths involves more than planning where the beam needs to be applied to generate a desired shape, but also the laser power and travel speed to produce the desired degree of bending using the appropriate forming mechanism. These requirements remain a challenge and have required researchers to design algorithms that plan a scan path and guesses appropriate lasing settings by consulting a database from experiments[99] or finite element simulations (**Figure 2.9b**).[53,121,149] Despite the known disagreement between experimental results and simulations,[38] these scan strategies are able to produce the final desired structures with a high degree of accuracy.[53,121] One limitation of these design systems is the

limited degree of bending required in the validation structures. As the bend angles required per point are small to moderate, the relationships between bend angle and line energy (laser power divided by scan speed) is approximately linear.[98,99] As the laser spot size gets smaller and the required bending angle approaches 90 degrees, this linear relation fails to hold[88,151] and none of these design strategies account for this deviation. These limitations are more prominent as engineers have started using laser forming to produce highly complex structures.

Realizing that laser forming was not limited to moderate bending but could be used for larger folds (up to ninety degrees or higher), our group began envisioning what origami structures can be produced with laser forming. Laser forming with TGM is limited to ninety-degree bends as further bending results in the workpiece blocking the laser path, but this limitation does not exist if using the buckling mechanism to bend away from the laser. Using both mechanisms, we were able to produce complex objects, such as cubes (**Figure 2.10a**) and airplanes, (**Figure 2.10b**) without the need for human intervention.[59] Similar to the car door forming,[33] the outline of the shape was manufactured from metal sheets by using the laser to also cut the final structure, releasing it from the sheet. By using a Nd:YAG laser instead of a CO_2 laser, an absorbing coating was not needed, allowing for marking of the metal at low powers. Rapidly producing these structures from a blank metal sheet using multiple bending modes and laser cutting demonstrated the potential for laser forming to be a viable rapid prototyping strategy.

Soon after, we showed that laser forming could be used to produce electronic devices such as antennas[152] and inductors.[88] When producing the antennas, a blank metal sheet was clamped on all sides before laser cutting the slots for the array antenna and the perimeter of the waveguide was laser cut from the metal sheet before the entire structure was bent to produce the

final structure, a rectangular prism (**Figure 2.10c**).[152] It was worth noting that the laser cutting made more precise cuts than electro-discharge machining, the usual technology used to produce the slots in the waveguide. In fact, the entire laser process of cutting and bending was faster than conventional machining that only produces the slots. Efficient waveguides require smooth surfaces to minimize losses[153] so new manufacturing techniques need to show that they do not greatly alter the metal surface. The impact of laser forming is limited to the laser scan paths and even after 100 passes only showed a modest increase of the surface roughness of 0.5 μm.[154] Similarly, the coils for the inductor were cut from a blank piece of copper before being bent out of plane to generate a toroidal inductor (**Figure 2.10d**).[88] Laser forming can also be used to produce an inductor with an overpass or bending the inductor out of plane. Bending inductors out of plane offers a way to improve the Q-factor as eddy currents and skin effects are minimized,[155] which is especially important for integrating these elements on semiconductor integrated circuits. Both reports demonstrated that laser forming could be used to rapidly prototype functional devices as the designs can easily be iterated as it only requires changing the location or size of lines in a 2D CAD drawing. This process, however, still requires human input to exchange the metal sheets between design iterations which would limit the industrial adoption of laser forming for rapid prototyping or producing custom parts.

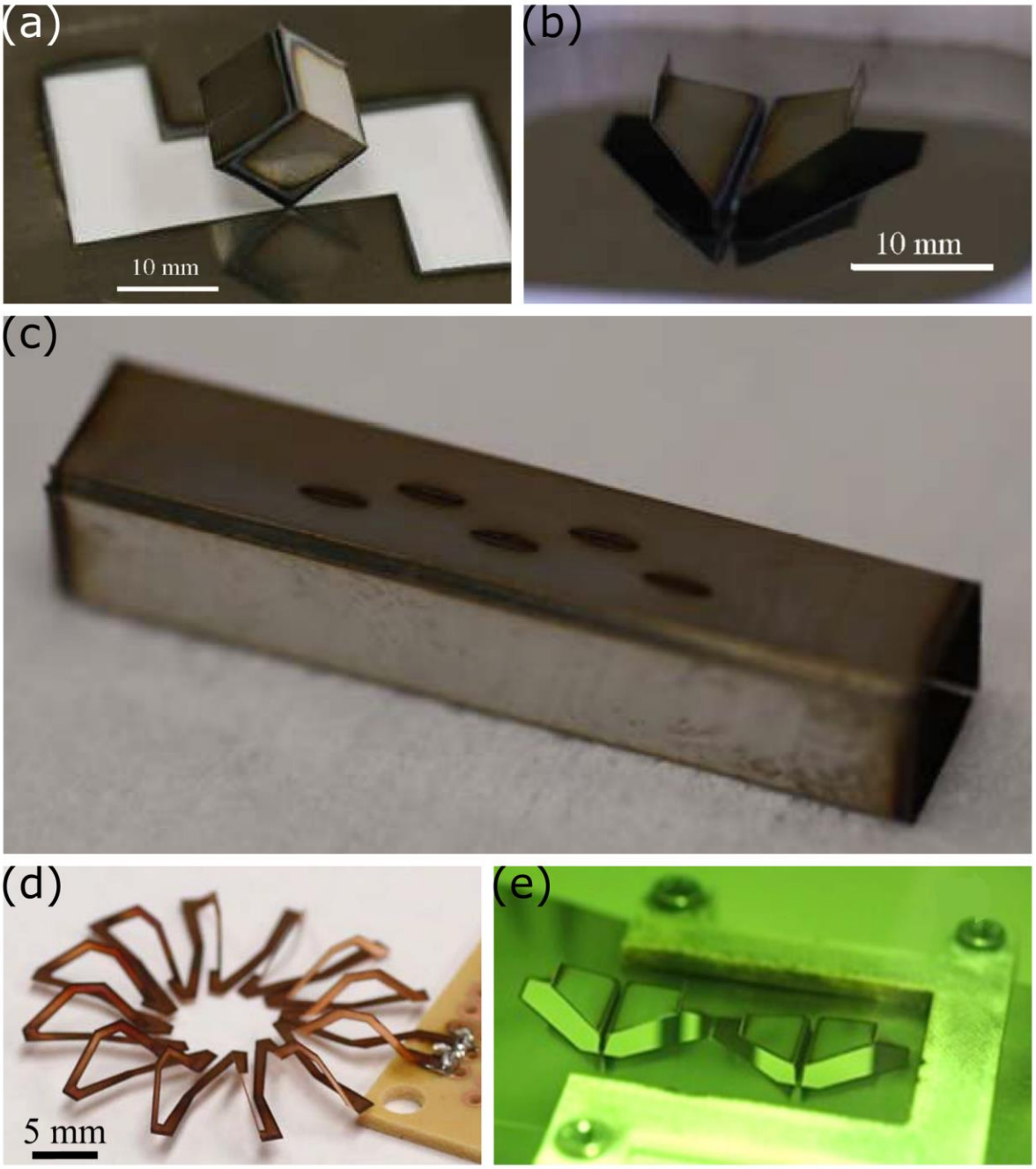

Figure 2.10. Laser forming can be used to produce complex and functional structures without the need for mechanical input. 3D structures that were cut and laser formed from nickel foil using a 20W Nd:YAG laser include (a) cubes and (b) airplanes.[59] (a,b) Reprinted with permission from John Wiley and Sons, copyright 2013. Laser forming can be used to produce functional structures as well such as (c) slotted waveguide for antennas from stainless steel[152] and even (d) toroidal inductors from copper.[88] (c) Reprinted with permission from IEEE, copyright 2018. (d) Reprinted with permission from IEEE, copyright 2018. New metal sheets are required between samples, but (e) continuous laser forming can be realized by combining it with roll-to-roll processing.[63]. Reprinted with permission from Springer Nature, copyright 2018.

Working to automate the entire laser forming process, our group developed a roll-to-roll laser forming system with the metal feedstock passing through the focal plane of the laser.[63] This set up allowed features to be readily cut and folded from the sheet metal using the TGM. Additionally, the metal sheet had a pre-strain from being wound onto a roll that was used to reliably generate downward bending using the buckling mechanism, producing the same complex shapes from our previous work in an automated process (**Figure 2.10e**). Once the piece was formed, it was released from the sheet and fell down a chute before the rolls were spun to introduce a new working area. This was the first demonstration of a fully automated laser forming process to produce complex 3D structures. While impressive, producing these structures relied on our previously designed scan paths and laser settings. For many of the structures, we relied on the self-limiting nature of ninety-degree bends so that precise control over the laser settings was not needed. Accurately determining the laser power, speed, and number of passes would be required if the desired structures included intermediate bends.

Figuring out what scan path and what lasing setting are needed to produce a desired structure is known as the inverse design problem and has been intensively studied.[53,66,99,147–149] Part of the difficulty of designing laser scan strategies is the highly-coupled and nonlinear thermo-mechanical nature of laser forming so many of the previously proposed strategies are limited in the number of scan lines[66,99,149] or are computationally intensive, relying on full finite-element models.[147,148] Recently, researchers introduced an algorithm that takes a desired 3D structure as an input and simultaneously unfolds the structure into a planar net and plans the cutting and bending paths for this net.[62] For normal origami, the planar net and the bending path can be solved for separately because the craftsmen is able to access all needed fold lines at any

given time.[6] As current laser forming setups rely on an unobstructed optical path between the laser and the fold line, this visibility constraint effectively couples the two problems.

Over the years, laser forming has emerged as a viable rapid prototyping strategy that is complementary to metal 3D printing. Understanding of the sub-mechanisms has allowed researchers to develop scan strategies for many 3D shapes, but the complex thermomechanical process makes it near mandatory to automate this process. This need becomes most pronounced when more complex 3D structures and devices are being laser formed, especially ones that require multiple forming mechanisms. Solutions to this inverse design problem are rapidly developing and will hopefully make laser forming as accessible as 3D printing.

2.4 Conclusion and Outlook

Laser forming has developed dramatically over the past forty years, from a mechanistic understanding of the process to the successful laser origami of complex 3D shapes and the algorithms to design their laser scan patterns. As the field matures and laser forming is adopted as a viable rapid prototyping strategy, new research opportunities abound. Like any other prototyping technology, laser forming is valuable for certain structures, while not being preferable for others. Deciding if laser forming is the preferred fabrication methods requires design heuristics that have yet to be clarified. Continued research efforts should be focused on clarifying these heuristics while expanding the capabilities of the laser forming by developing it as a robust technology that is able to reliably produce functional, near-arbitrary 3D structures from flat substrates in an automated manufacturing environment. To this end, researchers will need to address current gaps in the understanding of the laser forming process, which will inform the design and control algorithms.

Laser forming involves rapid heating and cooling cycles that can cause changes in the microstructure of the metal during the process. Microstructural control is very important for titanium pieces in the aerospace industry as the mechanical properties and fatigue resistance of titanium and its alloys is highly dependent on having precise control over the grains. Preliminary reports suggest that laser forming leads to unfavorable grain structures in titanium.[27,95,156] Other industries and applications might not have as stringent requirements on the grain structure, but these reports suggest there may be some degradation in the mechanical properties of laser formed parts compared to mechanically bent structures, an area that needs further investigation.

The microstructure of a material influences more than mechanical properties and so these other properties need to be considered when deciding to laser form an object. Of particular concern to the shipbuilding industry might be corrosion resistance to the salty ocean water. The corrosion resistance of some laser formed metals has been briefly investigated[96,115,157,158] with many metals demonstrating a reduced corrosion resistance resulting from the disturbed microstructure. Interestingly, some alloys showed an increased corrosion resistance after being laser formed[158] though the role of the lasing parameters on this phenomenon was underexplored. There is a need to study systematically the suitability of a laser formed material for use in a corrosive environment as a function of the material's properties, the nature of the corrosive species, and the laser forming parameters. Applications could include ship hulls in salt water, or a laser bent tube in a chemical processing plant.

For laser forming to move from academic research to an industrial process, stronger control schemes and predictive modelling need to be developed. The state-of-the-art algorithms either develop the optimal laser settings for relatively simple shapes based on finite element modelling, or they use experimental data to develop a laser scan path to produce near-arbitrary

3D shapes. The next step would be to develop an algorithm that combines these methods to develop a scan path for near-arbitrary shapes and the optimal laser settings to produce this shape as some regions might only need bending while others require shortening. Combining these algorithms would enable additional constraints to be designed around as the laser-substrate interaction does more than just bend the workpiece.

Most laser forming setups are run in a batch process with one sheet being bent at a time. A recent report demonstrated a way to transform lase forming into a continuous roll-to-roll process by combining laser cutting and bending. [63] Lasers are used to do much more, such as welding,[120,159] marking,[160,161] laser-induced chemistry,[162–164] and are even used in analytical techniques.[165,166] Taken together, one could imagine a fully automated process wherein blank sheet metal is fed, then different lasers will cut, mark, chemically pattern, and then fold it into a desired 3D structure with inline quality control. Developing such a system will require developing further control schemes to know when and where to bend the structure in this complex process to yield the desired result.

Laser forming is a valuable technology that is poised to address two notable shortcomings of metal 3D printing—large structures and thin structures. Fully realizing this potential will require developing a detailed understanding of how the laser forming process impacts material properties to produce advanced planning and control schemes. With a completely automated process, laser forming will be available to make the rapid prototyping of metallic structures even lighter.

2.5 Acknowledgements

We gratefully acknowledge the financial sponsorship from the Army Research Laboratory and research was accomplished under Cooperative Agreement Number W911NF-20-

2-0243. The views and conclusions contained in this document are those of the authors and should not be interpreted as representing the official policies, either expressed or implied, of the Army Research Laboratory or the U.S. Government. The U.S. Government is authorized to reproduce and distribute reprints for Government purposes notwithstanding any copyright notation herein.

2.6 References

1. Turner, N.; Goodwine, B.; Sen, M. A review of origami applications in mechanical engineering. *Proceedings of the Institution of Mechanical Engineers, Part C: Journal of Mechanical Engineering Science* **2016**, *230*, 2345–2362, doi:10.1177/0954406215597713.

2. Hernandez, E.A.P.; Hartl, D.J.; Lagoudas, D.C. Introduction to Active Origami Structures. In *Active Origami*; Springer, Cham, 2019; pp. 1–53 ISBN 978-3-319-91865-5.

3. Felton, S.; Tolley, M.; Demain, E.; Rus, D.; Wood, R. A method for building self-folding machines. *Science* **2014**, *345*, 644–646.

4. Taylor, A.; Miller, M.; Fok, M.; Nilsson, K.; Tsz Ho Tse, Z. Intracardiac Magnetic Resonance Imaging Catheter With Origami Deployable Mechanisms1. *Journal of Medical Devices* **2016**, *10*, 020957, doi:10.1115/1.4033151.

5. Takano, T.; Miura, K.; Natori, M.; Hanayama, E.; Inoue, T.; Noguchi, T.; Miyahara, N.; Nakaguro, H. Deployable antenna with 10-m maximum diameter for space use. *IEEE Transactions on Antennas and Propagation* **2004**, *52*, 2–11, doi:10.1109/TAP.2003.820968.

6. Tachi, T. Origamizing Polyhedral Surfaces. *IEEE Transactions on Visualization and Computer Graphics* **2010**, *16*, 298–311, doi:10.1109/TVCG.2009.67.

7. Zirbel, S.A.; Lang, R.J.; Thomson, M.W.; Sigel, D.A.; Walkemeyer, P.E.; Trease, B.P.; Magleby, S.P.; Howell, L.L. Accommodating Thickness in Origami-Based Deployable Arrays. *J. Mech. Des* **2013**, *135*, doi:10.1115/1.4025372.

8. Lang, R.J.; Tolman, K.A.; Crampton, E.B.; Magleby, S.P.; Howell, L.L. A Review of Thickness-Accommodation Techniques in Origami-Inspired Engineering. *Applied Mechanics Reviews* **2018**, *70*, 010805, doi:10.1115/1.4039314.

9. Tachi, T.; Hull, T.C. Self-Foldability of Rigid Origami. *J. Mechanisms Robotics* **2017**, *9*, doi:10.1115/1.4035558.

10. Lang, R.J.; Howell, L. Rigidly Foldable Quadrilateral Meshes From Angle Arrays. *Journal of Mechanisms and Robotics* **2018**, *10*, 021004, doi:10.1115/1.4038972.

11. Zirbel, S.A.; Trease, B.P.; Magleby, S.P.; Howell, L.L. Deployment Methods for an Origami-Inspired Rigid-Foldable Array. 6.

12. Morgan, J.; Magleby, S.P.; Howell, L.L. An Approach to Designing Origami-Adapted Aerospace Mechanisms. *J. Mech. Des* **2016**, *138*, doi:10.1115/1.4032973.

13. Whitney, J.P.; Sreetharan, P.S.; Ma, K.Y.; Wood, R.J. Pop-up book MEMS. *J. Micromech. Microeng.* **2011**, *21*, 115021, doi:10.1088/0960-1317/21/11/115021.

14. Ahmed, S.; McGough, K.; Ounaies, Z.; Frecker, M. Origami-Inspired Folding and Unfolding of Structures: Fundamental Investigations of Dielectric Elastomer-Based Active Materials. In Proceedings of the ASME Proceedings; 2013; p. V001T01A029/1-6.

15.Hayes, G.J.; Liu, Y.; Genzer, J.; Lazzi, G.; Dickey, M.D. Self-Folding Origami Microstrip Antennas. *IEEE Transactions on Antennas and Propagation* **2014**, *62*, 5416–5419, doi:10.1109/TAP.2014.2346188.

16. Tolley, M.T.; Felton, S.M.; Miyashita, S.; Aukes, D.; Rus, D.; Wood, R.J. Self-folding origami: shape memory composites activated by uniform heating. *Smart Mater. Struct.* **2014**, *23*, 094006/1–9, doi:10.1088/0964-1726/23/9/094006.

17. Wang, D.H.; Tan, L.-S. Origami-Inspired Fabrication: Self-Folding or Self-Unfolding of Cross-Linked-Polyimide Objects in Extremely Hot Ambience. *ACS Macro Lett.* **2019**, *8*, 546–552, doi:10.1021/acsmacrolett.9b00198.

18. Upcraft, S.; Fletcher, R. The rapid prototyping technologies. *Assembly Automation* **2003**, *23*, 318–330, doi:10.1108/01445150310698634.

19. Ligon, S.C.; Liska, R.; Stampfl, J.; Gurr, M.; Mülhaupt, R. Polymers for 3D Printing and Customized Additive Manufacturing. *Chem. Rev.* **2017**, *117*, 10212–10290, doi:10.1021/acs.chemrev.7b00074.

20. Das, S.; Bourell, D.L.; Babu, S.S. Metallic materials for 3D printing. *MRS Bulletin* **2016**, *41*, 729–741, doi:10.1557/mrs.2016.217.

21. Bak, D. Rapid prototyping or rapid production? 3D printing processes move industry towards the latter. *Assem. Autom.* **2003**, *23*, 340–345, doi:10.1108/01445150310501190.

22. Agarwala, M.; Bourell, D.; Beaman, J.; Marcus, H.; Barlow, J. Direct selective laser sintering of metals. *Rapid Prototyping Journal* **1995**, *1*, 26–36, doi:10.1108/13552549510078113.

23. Duda, T.; Raghavan, L.V. 3D Metal Printing Technology. *IFAC-PapersOnLine* **2016**, *49*, 103–110, doi:10.1016/j.ifacol.2016.11.111.

24. Panchagnula, J.S.; Simhambhatla, S. Manufacture of complex thin-walled metallic objects using weld-deposition based additive manufacturing. *Robotics and Computer-Integrated Manufacturing* **2018**, *49*, 194–203, doi:10.1016/j.rcim.2017.06.003.

25. Hu, J.; Marciniak, Z.; Duncan, J. *Mechanics of Sheet Metal Forming*; Elsevier, 2002; ISBN 978-0-08-049651-1.

26. Qattawi, A.; Abdelhamid, M.; Mayyas, A.; Omar, M. Design Analysis for Origami-Based Folded Sheet Metal Parts. *SAE Int. J. Mater. Manf.* **2014**, *7*, 488–498, doi:10.4271/2014-01-9098.

27. Walczyk, D.F.; Vittal, S. Bending of Titanium Sheet Using Laser Forming. *Journal of Manufacturing Processes* **2000**, *2*, 258–269, doi:10.1016/S1526-6125(00)70027-2.

28. Cleveland, R.M.; Ghosh, A.K. Inelastic effects on springback in metals. *International Journal of Plasticity* **2002**, *18*, 769–785, doi:10.1016/S0749-6419(01)00054-7.

29. Tseng, A.A.; Jen, K.P.; Chen, T.C.; Kondetimmamhalli, R.; Murty, Y.V. Forming properties and springback evaluation of copper beryllium sheets. *MMTA* **1995**, *26*, 2111–2121, doi:10.1007/BF02670682.

30. Wagoner, R.H.; Lim, H.; Lee, M.-G. Advanced Issues in springback. *International Journal of Plasticity* **2013**, *45*, 3–20, doi:10.1016/j.ijplas.2012.08.006.

31. Abvabi, A.; Rolfe, B.; Hodgson, P.D.; Weiss, M. The influence of residual stress on a roll forming process. *International Journal of Mechanical Sciences* **2015**, *101–102*, 124–136, doi:10.1016/j.ijmecsci.2015.08.004.

32. Martin, J.H.; Yahata, B.D.; Hundley, J.M.; Mayer, J.A.; Schaedler, T.A.; Pollock, T.M. 3D printing of high-strength aluminium alloys. *Nature* **2017**, *549*, 365–369, doi:10.1038/nature23894.

33. Thomson, G.; Pridham, M.S. Controlled laser forming for rapid prototyping. *Rapid Prototyping Journal* **1997**, *3*, 137–143, doi:10.1108/13552549710191845.

34. Bisgaard Clausen, H.; Technical University of Denmark; Department of Naval Architecture and Offshore Engineering; DTU Plate forming by line heating., Lyngby, 2000.

35. Scully, Kevin Laser Line Heating. *Journal of Ship Production* **1987**, *3*, 237–246.

36. Magee, J.; Watkins, K.G.; Steen, W.M. Advances in laser forming. *Journal of Laser Applications* **1998**, *10*, 235–246, doi:10.2351/1.521859.

37. Geiger, M.; Vollertsen, F. The Mechanisms of Laser Forming. *CIRP Annals* **1993**, *42*, 301–304, doi:10.1016/S0007-8506(07)62448-2.

38. Shen, H.; Vollertsen, F. Modelling of laser forming – An review. *Computational Materials Science* **2009**, *46*, 834–840, doi:10.1016/j.commatsci.2009.04.022.

39. Cheng, P.; Fan, Y.; Zhang, J.; Yao, Y.L.; Mika, D.P.; Zhang, W.; Graham, M.; Marte, J.; Jones, M. Laser Forming of Varying Thickness Plate—Part I: Process Analysis. *J. Manuf. Sci. Eng* **2006**, *128*, 634–641, doi:10.1115/1.2172280.

40. Li, W.; Yao, Y.L. Laser Bending of Tubes: Mechanism, Analysis, and Prediction. *J. Manuf. Sci. Eng* **2001**, *123*, 674–681, doi:10.1115/1.1392992.

41. Tam, A.C.; Poon, C.C.; Crawforth, L. Laser Bending of Ceramics and Application to Manufacture Magnetic Head Sliders in Disk Drives. *Analytical Sciences/Supplements* **2002**, *17icpp*, s419–s421, doi:10.14891/analscisp.17icpp.0.s419.0.

42. Folkersma, G.; Römer, G.-W.; Brouwer, D.; Veld, B.H. in 't In-plane laser forming for high precision alignment. *OE* **2014**, *53*, 126105, doi:10.1117/1.OE.53.12.126105.

43. Hu, Y.; Xu, X.; Yao, Z.; Hu, J. Laser peen forming induced two way bending of thin sheet metals and its mechanisms. *Journal of Applied Physics* **2010**, *108*, 073117, doi:10.1063/1.3486218.

44. Yocom, C.J.; Zhang, X.; Liao, Y. Research and development status of laser peen forming: A review. *Optics & Laser Technology* **2018**, *108*, 32–45, doi:10.1016/j.optlastec.2018.06.032.

45. Arcella, F.G.; Froes, F.H. Producing titanium aerospace components from powder using laser forming. *JOM* **2000**, *52*, 28–30, doi:10.1007/s11837-000-0028-x.

46. Laeng, J.; Stewart, J.G.; Liou, F.W. Laser metal forming processes for rapid prototyping - A review. *International Journal of Production Research* **2000**, *38*, 3973–3996, doi:10.1080/00207540050176111.

47. Kant, R.; Joshi, S.N.; Dixit, U.S. 4 - Research issues in the laser sheet bending process. In *Materials Forming and Machining*; Davim, J.P., Ed.; Woodhead Publishing Reviews: Mechanical Engineering Series; Woodhead Publishing, 2016; pp. 73–97 ISBN 978-0-85709-483-4.

48. Omidvar, M.; Fard, R.K.; Sohrabpoor, H.; Teimouri, R. Selection of laser bending process parameters for maximal deformation angle through neural network and teaching–learning-based optimization algorithm. *Soft Comput* **2015**, *19*, 609–620, doi:10.1007/s00500-014-1282-0.

49. Lambiase, F. An Analytical Model for Evaluation of Bending Angle in Laser Forming of Metal Sheets. *J. of Materi Eng and Perform* **2012**, *21*, 2044–2052, doi:10.1007/s11665-012-0163-x.

50. Dearden, G.; Edwardson, S.P. Some recent developments in two-and three-dimensional laser forming for macro and micro applications. *Journal of Optics A: Pure and Applied Optics* **2003**, *5*, S8–S15, doi:10.1088/1464-4258/5/4/352.

51. Shi, Y.; Yao, Z.; Shen, H.; Hu, J. Research on the mechanisms of laser forming for the metal plate. *International Journal of Machine Tools and Manufacture* **2006**, *46*, 1689–1697, doi:10.1016/j.ijmachtools.2005.09.016.

52. Arnet, H.; Vollertsen, F. Extending Laser Bending for the Generation of Convex Shapes. *Proceedings of the Institution of Mechanical Engineers, Part B: Journal of Engineering Manufacture* **1995**, *209*, 433–442, doi:10.1243/PIME_PROC_1995_209_107_02.

53. Liu, C.; Yao, Y.L.; Srinivasan, V. Optimal Process Planning for Laser Forming of Doubly Curved Shapes. *J. Manuf. Sci. Eng* **2004**, *126*, 1–9, doi:10.1115/1.1643077.

54. S.P. Edwardson; G. Dearden Laser Assisted Forming for Ship Building. 14.

55. Steen, W.M.; Mazumder, J. Laser Bending or Forming. In *Laser Material Processing*; Steen, W.M., Mazumder, J., Eds.; Springer: London, 2010; pp. 389–416 ISBN 978-1-84996-062-5.

56. Che Jamil, M.S.; Sheikh, M.A.; Li, L. A study of the effect of laser beam geometries on laser bending of sheet metal by buckling mechanism. *Optics & Laser Technology* **2011**, *43*, 183–193, doi:10.1016/j.optlastec.2010.06.011.

57. Vollertsen, F.; Komel, I.; Kals, R. The laser bending of steel foils for microparts by the buckling mechanism-a model. *Modelling and Simulation in Materials Science and Engineering* **1995**, *3*, 107–119, doi:10.1088/0965-0393/3/1/009.

58. Experimental and numerical modeling of buckling instability of laser sheet forming. *International Journal of Machine Tools and Manufacture* **2002**, *42*, 1427–1439, doi:10.1016/S0890-6955(02)00075-5.

59. Lazarus, N.; Smith, G.L. Laser Forming for Complex 3D Folding. *Advanced Materials Technologies* **2017**, *2*, 1700109, doi:10.1002/admt.201700109.

60. Shi, Y.; Liu, Y.; Yao, Z.; Shen, H. A study on bending direction of sheet metal in laser forming. *Journal of Applied Physics* **2008**, *103*, 053101, doi:10.1063/1.2887995.

61. Li, W.; Yao, Y.L. Buckling based laser forming process: Concave or convex. *ICALEO* **2000**, *2000*, D220–D229, doi:10.2351/1.5059467.

62. Hao, Y.; Lien, J.-M. Computational laser forming origami of convex surfaces. In Proceedings of the Proceedings of the ACM Symposium on Computational Fabrication - SCF '19; ACM Press: Pittsburgh, Pennsylvania, 2019; pp. 1–11.

63. Lazarus, N.; Smith, G.L. Laser Folding in a Roll-to-Roll Manufacturing Process. *Lasers in Manufacturing and Materials Processing* **2018**, *5*, 237–247, doi:10.1007/s40516-018-0064-4.

64. Shen, H. Mechanism of laser micro-adjustment. *J. Phys. D: Appl. Phys.* **2008**, *41*, 245106, doi:10.1088/0022-3727/41/24/245106.

65. Lawrence, S. Developable Surfaces: Their History and Application. *Nexus Netw J* **2011**, *13*, 701–714, doi:10.1007/s00004-011-0087-z.

66. Maji, K.; Pratihar, D.K.; Nath, A.K. Forward and inverse predictions of deformations in laser forming of shaped surfaces under coupling mechanism. *Journal of Laser Applications* **2018**, *30*, 032011, doi:10.2351/1.5033450.

67. Chen, G.; Xu, X. Experimental and 3D Finite Element Studies of CW Laser Forming of Thin Stainless Steel Sheets. *Journal of Manufacturing Science and Engineering* **2000**, *123*, 66–73, doi:10.1115/1.1347036.

68. Vásquez-Ojeda, C.; Ramos-Grez, J. Bending of stainless steel thin sheets by a raster scanned low power CO2 laser. *Journal of Materials Processing Technology* **2009**, *209*, 2641–2647, doi:10.1016/j.jmatprotec.2008.06.026.

69. Paunoiu, V.; Squeo, E.A.; Quadrini, F.; Gheorghies, C.; Nicoara, D. Laser Bending of Stainless Steel Sheet Metals. *Int J Mater Form* **2008**, *1*, 1371–1374, doi:10.1007/s12289-008-0119-8.

70. Zaeh, M.F.; Hornfeck, T. Development of a robust laser beam bending process for aluminum fuselage structures. *Prod. Eng. Res. Devel.* **2008**, *2*, 149–155, doi:10.1007/s11740-008-0100-x.

71. Geiger, M.; Merklein, M.; Pitz, M. Laser and forming technology—an idea and the way of implementation. *Journal of Materials Processing Technology* **2004**, *151*, 3–11, doi:10.1016/j.jmatprotec.2004.04.004.

72. Lubiano, G.; Ramos, J.A.; Magee, J. Laser Bending of Thin Metal Sheets by Means of a Low Power CO2 Laser. 12.

73. Magee, J.; Watkins, K.G.; Steen, W.M.; Calder, N.J.; Sidhu, J.; Kirby, J. Laser forming of aerospace alloys. *ICALEO* **1997**, *1997*, E156–E165, doi:10.2351/1.5059678.

74. Kitada, K.; Asahi, N. Laser adjustment of beryllium copper sheet using temperature gradient mechanism. In Proceedings of the Third International Symposium on Laser Precision Microfabrication; International Society for Optics and Photonics, 2003; Vol. 4830, pp. 30–35.

75. Jiang, S.Q.; Liu, A.H.; Wang, X.X.; Chen, Z. The Bending Forming Mechanism of Copper Alloy by Different Lasers. *AMR* **2014**, *968*, 142–145, doi:10.4028/www.scientific.net/AMR.968.142.

76. Gärtner, E.; Frühauf, J.; Löschner, U.; Exner, H. Laser bending of etched silicon microstructures. *Microsystem Technologies* **2001**, *7*, 23–26, doi:10.1007/s005420000065.

77. Xu, W.; Zhang, L.C.; Wang, X. Laser Bending of Silicon Sheet: Absorption Factor and Mechanisms. *J. Manuf. Sci. Eng* **2013**, *135*, doi:10.1115/1.4025579.

78. Wu, D.-J.; Ma, G.-Y.; Liu, S.; Wang, X.-Y.; Guo, D.-M. Experiments and simulation on laser bending of silicon sheet with different thicknesses. *Appl. Phys. A* **2010**, *101*, 517–521, doi:10.1007/s00339-010-5889-4.

79. Wu, D.; Zhang, Q.; Ma, G.; Guo, Y.; Guo, D. Laser bending of brittle materials. *Optics and Lasers in Engineering* **2010**, *48*, 405–410, doi:10.1016/j.optlaseng.2009.09.009.

80. Wu, D.; Ma, G.; Niu, F.; Guo, D. Temperature Gradient Mechanism on Laser Bending of Borosilicate Glass Sheet. *J. Manuf. Sci. Eng* **2010**, *132*, doi:10.1115/1.4000722.

81. Bucher, T.; Cardenas, S.; Verma, R.; Li, W.; Lawrence Yao, Y. Laser Forming of Sandwich Panels With Metal Foam Cores. *Journal of Manufacturing Science and Engineering* **2018**, *140*, 111015, doi:10.1115/1.4040959.

82. Guglielmotti, A.; Quadrini, F.; Squeo, E.A.; Tagliaferri, V. Laser Bending of Aluminum Foam Sandwich Panels. *Advanced Engineering Materials* **2009**, *11*, 902–906, doi:10.1002/adem.200900111.

83. Gisario, A.; Barletta, M. Laser forming of glass laminate aluminium reinforced epoxy (GLARE): On the role of mechanical, physical and chemical interactions in the multi-layers material. *Optics and Lasers in Engineering* **2018**, *110*, 364–376, doi:10.1016/j.optlaseng.2018.06.013.

84. Seong, W.-J.; Jeon, Y.-C.; Na, S.-J. Ship-hull plate forming of saddle shape by geometrical approach. *Journal of Materials Processing Technology* **2013**, *213*, 1885–1893, doi:10.1016/j.jmatprotec.2013.04.017.

85. Okamoto Y.; Uno Y.; Ohta K.; Shibata T.; Kubota S.; Namba Y. Study on Precision Laser Forming of Plastic with YAG Laser. *Journal of the Japan Society for Precision Engineering* **2000**, *66*, 891–895, doi:10.2493/jjspe.66.891.

86. Okamoto, Y.; Miyamoto, I.; Uno, Y.; Takenaka, T. Deformation characteristics of plastics in YAG laser forming. In Proceedings of the Fifth International Symposium on Laser Precision Microfabrication; International Society for Optics and Photonics, 2004; Vol. 5662, pp. 576–581.

87. Cheng, P.; Fan, Y.; Zhang, J.; Yao, Y.L.; Mika, D.P.; Zhang, W.; Graham, M.; Marte, J.; Jones, M. Laser Forming of Varying Thickness Plate—Part II: Process Synthesis. *J. Manuf. Sci. Eng* **2006**, *128*, 642–650, doi:10.1115/1.2162912.

88. Lazarus, N.; Bedair, S.S.; Smith, G.L. Origami Inductors: Rapid Folding of 3-D Coils on a Laser Cutter. *IEEE Electron Device Letters* **2018**, *39*, 1046–1049, doi:10.1109/LED.2018.2841638.

89. Gautam, S.S.; Singh, S.K.; Dixit, U.S. Laser Forming of Mild Steel Sheets Using Different Surface Coatings. In *Lasers Based Manufacturing: 5th International and 26th All India Manufacturing Technology, Design and Research Conference, AIMTDR 2014*; Joshi, S.N., Dixit, U.S., Eds.; Topics in Mining, Metallurgy and Materials Engineering; Springer India: New Delhi, 2015; pp. 17–39 ISBN 978-81-322-2352-8.

90. Axelevitch, A.; Gorenstein, B.; Golan, G. Investigation of Optical Transmission in Thin Metal Films. *Physics Procedia* **2012**, *32*, 1–13, doi:10.1016/j.phpro.2012.03.510.

91. *CRC Handbook of Chemistry and Physics*; Rumble, J., Ed.; 101st edition.; CRC Press: Boca Raton, FL, USA, 2020; ISBN 978-0-367-41724-6.

92. Shidid, D.P.; Gollo, M.H.; Brandt, M.; Mahdavian, M. Study of effect of process parameters on titanium sheet metal bending using Nd: YAG laser. *Optics & Laser Technology* **2013**, *47*, 242–247, doi:10.1016/j.optlastec.2012.07.033.

93. Yau, C.L.; Chan, K.C.; Lee, W.B. Laser bending of leadframe materials. *Journal of Materials Processing Technology* **1998**, *82*, 117–121, doi:10.1016/S0924-0136(98)00012-0.

94. Hennige, T.; Holzer, S.; Vollertsen, F.; Geiger, M. On the working accuracy of laser bending. *Journal of Materials Processing Technology* **1997**, *71*, 422–432, doi:10.1016/S0924-0136(97)00108-8.

95. Fidder, H.; Ocelík, V.; Botes, A.; De Hosson, J.T.M. Response of Ti microstructure in mechanical and laser forming processes. *J Mater Sci* **2018**, *53*, 14713–14728, doi:10.1007/s10853-018-2650-4.

96. Walczak, M.; Ramos-Grez, J.; Celentano, D.; Lima, E.B.F. Sensitization of AISI 302 stainless steel during low-power laser forming. *Optics and Lasers in Engineering* **2010**, *48*, 906–914, doi:10.1016/j.optlaseng.2010.03.014.

97. Patel, C.K.N. Continuous-Wave Laser Action on Vibrational-Rotational Transitions of C${\mathrm{O}}_{2}$. *Phys. Rev.* **1964**, *136*, A1187–A1193, doi:10.1103/PhysRev.136.A1187.

98. Lawrence, J. A comparative investigation of the efficacy of CO_2 and high-power diode lasers for the forming of EN3 mild steel sheets. *Proceedings of the Institution of Mechanical Engineers, Part B: Journal of Engineering Manufacture* **2002**, *216*, 1481–1491, doi:10.1243/095440502320783521.

99. Kim, J.; Na, S.J. Development of irradiation strategies for free curve laser forming. *Optics & Laser Technology* **2003**, *35*, 605–611, doi:10.1016/S0030-3992(03)00088-4.

100. Silve, S.; Podschies, B.; Steen, W.M.; Watkins, K.G. Laser Forming - A New Vocabulary for Objects. In Proceedings of the ICALEO 1999; San Diego, UNITED STATES, 1999; Vol. F, pp. 87–96.

101. Shi, Y.; Shen, H.; Yao, Z.; Hu, J. Temperature gradient mechanism in laser forming of thin plates. *Optics & Laser Technology* **2007**, *39*, 858–863, doi:10.1016/j.optlastec.2005.12.006.

102. Magee, J.; Sidhu, J.; Cooke, R.L. A Prototype laser forming system. *Optics and Lasers in Engineering* **2000**, *34*, 339–353, doi:10.1016/S0143-8166(00)00069-5.

103. Namba, Y. Laser Forming in Space. In Proceedings of the Proceedings of the International Conference on Lasers ’85; Las Vegas, NV, 1985; pp. 403–407.

104. Liu, J.; Sun, S.; Guan, Y.; Ji, Z. Experimental study on negative laser bending process of steel foils. *Optics and Lasers in Engineering* **2010**, *48*, 83–88, doi:10.1016/j.optlaseng.2009.07.019.

105. Yoshioka, S.; Miyazaki, T.; Misu, T.; Oba, R.; Saito, M. Laser forming of thin foil by a newly developed sample holding method. *J. Laser Appl.* **2003**, *15*, 6.

106. Shen, H.; Peng, L.; Hu, J.; Yao, Z. Study on the mechanical behavior of laser micro-adjustment of two-bridge actuators. *J. Micromech. Microeng.* **2010**, *20*, 115010, doi:10.1088/0960-1317/20/11/115010.

107. Tetzel, H.; Grden, M.; Vollertsen, F. Stress analysis based on strain measurement in sheet metal laser bending. *Prod. Eng. Res. Devel.* **2013**, *7*, 647–655, doi:10.1007/s11740-013-0488-9.

108. Cheng, J.; Yao, Y.L. Cooling effects in multiscan laser forming. *Journal of Manufacturing Processes; Dearborn* **2001**, *3*, 60–72.

109. Lambiase, F.; Di Ilio, A.; Paoletti, A. An experimental investigation on passive water cooling in laser forming process. *Int J Adv Manuf Technol* **2013**, *64*, 829–840, doi:10.1007/s00170-012-4072-9.

110. Seyedkashi, S.M.H.; Cho, J.R.; Lee, S.H.; Moon, Y.H. Feasibility of underwater laser forming of laminated metal composites. *Materials & Manufacturing Processes* **2018**, *33*, 546–551, doi:10.1080/10426914.2017.1376075.

111. Shen, H.; Ran, M.; Hu, J.; Yao, Z. An experimental investigation of underwater pulsed laser forming. *Optics and Lasers in Engineering* **2014**, *62*, 1–8, doi:10.1016/j.optlaseng.2014.04.011.

112. Paramasivan, K.; Das, S.; Marimuthu, S.; Misra, D. Increment in laser bending angle by forced bottom cooling. *Int J Adv Manuf Technol* **2018**, *94*, 2137–2147, doi:10.1007/s00170-017-1035-1.

113. Shen, H.; Hu, J.; Yao, Z.Q. Cooling Effects in Laser Forming. *MSF* **2010**, *663–665*, 58–63, doi:10.4028/www.scientific.net/MSF.663-665.58.

114. Lambiase, F.; Di Ilio, A.; Paoletti, A. Productivity in multi-pass laser forming of thin AISI 304 stainless steel sheets. *Int J Adv Manuf Technol* **2016**, *86*, 259–268, doi:10.1007/s00170-015-8150-7.

115. Chinizadeh, M.; Kiahosseini, S.R. Deformation, microstructure, hardness, and pitting corrosion of 316 stainless steel after laser forming: A comparison between natural and forced cooling. *Journal of Materials Research* **2017**, *32*, 3046–3054, doi:10.1557/jmr.2017.146.

116. Arora, H.; Singh, R.; Brar, G.S. Thermal and structural modelling of arc welding processes: A literature review. *Measurement and Control* **2019**, *52*, 955–969, doi:10.1177/0020294019857747.

117. Geiger, M.; Vollertsen, F.; Deinzer, G. Flexible Straightening of Car Body Shells by Laser Forming.; 1993; p. 930279.

118. Dearden, G.; Edwardson, S.P.; Abed, E.; Watkins, K.G. Laser forming for the correction of distortion and design shape in aluminium structures. 6.

119. Gurova, T.; Estefen, S.F.; Leontiev, A.; de Oliveira, F. a. L. Welding residual stresses: a daily history. *Science & Technology of Welding & Joining* **2015**, *20*, 616–621, doi:10.1179/1362171815Y.0000000047.

120. Stavridis, J.; Papacharalampopoulos, A.; Stavropoulos, P. Quality assessment in laser welding: a critical review. *Int J Adv Manuf Technol* **2018**, *94*, 1825–1847, doi:10.1007/s00170-017-0461-4.

121. Shi, Y.J.; Chen, J.; Qi, Y.G.; Yao, Z.Q. Processing strategy for laser forming of complicated singly curved shapes. *Materials Science and Technology* **2009**, *25*, 925–930, doi:10.1179/174328408X365847.

122. Mehrpouya, M.; Huang, H.; Venettacci, S.; Gisario, A. LaserOrigami (LO) of three-dimensional (3D) components: Experimental analysis and numerical modeling-part II. *Journal of Manufacturing Processes* **2019**, *39*, doi:10.1016/j.jmapro.2019.02.026.

123. Castle, T.; Cho, Y.; Gong, X.; Jung, E.; Sussman, D.M.; Yang, S.; Kamien, R.D. Making the Cut: Lattice Kirigami Rules. *Phys. Rev. Lett.* **2014**, *113*, 245502, doi:10.1103/PhysRevLett.113.245502.

124. Cheng, J.; Yao, Y.L. Process Design of Laser Forming for Three-Dimensional Thin Plates. *Journal of Manufacturing Science and Engineering* **2004**, *126*, 217–225, doi:10.1115/1.1751187.

125. Ibraheem Imhan, K.; Btht, B.; Zakaria, A.; Shah B Ismail, M.I.; Hadi Alsabti, N.M.; Ahmad, A.K. Features of Laser Tube Bending processing based on Laser Forming: A Review. *J Laser Opt Photonics* **2018**, *05*, doi:10.4172/2469-410X.1000174.

126. Wang, X.Y.; Wang, J.; Xu, W.J.; Guo, D.M. Scanning path planning for laser bending of straight tube into curve tube. *Optics & Laser Technology* **2014**, *56*, 43–51, doi:10.1016/j.optlastec.2013.07.001.

127. Guglielmotti, A.; Quadrini, F.; Squeo, E.A.; Tagliaferri, V. Diode laser bending of tongues from slotted steel tubes. *Int J Mater Form* **2009**, *2*, 107–111, doi:10.1007/s12289-009-0396-x.

128. Che Jamil, M.S.; Imam Fauzi, E.R.; Juinn, C.S.; Sheikh, M.A. Laser bending of pre-stressed thin-walled nickel micro-tubes. *Optics & Laser Technology* **2015**, *73*, 105–117, doi:10.1016/j.optlastec.2015.04.012.

129. Campbell, R.C.; Campbell, B.R.; Lehecka, T.M.; Palmer, J.A.; Knorovsky, G.A. Precision laser bending of thin precious metal alloys. In Proceedings of the Laser-based Micro- and Nanopackaging and Assembly; International Society for Optics and Photonics, 2007; Vol. 6459, p. 64590U.

130. Frühauf, J.; Gärtner, E.; Jänsch, E. Silicon as a plastic material. *J. Micromech. Microeng.* **1999**, *9*, 305–312, doi:10.1088/0960-1317/9/4/304.

131. Schmidt, M.; Dirscherl, M.; Rank, M.; Zimmermann, M. Laser micro adjustment—from new basic process knowledge to the application. *J. Laser Appl.* **2007**, *19*, 10.

132. Widlaszewski, Jacek Applications of laser forming in micro technologies. In *Selected Problems of Modeling and Control in Mechanics*; Kielce, 2011.

133. Hoving, W. Accurate manipulation using laser technology.; Beckmann, L.H.J.F., Ed.; Munich, Germany, 1997; pp. 284–295.

134. Zhuang, Z.; Lu, Z.; Huang, Z.; Liu, C.; Qin, W.; School of Mechanical Engineering, Shanghai Jiao Tong University, 200240, Shanghai, China Experimental study on edge effects in laser bending. *Mathematical Biosciences and Engineering* **2019**, *16*, 4491–4505, doi:10.3934/mbe.2019224.

135. Shen, H.; Wang, H.; Hu, J.; Yao, Z. Processing Optimization in Multiheating Positions for Laser Thermal Adjustment of Actuators. *J. Manuf. Sci. Eng* **2016**, *138*, doi:10.1115/1.4032806.

136. Zhang, X.R.; Xu, X. Laser bending for high-precision curvature adjustment of microcantilevers. *Appl. Phys. Lett.* **2005**, *86*, 021114, doi:10.1063/1.1851617.

137. Inoue, M.; Kawamata, H.; Tanaka, H. Thin plate formation method, thin plate and suspension correction apparatus, and correction method 2011.

138. Murata, A.; Mukae, H.; Maegawa, T.; Higashionji, M.; Okada, T. Rotary head adjuster 1992.

139. Murata, A.; Mukae, H.; Maegawa, T.; Higashionji, M.; Okada, T. Rotary magnetic head having head base which is bent along thermal plastic deformation line 2001.

140. Folkersma, K.G.P.; Römer, G.R.B.E.; Brouwer, D.M.; Herder, J.L. High precision optical fiber alignment using tube laser bending. *Int J Adv Manuf Technol* **2016**, *86*, 953–961, doi:10.1007/s00170-015-8143-6.

141. Folkersma, G.; Brouwer, D.; Römer, G.-W. Microtube Laser Forming for Precision Component Alignment. *J. Manuf. Sci. Eng* **2016**, *138*, doi:10.1115/1.4033389.

142. Thompson, Y.; Gonzalez-Gutierrez, J.; Kukla, C.; Felfer, P. Fused filament fabrication, debinding and sintering as a low cost additive manufacturing method of 316L stainless steel. *Additive Manufacturing* **2019**, *30*, 100861, doi:10.1016/j.addma.2019.100861.

143. Lathers, S.; Mousa, M.; La Belle, J. Additive Manufacturing Fused Filament Fabrication Three-Dimensional Printed Pressure Sensor for Prosthetics with Low Elastic Modulus and High Filler Ratio Filament Composites. *3D Printing and Additive Manufacturing* **2017**, *4*, 30–40, doi:10.1089/3dp.2016.0051.

144. Hegde, M.; Meenakshisundaram, V.; Chartrain, N.; Sekhar, S.; Tafti, D.; Williams, C.B.; Long, T.E. 3D Printing All-Aromatic Polyimides using Mask-Projection Stereolithography: Processing the Nonprocessable. *Advanced Materials* **2017**, *29*, 1701240, doi:10.1002/adma.201701240.

145. Hull, C.W. Apparatus for production of three-dimensional objects by stereolithography 1986.

146. Negi, S.; Dhiman, S.; Sharma, R.K. BASICS, APPLICATIONS AND FUTURE OF ADDITIVE MANUFACTURING TECHNOLOGIES: A REVIEW. 23.

147. Gao, H.; Sheikholeslami, G.; Dearden, G.; Edwardson, S.P. Development of Scan Strategies for Controlled 3D Laser Forming of Sheet Metal Components. *Physics Procedia* **2016**, *83*, 286–295, doi:10.1016/j.phpro.2016.08.027.

148. Gao, H.; Sheikholeslami, G.; Dearden, G.; Edwardson, S.P. Reverse Analysis of Scan Strategies for Controlled 3D Laser Forming of Sheet Metal. *Procedia Engineering* **2017**, *183*, 369–374, doi:10.1016/j.proeng.2017.04.054.

149. Kim, J.; Na, S.J. 3D laser-forming strategies for sheet metal by geometrical information. *Optics & Laser Technology* **2009**, *41*, 843–852, doi:10.1016/j.optlastec.2008.12.001.

150. Kim, J.; Na, S.J. Feedback control for 2D free curve laser forming. *Optics & Laser Technology* **2005**, *37*, 139–146, doi:10.1016/j.optlastec.2004.03.001.

151. Edwardson, S.P.; Abed, E.; Bartkowiak, K.; Dearden, G.; Watkins, K.G. Geometrical influences on multi-pass laser forming. *J. Phys. D: Appl. Phys.* **2006**, *39*, 382–389, doi:10.1088/0022-3727/39/2/021.

152. Smith, G.L.; Lazarus, N.; McCormick, S. Laser Folded Antenna. In Proceedings of the 2018 IEEE MTT-S International Microwave Workshop Series on Advanced Materials and Processes for RF and THz Applications (IMWS-AMP); 2018; pp. 1–3.

153. Morgan, S.P. Effect of Surface Roughness on Eddy Current Losses at Microwave Frequencies. *Journal of Applied Physics* **1949**, *20*, 352–362, doi:10.1063/1.1698368.

154. Kügler, H.; Vollertsen, F. Determining Absorptivity Variations of Multiple Laser Beam Treatments of Stainless Steel Sheets. *Journal of Manufacturing and Materials Processing* **2018**, *2*, 84, doi:10.3390/jmmp2040084.

155. Chua, C.L.; Fork, D.K.; Schuylenbergh, K.V.; Jeng-Ping Lu Out-of-plane high-Q inductors on low-resistance silicon. *Journal of Microelectromechanical Systems* **2003**, *12*, 989–995, doi:10.1109/JMEMS.2003.820274.

156. Fidder, H.; Els-Botes, A.; Woudberg, S.; McGrath, P.J.; Ocelik, V.; Hosson, J.T.M. de A Study Of Microstructural Fatigue And Residual Stress Evolution In Titanium Plates Deformed By Mechanical And Laser Bending. *WIT Transactions on Engineering Sciences; Southampton* **2015**, *91*, 23–34.

157. Sami Yilbas, B.; Khaled, M.; Akhtar, S.; Karatas, C. Laser bending of steel sheets: corrosion testing of bended sections. *Industrial Lubrication and Tribology* **2011**, *63*, 367–372, doi:10.1108/00368791111154986.

158. Liu, Z.; Guzmán, C.; Liu, H.; Anacleto, A.; Francisco, T.; Abdoalshafie, M.; Ma, L.; Abodunrin, O.; Skeldon, P. Corrosion performance and restoration of laser-formed metallic alloy sheets. *Journal of Laser Applications* **2009**, *21*, 76–81, doi:10.2351/1.3110061.

159. Olsen, F.O.; Alting, L. Pulsed Laser Materials Processing, ND-YAG versus CO2 Lasers. *CIRP Annals* **1995**, *44*, 141–145, doi:10.1016/S0007-8506(07)62293-8.

160. Lazarus, N.; Wilson, A.A.; Smith, G.L. Contactless laser fabrication and propulsion of freely moving structures. *Extreme Mechanics Letters* **2018**, *20*, 46–50, doi:10.1016/j.eml.2018.01.003.

161. Noor, Y.Md.; Tam, S.C.; Lim, L.E.N.; Jana, S. A review of the Nd: YAG laser marking of plastic and ceramic IC packages. *Journal of Materials Processing Technology* **1994**, *42*, 95–133, doi:10.1016/0924-0136(94)90078-7.

162. Ehrlich, D.J.; Tsao, J.Y. A review of laser–microchemical processing. *Journal of Vacuum Science & Technology B: Microelectronics Processing and Phenomena* **1983**, *1*, 969–984, doi:10.1116/1.582718.

163. Osgood, R.M.; Deutsch, T.F. Laser-Induced Chemistry for Microelectronics. *Science* **1985**, *227*, 709–714, doi:10.1126/science.227.4688.709.

164. Kindle, C.; Castonguay, A.; McGee, S.; Tomko, J.A.; Hopkins, P.E.; Zarzar, L.D. Direct Laser Writing from Aqueous Precursors for Nano to Microscale Topographical Control, Integration, and Synthesis of Nanocrystalline Mixed Metal Oxides. *ACS Appl. Nano Mater.* **2019**, *2*, 2581–2586, doi:10.1021/acsanm.9b00360.

165. Wachs, I.E. Raman and IR studies of surface metal oxide species on oxide supports: Supported metal oxide catalysts. *Catalysis Today* **1996**, *27*, 437–455, doi:10.1016/0920-5861(95)00203-0.

166. Kalinushkin, V.P.; Uvarov, O.V.; Gladilin, A.A. Photoluminescent Tomography of Semiconductors by Two-Photon Confocal Microscopy Technique. *Journal of Elec Materi* **2018**, *47*, 5087–5091, doi:10.1007/s11664-018-6393-4.

Chapter 3 Self-folding PCB Kirigami: Rapid Prototyping of 3D Electronics via Laser Cutting and Forming

Adam L. Bachmann[a,b], Brendan Hanrahan[c], Michael D. Dickey,[b] and Nathan Lazarus[c*]

[a] *Oak Ridge Associated Universities (ORAU) Fellowship Program at US Army Research Laboratory, 2800 Powder Mill Road, Adelphi, Maryland 20783, United States*

[b] Department of Chemical and Biomolecular Engineering, North Carolina State University, Raleigh, North Carolina, 27695

[c] Sensors and Electron Devices Directorate, US Army Research Laboratory, 2800 Powder Mill Road, Adelphi, Maryland 20783, United States

This chapter has been published in the journal ACS Applied Materials & Interfaces (2022)

Abstract

This paper demonstrates laser forming, localized heating with a laser to induce plastic deformation, can self-fold 2D printed circuit boards (PCBs) into 3D structures with electronic function. There are many methods for self-folding, but few are compatible with electronic materials. We use a low-cost commercial laser writer to both cut and fold a commercial flexible PCB. Laser settings are tuned to select between cutting and folding, with higher power resulting in cutting and lower power resulting in localized heating for folding into 3D shapes. Since the thin copper traces used in commercial PCBs are highly reflective and difficult to directly fold, two approaches are explored for enabling folding: plating with a nickel/gold coating or using a single, high-power laser exposure to oxidize the surface and improve laser absorption. We characterized the physical effect of the exposure on the sample as well as the fold angle as a function of laser passes and demonstrate the ability to lift weights comparable with circuit packages and passive components. This technique can form complex, multi-fold structures with integrated electronics; as a demonstrator, we fold a commercial board with a common timing circuit. Laser forming to add a third dimension to printed circuit boards is an important technology to enable the rapid prototyping of complex 3D electronics.

3.1 Introduction

Origami, the Japanese art of paper folding, and Kirigami, origami that allows cutting,[1] have led to the development of powerful principles[2] that have been used in robotics,[3,4] and deployable structures,[5–7] to produce complex 3D systems from 2D materials. Many objects in daily life are 3D, yet a variety of high-throughput processes — including those used in the microfabrication of electronics — are inherently 2D. Folding can convert such planar electronics[8–11] into 3D objects to enable the production of reconfigurable devices[12], miniaturized components,[9] and multi-axis sensors.[13] In addition, devices with a third dimension can have unique or improved mechanical properties; for example, thin sheets are flexible but can be rendered stiff or extensible using corrugations.[14] Manual folding has been used to make 3D electronic devices,[8,10,15] but this approach presents challenges for automated manufacturing[9] and is also impossible for environments like space,[16] so there has been significant interest in shifting to self-folding techniques.[3,17–21]

Many self-folding systems rely on stimuli-responsive polymers that fold in response to heat, light, or solvents.[18,21–24] To date, most self-folding processes use materials that are either poor electrical conductors or incompatible with conventional electronic processing.[25] By carefully incorporating conductive materials, self-folding electronic devices have been demonstrated,[17,26,27] but integrating these methods with complex circuits and packaged electronics remains challenging.

Integration of packaged electronics with 3D structures has been attempted using other methods, most notably 3D printing.[26,28,29] The use of conductive inks or filaments offers the freedom to pattern arbitrary conductive patterns, but these traces tend to be much more resistive than metals. Near-metallic conductivity of 3D printed structures has been approached by

plating[30–32] conductive traces, but the harsh plating chemicals are often incompatible with the printed parts.[33] Furthermore, the use of 3D printing does not harness the high-resolution patterning or sophisticated processes developed over many decades to create complex electronics on planar substrates. Thus, it is appealing to start with conventional substrates, like printed circuit boards (PCBs), and fold them into desired shapes.

It is possible to manually fold flexible PCBs that consist of copper traces on thin polyimide substrates.[10] Stressed elastomer layers have been used to bend PCBs, but sharp folds are not possible.[34] While the terms bending and folding are often used interchangeably, folding[35] is a highly localized shape transformation unlike bending which is more distributed, generally over length scales larger than the material thickness. We thus sought a self-folding technique for flex PCBs based on recent advances in laser forming of micron-scale metal origami.[36,37]

Laser forming uses a scanned laser to generate thermal stresses that plastically deform a substrate, causing it to fold out of plane.[38] This technique, unlike alternatives such as ion-implantation,[39] can be done in ambient conditions and, unlike surface tension-driven folding,[40] works at multiple length scales.[36,41] Additionally, laser forming is nearly material agnostic with complex shapes formed out of steel plates,[42–45] nickel foils,[36] and copper,[37] in addition to simpler folding being demonstrated in more varied substrates like titanium,[46,47] metal foams,[48] and even non-metals such as silicon,[49] borosilicate glass,[50] and certain polymers.[51]

Laser forming is a viable rapid prototyping strategy[52–54] because laser writers enable fast patterning[55,56] and are compatible with roll-to-roll setups.[57] Recently, researchers have investigated laser forming as a means to cut and fold electronic devices such as antenna waveguides[45] and toroidal inductors[37] from flat metal sheets (~200 μm), paving the way for laser forming of complex electronic devices. Despite these advances, laser forming has not been used

to produce complex, 3D circuits as there remain no reports of laser forming metal/polymer bilayers which are essential to 3D electronics.

Herein, we successfully use a low-cost laser to both cut and fold a conventional flex PCB (copper-polyimide film stack). At high powers, the laser can locally ablate the PCB, thereby enabling cutting of a rectangular PCB into arbitrary 2D shapes. Folding the flex PCB required new methods to overcome the high reflectivity of copper with minimal cutting and without the use of a graphite coating which could cause electrical problems. Under certain conditions, the laser can drive surface oxidation of copper to drastically improve absorbance of the laser light. This increased absorbance allows lower powers to be used for folding, minimizing cutting during the folding process. To demonstrate that this technique is a viable method for the rapid prototyping of 3D electronics, we fabricate multi-fold structures with fully functional integrated electronics as well as the facile folding of complex, commercially fabricated flex-PCB circuits. The ability to use a low-cost laser system to fold commercial PCBs into 3D structures demonstrates a promising new way for rapid prototyping of 3D electronics.

3.2 Experimental

3.2.1 Sample Preparation

For this study, a 20W, pulsed (f = 20 kHz) fiber laser (λ = 1064 nm) with an 80 μm spot size (Full Spectrum Lasers MC Series) is used to successfully cut and fold a copper/polyimide bilayer which is commonly used for making flexible PCBs. Laser power is controlled using pulse-width modulation. The bilayer used in the folding characterizations was Pyralux®AC354500EV (DuPont) which is a single-sided laminate of 35 μm electrodeposited copper on 45 μm polyimide and was used as received. The flex PCB was clamped on all sides and 30 mm by 10 mm strips were cut out at P = 20 W at a scan speed of 100 mm/s. These strips

were then clamped on one side with 15 mm of the strip being in the clamp and the laser fold line 5 mm from the edge of the clamp. The laser power and scan speed were then adjusted to successfully laser form the samples while minimizing cutting.

Samples of patterned copper on polyimide were produced by placing Kapton tape on top of the copper and cutting out the desired pattern, with P = 6 W at 100 mm/s scan speed with 10 total laser passes. The cut Kapton tape is then removed manually. The sample is then placed in a ferric chloride copper etchant solution (MG Chemicals) for 15 minutes at 50 °C and then doubly rinsed in DI water. These samples are then used for laser forming after soldering surface mount LEDs across the gap.

Weighted samples were prepared by attaching different sized (M2.5, M3, M3.5, and M4) hex nuts to the polyimide side of the bilayer using double sided polyimide tape.

The astable 555 oscillator was designed in KiCAD and was fabricated by OSH Park. A standard trace width of 0.4 mm was used for the circuit paths, but a trace width of 2.5 mm was used for the folding region to make manual alignment easier. The 555-timer circuit was designed to have a frequency of 2 Hz (**Appendix A.1**) with all surface mount components bought from Digi-Key. The circuits were cut out from the board using the laser writer before soldering all surface mount components. Electrical connectivity was tested by connecting a 9V battery to the circuit and confirming the LED was blinking properly before, during, and after laser forming.

3.2.2 Characterization

After clamping, a single pass of the high-power mark (HPM) at P = 16 W scanned at 100 mm/s was followed by a 10 second cooling period. Folding was accomplished with P = 6 W laser passes at 100 mm/s. Laser folding was done with five laser passes followed by a 10 second

cooling period. Fold angles were measured by taking pictures during these cooling periods. The photos were then imported to ImageJ (https://imagej.nih.gov/ij/) to measure the fold angles. Laser-induced surface roughening was characterized using confocal microscopy (LEXT OLS4000). Laser induced oxidation was characterized using x-ray diffraction (Panalytical X'Pert3) in Bragg-Brentano geometry. Due to the large beam size, 2 cm by 2 cm squares were prepared by scanning multiple lines at P = 16 W and 100 mm/s with a 100 μm spacing between the lines to avoid multiple laser exposure.

3.3 Results and Discussion

We used a pulsed fiber laser to both cut and fold flexible PCBs that have been patterned and populated with surface mount components as depicted in **Figure 3.1a**. This technique was used to produce complex 3D structures with electronically functional circuits. At higher powers, the laser ablates the copper and the polyimide, but at lower powers, the substrate is simply heated, allowing the same laser system to be used for both cutting and laser forming of the flex PCBs.[36,37,45]

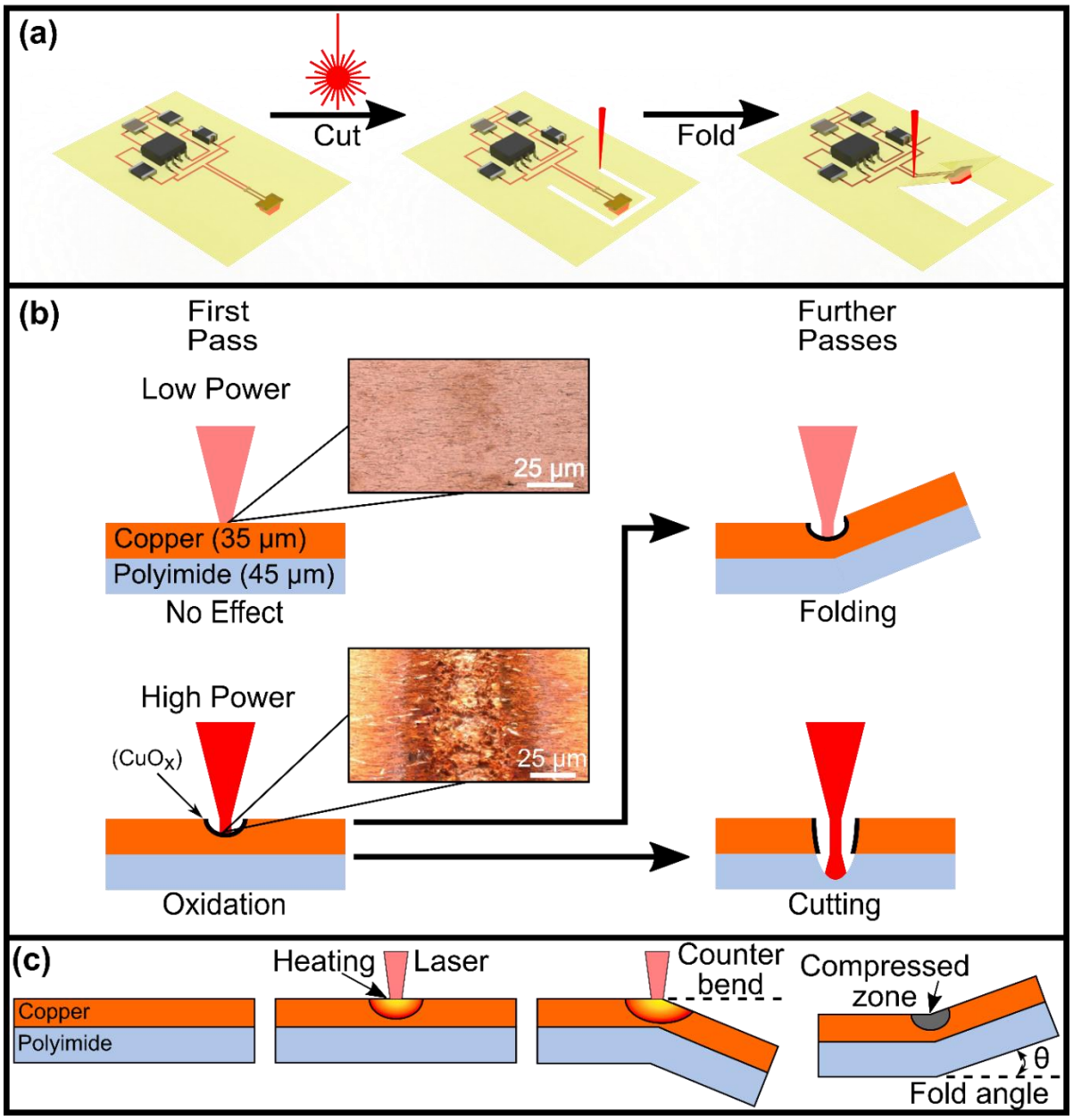

Figure 3.1. Schematic of the process (a) of cutting and laser forming (folding) a flexible printed circuit board (PCB) into a 3D shape using the same laser. Surface mount components are soldered to the board before the laser cuts out the fold region before laser forming to produce the 3D structure. The laser light is poorly absorbed (b) by copper, so nothing happens initially with low laser powers. A single pass at higher power causes mild ablation and some surface oxidation which enables folding with sustained low-power lasing. Repeated lasing with higher powers leads to cutting through the entire substrate. The temperature gradient mechanism (c) begins with a scanning laser heating the surface layers of the substrate. The thermal gradient leads to a thermal expansion gradient through the thickness of the material, causing the piece to initially bend away from the laser as the upper layers expands more. The thermal expansion is resisted by the cooler portions and is encoded as plastic compressive stresses that causes the piece to fold toward the laser after the laser has passed and the scan line cools, resulting in a permanent fold.

There are three main mechanisms for laser forming: the temperature gradient mechanism (TGM), the buckling mechanism (BM), and the upsetting mechanism (UM). Only the TGM and BM can produce out-of-plane bending or folding. The dominant mechanism depends on how the thermal gradients are established. Since the TGM was the mechanism used in this paper, we explain it briefly, but the reader is referred to reviews that cover all these mechanisms in more detail.[54,58]

The TGM relies on a steep thermal gradient through the thickness of the material and results in folding toward the laser.[38,58] The steep thermal gradient between the lased and unlased side (**Figure 3.1c**) is realized with moderate laser powers and a high scan speed. This thermal gradient causes the top layers to expand more than the bottom layers resulting in an initial bend *away* from the laser called the counter bend. This expansion, however, is resisted by the surrounding, cooler metal. At the elevated temperatures during the laser pulse, the mechanical properties change dramatically, most notably the yield stress and the flow stress decrease. The stresses generated by the thermal expansion are sufficient to overcome the reduced yield stress and enter the plastic regime. Once in the plastic regime, the thermal stresses continue to generate plastic deformation when the flow stress is exceeded in the heated region. Once the laser has passed, the substrate begins to cool and the heated sections return to their original sizes, but the compressive stresses remain from the plastically deformed region. These stresses act on the scanned region, compressing it and cause the workpiece to fold toward the laser by an incremental folding angle, θ. Single passes lead to small fold angles, but larger angles are possible through repeated laser passes.[36,59]

Laser forming is nearly material agnostic, but laser forming of copper, the typical metal used in PCBs, is quite rare[37] as copper's high thermal conductivity makes it difficult to establish

the needed thermal gradients. This difficulty is compounded by copper being highly reflective to all wavelengths above its absorption edge that occurs near 600 nm wavelengths (**Figure 3.2a**).[60] Conventional laser forming uses CO_2 lasers but metals are highly reflective to the 10.6 μm wavelength laser so a graphite coating is often used to improve absorbance of the laser.[51,61,62] Such a coating is unnecessary when laser forming metals with shorter wavelength lasers[36,45,46,63,64] as metals tend to be less reflective to shorter wavelengths.[60] Consequently, visible[65] (532 nm) and UV[66] (355 nm) lasers are desirable when patterning copper as they do not need graphite coatings that can cause short circuits. Due to the non-linear optical elements needed, these frequency-doubled (532 nm) and frequency-tripled (355 nm) lasers are expensive compared to fiber lasers of a comparable power. Owing to their lower cost and that laser forming of bulk copper has been demonstrated,[37] a pulsed fiber laser (1064 nm) was chosen. As reported, surface cutting ~100 μm was observed which limits their approach to substrates ~200 μm or thicker and is incompatible with flex PCBs as their copper layers are typically 35 μm or thinner. Careful control, however, of the laser settings should allow enough heat to enter the copper without cutting it, enabling laser forming of thin metal traces despite the high reflectivity.

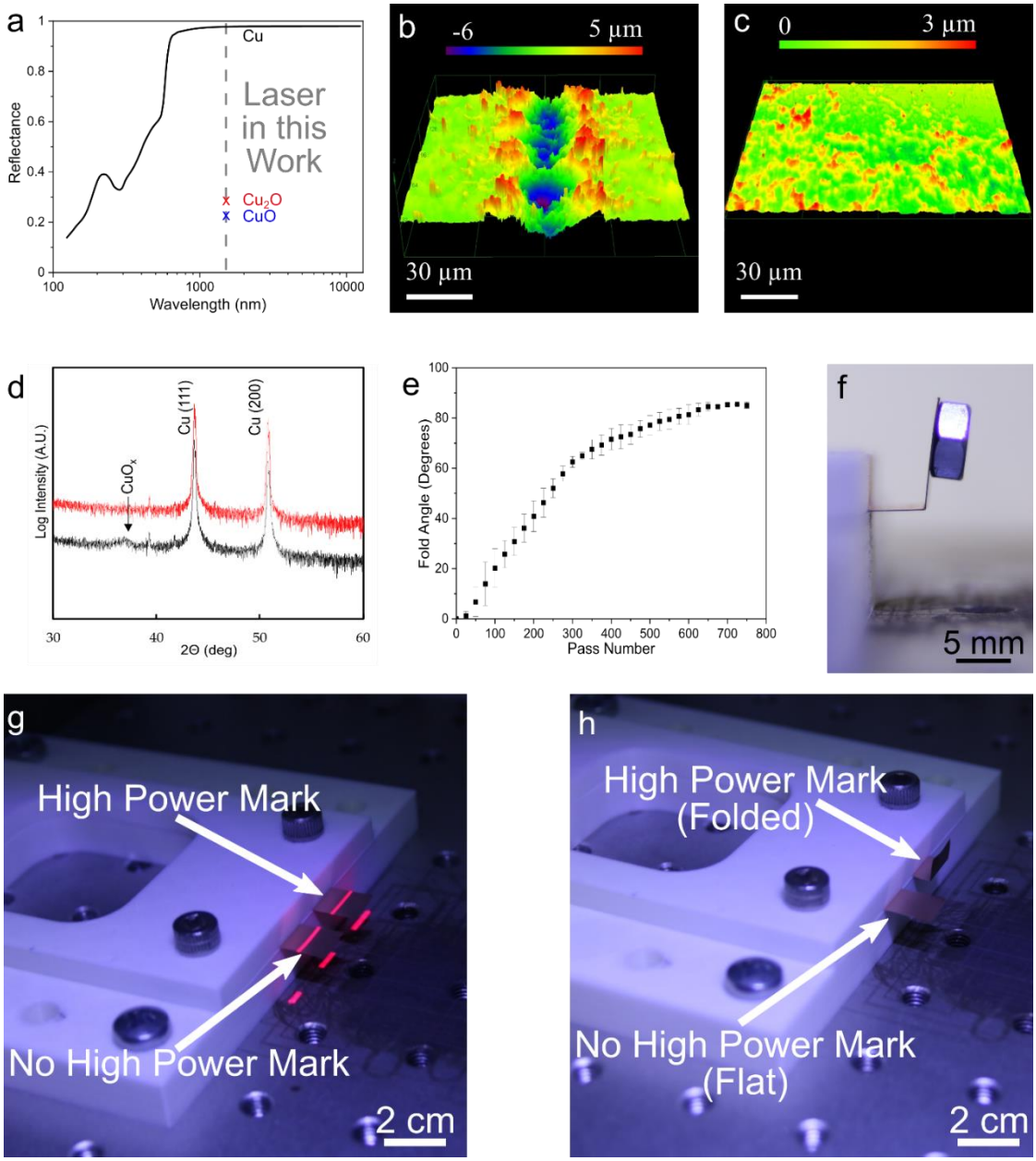

Figure 3.2. The reflectivity of bare copper (a) is extremely high at the fiber laser wavelength, but the high-power mark (HPM) allows bare copper to be successfully laser formed with minimal cutting by oxidizing the surface. The copper oxides are much less reflective at the laser wavelength. Copper reflectivity adopted from [60] and copper oxide reflectivity from.[67] A single pass of the HPM (b) greatly roughens the surface compared to a single pass of the laser folding settings (c) which has almost no noticeable effect on the surface. The HPM also oxidizes the copper surface (d) which leads to enhanced laser absorption. Folding (e) can be realized at lower power settings that avoid cutting. The forces generated during laser forming are large enough to fold the sample with weights attached to it (f). The HPM is essential for laser forming copper (g) as two samples were laser formed using the same settings but only one received the HPM and this one folds (h) despite the laser passing over both samples.

Based on previous work,[37] we held the scan speed constant at 100 mm/s and varied the power to find the minimum power setting needed to still observe folding. Based on prior work of laser carbonization of polyimide,[68] we sought to carbonize the polyimide to generate an absorbing coating. Unfortunately, even the lowest power settings ablated the polyimide thoroughly and we observed no bending, so we turned our attention to conventional laser forming by having the metal exposed to the laser. The first pass at higher powers left a black mark on the copper we call the high-power mark (HPM) in the remainder of the paper. We reasoned this black mark should improve the laser absorption like graphite coatings.[61] The improved absorbance allows lower powers for laser forming, thus minimizing cutting. Further testing found the most consistent folding using an HPM of P = 16 W. Two main mechanisms explain the enhanced laser absorption: surface roughening and oxidation. Confocal micrographs show significant roughness on a single pass of the HPM (**Figure 3.2b**) relative to a single pass of the laser settings used for folding, P = 6 W and 100 mm/s (**Figure 3.2c**).

The low-power folding passes cause no noticeable changes to the copper surface unlike the HPM which cuts a micro-sized valley into the surface. This cutting is minimal, about 15%, so the sample still folds while maintaining electrical connectivity. This 15% reduction in the cross-sectional area minimally contributes to the resistance of the entire trace because the trench is narrow. Based on theoretical calculations, an ablation width of 70 μm increases the total resistance of a 2 cm trace by 0.6%. The surface roughening from the HPM, however, is insufficient to explain the drastic increase in laser absorption, as the shallow, wide features are expected to show only a modest increase[69] and is inconsistent with experiments on oven heated metals which show increased optical absorption with minimal change in surface roughness.[70] Taken in sum, the enhanced absorption from the HPM is best explained by surface oxidation.

Surface oxidation from the HPM was confirmed with x-ray diffraction (**Figure 3.2d**). The control sample shows that the as-received samples have minimal surface oxides. In contrast, CuO_x peaks are observed in the diffraction spectrum of the HPM sample. Both copper oxides, Cu_2O and CuO, have similar diffraction patterns but are hard to distinguish via XRD as these surface oxides are only a small percentage of the interaction volume with the x-ray beam. Either oxide could be responsible for the increased absorption as Cu_2O has a reflectivity ~23% while CuO has a reflectivity ~21% at the laser wavelength[67] compared to the 98% reflectivity of bare copper.[60] Previous work suggests that both copper oxides would be formed for laser heating of copper in air.[71]

The improved laser absorbance from surface oxidation allowed reliable folding without cutting by using a lower power. The samples were able to self-fold almost vertically (90 degrees, **Figure 3.2e**). Near 90 degrees, the substrate begins to interfere with the focusing path of the laser beam and folding stops. This self-limiting behavior of the TGM has been reported previously,[36] and serves as a natural control mechanism for preparing samples with right angle folds.

With the ability to fold flex PCBs near vertically, we began envisioning laser forming as a viable rapid prototyping strategy for 3D electronic devices with packaged electronics like resistors, capacitors, and diodes. Despite the thin bilayer substrate (~80 μm), the samples were able to be laser formed to nearly 90 degrees even with an attached weight ~0.7g, (**Figure 3.2f**) which is much greater than the average weight of common surface mount components, about 77 mg for SOIC-8 packages. Flex PCBs can come in a variety of copper and polyimide thicknesses and the laser formability of these different bilayers is impacted by the thickness of each layer as

well as the ratio of their thicknesses. Materials resist bending and folding from their flexural rigidity which is

$$Flexural\ stiffness = \frac{Ebh^3}{12}$$

Where E is the Young's Modulus, b and h are the width and thickness of the layer, respectively. Copper is a much stiffer material (E = 130 GPa) compared to polyimide (E ~ 3 GPa) so for comparable thickness ratios, the forces generated during laser forming that can fold the copper are more than sufficient for folding the polyimide layer. Since the stiffness scales as h^3, polyimide layers substantially thicker than the copper layer could inhibit laser forming entirely.

The HPM is required for low-power laser forming of bare copper as the high reflectivity of copper prevents enough heat from entering the substrate, even over hundreds of laser passes. To demonstrate this, a control experiment was done in which two samples were exposed to the same laser settings for folding, but only one substrate received the HPM before exposure (**Figure 3.2g**). As expected, the copper that does not receive the HPM remained flat while the one that was marked bent toward the laser (**Figure 3.2h**). Even the repeated lasing at the folding settings is insufficient to oxidize the surface and introduce folding so only the HPM allows the bilayer to reach a 90-degree fold. Despite the high temperatures generated during laser forming, the copper efficiently spreads and dissipates the heat. After folding, we tried to measure the conductivity through the thickness of the bilayer, but were unable to measure anything, suggesting that any carbonization is highly localized and does not extend through the thickness of the polyimide layer.

Having demonstrated folding of a metal/polymer bilayer with added weight, we tried laser forming flexible PCBs with surface mount components. Flex PCBs are easily patterned by

lithography and integrated with pick-and-place machinery,[3,72] so their successful laser forming would enable rapid prototyping of three-dimensional electronics from existing processes and equipment. As an initial demonstration, a flex PCB was pattered by etching a 2 mm wide trace in the middle of the flex PCB, electrically isolating the two halves. A surface mount LED was soldered to the plates and connected to a circuit containing a resistor and a 9 V battery (**Figure 3.3**). The fiber laser cut through the bilayer to form a Z-shape net as it is laser formable unlike the T-shape nets.[73] A narrow (500 µm) metal bridge between each half of the cube maintained mechanical and electrical connectivity with the flex PCB during the forming process. The exposed polyimide does not contribute to the folding as even the low-power folding passes are able to cut through.

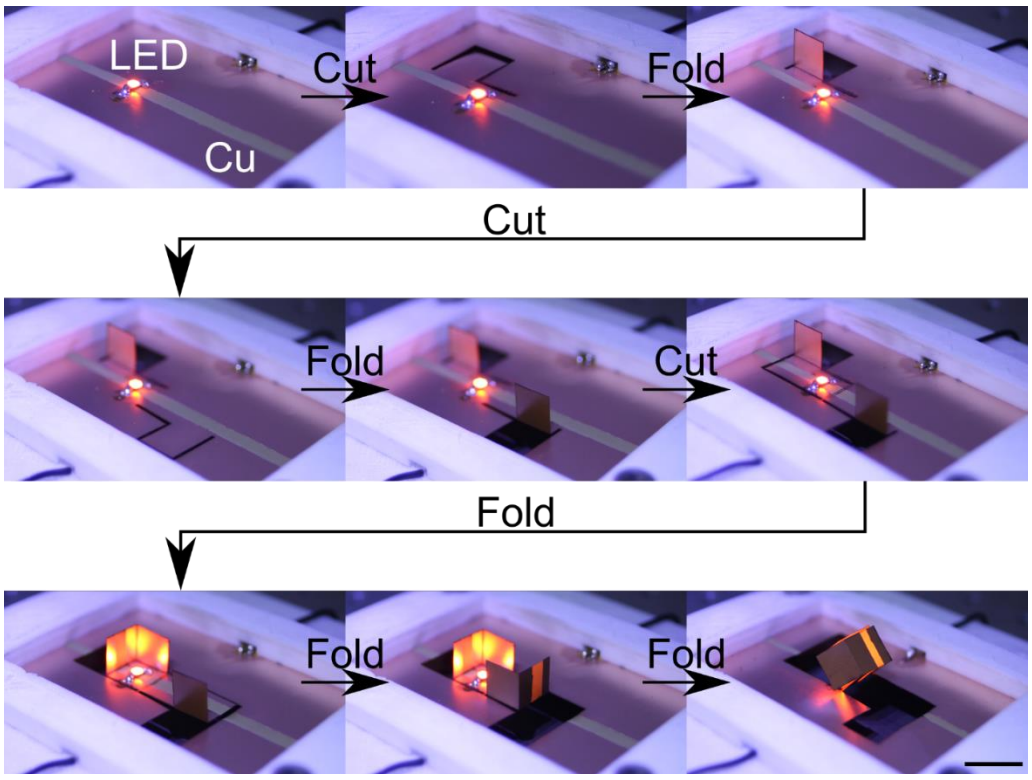

Figure 3.3. A step-by-step folding of a cube with a functioning electronic circuit. An etching process (not shown) removed the copper from a strip in the middle of the sample. The first frame (top left) shows an LED that bridges across this etched region to make electrical connections with copper on each side. The LED maintains electrical connectivity throughout the cutting and folding process and can be folded out-of-plane. Scale bar is 1 cm.

Based on the successful folding with a single integrated electronic component, we sought to laser form a more complex circuit: an astable 555 timer, (**Appendix A.1**) which comprises multiple surface mount components including an integrated circuit. The blinking pattern of the LED allows easy verification of electrical connection during folding of the commercial PCB.

Commercial flex PCBs typically cover all exposed copper with ENIG (electroless nickel immersion gold) to prevent copper oxidation. The gold surface presents a challenge for laser forming because gold is highly reflective to the fiber laser wavelength and does not oxidize. Despite these challenges, the immersion gold layer is thin enough (~100 nm) to not interfere with the laser forming process. Straightforward application of the HPM followed by the folding passes leads to more substantial cutting compared to the samples with exposed copper, breaking the electrical connection. The HPM cuts deeply into the ENIG coated samples (**Appendix A.2**) and breaks the electrical circuit. Fortunately, the low-power folding settings can fold the ENIG coated samples without the HPM.

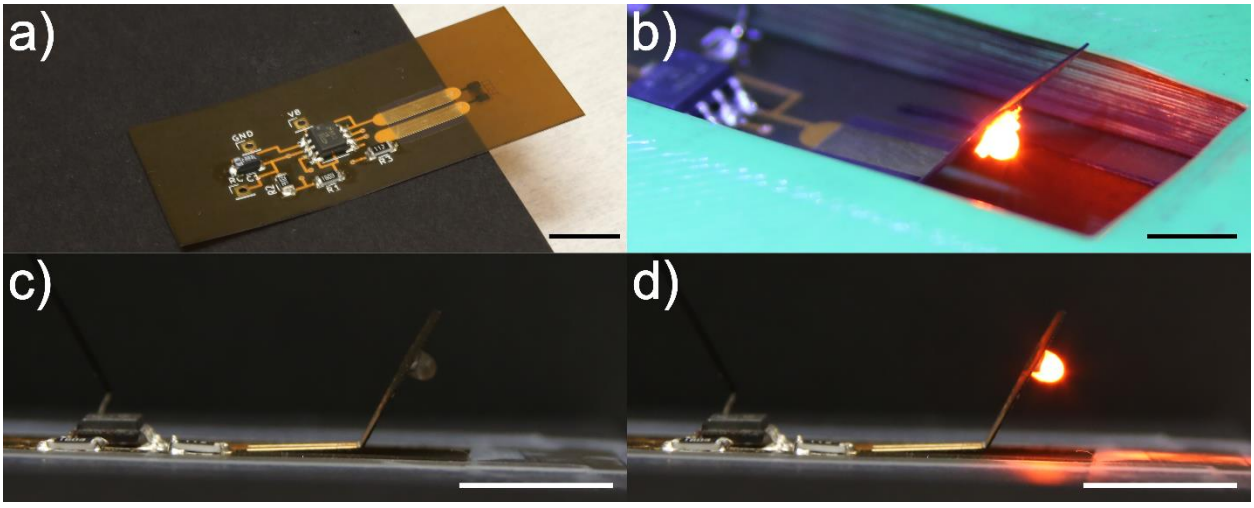

Figure 3.4. The commercially fabricated flex PCB (a) is populated with surface mount components before being mounted into the laser system. The flex PCB is cut and folded (b) while the circuit still functions. The permanently folded circuit continues to blink (c and d) after removal from the laser system. All scale bars are 1 cm.

The populated board (**Figure 3.4a**) is then clamped at the focal plane of the laser before high power laser passes were used to cut a tab around the LED to be bent. The standard folding pass settings are then used to fold the LED out of plane (**Figure 3.4b**) while maintaining electrical connectivity. After laser forming, the sample can be removed from the clamp and retains its fold while the LED still blinks (**Figure 3.4c and 3.4d**). The trace width for the folding region is much larger than in conventional PCBs to make manual alignment easier. Previous reports of laser forming of silicon microsctructures[74] suggest that this linewidth is not an inherent limitation of the process and with automatic alignment systems, conventional trace widths can be used. While this technique was developed for flexible PCBs, it should also be applicable to printed copper electronics[75] provided the printed traces are sufficiently thick.

3.4 Conclusions

In this work, we demonstrated the laser forming of metal/polymer bilayers using a fiber laser writer. The same laser writer can be used to drive surface oxidation on the copper and improve the absorption properties, allowing laser forming without cutting the thin copper layers. Having demonstrated simple bilayer folding of copper on polyimide, we further showed that this technique can laser form complex structures with patterned electrodes and integrated surface mount components. The easy integration of laser forming with conventional PCB fabrication makes it a promising method for rapid prototyping of 3D electronics.

3.5 Acknowledgements

We gratefully acknowledge the financial sponsorship from the Army Research Laboratory and research was accomplished under Cooperative Agreement Number W911NF-20-2-0243. The views and conclusions contained in this document are those of the authors and should not be interpreted as representing the official policies, either expressed or implied, of the

3.6 References

(1) Blees, M. K.; Barnard, A. W.; Rose, P. A.; Roberts, S. P.; McGill, K. L.; Huang, P. Y.; Ruyack, A. R.; Kevek, J. W.; Kobrin, B.; Muller, D. A.; McEuen, P. L. Graphene Kirigami. *Nature* **2015**, *524* (7564), 204–207. https://doi.org/10.1038/nature14588.

(2) Ishida, S.; Hagiwara, I. Introduction to Mathematical Origami and Origami Engineering. In *Applications + Practical Conceptualization + Mathematics = fruitful Innovation*; Anderssen, R. S., Broadbridge, P., Fukumoto, Y., Kajiwara, K., Takagi, T., Verbitskiy, E., Wakayama, M., Eds.; Mathematics for Industry; Springer Japan: Tokyo, 2016; pp 41–49. https://doi.org/10.1007/978-4-431-55342-7_4.

(3) Felton, S.; Tolley, M.; Demain, E.; Rus, D.; Wood, R. A Method for Building Self-Folding Machines. *Science* **2014**, *345* (6197), 644–646.

(4) Cha, W.; Campbell, M. F.; Popov, G. A.; Stanczak, C. H.; Estep, A. K.; Steager, E. B.; Sung, C. R.; Yim, M. H.; Bargatin, I. Microfabricated Foldable Wings for Centimeter-Scale Microflyers. *Journal of Microelectromechanical Systems* **2020**, *29* (5), 1127–1129. https://doi.org/10.1109/JMEMS.2020.3013813.

(5) Zirbel, S. A.; Lang, R. J.; Thomson, M. W.; Sigel, D. A.; Walkemeyer, P. E.; Trease, B. P.; Magleby, S. P.; Howell, L. L. Accommodating Thickness in Origami-Based Deployable Arrays. *J. Mech. Des* **2013**, *135* (11). https://doi.org/10.1115/1.4025372.

(6) Melancon, D.; Gorissen, B.; García-Mora, C. J.; Hoberman, C.; Bertoldi, K. Multistable Inflatable Origami Structures at the Metre Scale. *Nature* **2021**, *592* (7855), 545–550. https://doi.org/10.1038/s41586-021-03407-4.

(7) Zhai, Z.; Wang, Y.; Jiang, H. Origami-Inspired, on-Demand Deployable and Collapsible Mechanical Metamaterials with Tunable Stiffness. *PNAS* **2018**, *115* (9), 2032–2037. https://doi.org/10.1073/pnas.1720171115.

(8) Shah, S. I. H.; Tentzeris, M. M.; Lim, S. Low-Cost Circularly Polarized Origami Antenna. *IEEE Antennas and Wireless Propagation Letters* **2017**, *16*, 2026–2029. https://doi.org/10.1109/LAWP.2017.2694138.

(9) Rogers, J.; Huang, Y.; Schmidt, O. G.; Gracias, D. H. Origami MEMS and NEMS. *MRS Bull.* **2016**, *41* (2), 123–129. https://doi.org/10.1557/mrs.2016.2.

(10) Sterman, Y.; Demaine, E. D.; Oxman, N. PCB Origami: A Material-Based Design Approach to Computer-Aided Foldable Electronic Devices. *Journal of Mechanical Design* **2013**, *135* (114502). https://doi.org/10.1115/1.4025370.

(11) Yamaoka, J.; Dogan, M. D.; Bulovic, K.; Saito, K.; Kawahara, Y.; Kakehi, Y.; Mueller, S. FoldTronics: Creating 3D Objects with Integrated Electronics Using Foldable Honeycomb Structures. In *Proceedings of the 2019 CHI Conference on Human Factors in Computing Systems*; Association for Computing Machinery: New York, NY, USA, 2019; pp 1–14.

(12) Liu, X.; Yao, S.; Cook, B. S.; Tentzeris, M. M.; Georgakopoulos, S. V. An Origami Reconfigurable Axial-Mode Bifilar Helical Antenna. *IEEE Transactions on Antennas and Propagation* **2015**, *63* (12), 5897–5903. https://doi.org/10.1109/TAP.2015.2481922.

(13) Efimovskaya, A.; Lin, Y.-W.; Shkel, A. M. Origami-Like 3-D Folded MEMS Approach for Miniature Inertial Measurement Unit. *Journal of Microelectromechanical Systems* **2017**, *26* (5), 1030–1039. https://doi.org/10.1109/JMEMS.2017.2703594.

(14) Hubbard, A. M.; Patel, J. K.; Wagner, S.; Chang, C.-H.; Genzer, J.; Dickey, M. D. Stiff or Extensible in Seconds: Light-Induced Corrugations in Thin Polymer Sheets. *Advanced Materials Technologies* **2021**, *6* (1), 2000789. https://doi.org/10.1002/admt.202000789.

(15) Ahn, B. Y.; Shoji, D.; Hansen, C. J.; Hong, E.; Dunand, D. C.; Lewis, J. A. Printed Origami Structures. *Advanced Materials* **2010**, *22* (20), 2251–2254. https://doi.org/10.1002/adma.200904232.
(16) Zirbel, S. A.; Trease, B. P.; Magleby, S. P.; Howell, L. L. Deployment Methods for an Origami-Inspired Rigid-Foldable Array. In *NASA Center for AeroSpace Information (CASI). Conference Proceedings*; NASA/Langley Research Center: Hampton, United States, 2014.
(17) van Manen, T.; Janbaz, S.; Ganjian, M.; Zadpoor, A. A. Kirigami-Enabled Self-Folding Origami. *Materials Today* **2020**, *32*, 59–67. https://doi.org/10.1016/j.mattod.2019.08.001.
(18) Liu, Y.; Boyles, J. K.; Genzer, J.; Dickey, M. D. Self-Folding of Polymer Sheets Using Local Light Absorption. *Soft Matter* **2012**, *8* (6), 1764–1769. https://doi.org/10.1039/C1SM06564E.
(19) Gracias, D.; Cho, J.-H.; Hu, S. A Three Dimensional Self-Folding Package (SFP) for Electronics. *MRS Online Proceedings Library (OPL)* **2010**, *1249*. https://doi.org/10.1557/PROC-1249-F09-07.
(20) Tolley, M. T.; Felton, S. M.; Miyashita, S.; Aukes, D.; Rus, D.; Wood, R. J. Self-Folding Origami: Shape Memory Composites Activated by Uniform Heating. *Smart Mater. Struct.* **2014**, *23* (9), 094006. https://doi.org/10.1088/0964-1726/23/9/094006.
(21) Wang, D. H.; Tan, L.-S. Origami-Inspired Fabrication: Self-Folding or Self-Unfolding of Cross-Linked-Polyimide Objects in Extremely Hot Ambience. *ACS Macro Lett.* **2019**, *8* (5), 546–552. https://doi.org/10.1021/acsmacrolett.9b00198.
(22) Abdullah, A. M.; Li, X.; Braun, P. V.; Rogers, J. A.; Hsia, K. J. Self-Folded Gripper-Like Architectures from Stimuli-Responsive Bilayers. *Advanced Materials* **2018**, *30*, 1801669. https://doi.org/10.1002/adma.201801669.
(23) Stuart, M. A. C.; Huck, W. T. S.; Genzer, J.; Müller, M.; Ober, C.; Stamm, M.; Sukhorukov, G. B.; Szleifer, I.; Tsukruk, V. V.; Urban, M.; Winnik, F.; Zauscher, S.; Luzinov, I.; Minko, S. Emerging Applications of Stimuli-Responsive Polymer Materials. *Nature Materials* **2010**, *9* (2), 101–113. https://doi.org/10.1038/nmat2614.
(24) Zarek, M.; Layani, M.; Cooperstein, I.; Sachyani, E.; Cohn, D.; Magdassi, S. 3D Printing of Shape Memory Polymers for Flexible Electronic Devices. *Advanced Materials* **2016**, *28* (22), 4449–4454. https://doi.org/10.1002/adma.201503132.
(25) Guan, J. J.; He, H. Y.; Hansford, D. J.; Lee, L. J. Self-Folding of Three-Dimensional Hydrogel Microstructures. *J. Phys. Chem. B* **2005**, *109* (49), 23134–23137. https://doi.org/10.1021/jp054341g.
(26) Sundaram, S.; Kim, D. S.; Baldo, M. A.; Hayward, R. C.; Matusik, W. 3D-Printed Self-Folding Electronics. *ACS Appl. Mater. Interfaces* **2017**, *9* (37), 32290–32298. https://doi.org/10.1021/acsami.7b10443.
(27) Hayes, G. J.; Liu, Y.; Genzer, J.; Lazzi, G.; Dickey, M. D. Self-Folding Origami Microstrip Antennas. *IEEE Transactions on Antennas and Propagation* **2014**, *62* (10), 5416–5419. https://doi.org/10.1109/TAP.2014.2346188.
(28) Flowers, P. F.; Reyes, C.; Ye, S.; Kim, M. J.; Wiley, B. J. 3D Printing Electronic Components and Circuits with Conductive Thermoplastic Filament. *Additive Manufacturing* **2017**, *18*, 156–163. https://doi.org/10.1016/j.addma.2017.10.002.
(29) Ahn, B. Y.; Duoss, E. B.; Motala, M. J.; Guo, X.; Park, S.-I.; Xiong, Y.; Yoon, J.; Nuzzo, R. G.; Rogers, J. A.; Lewis, J. A. Omnidirectional Printing of Flexible, Stretchable, and Spanning Silver Microelectrodes. *Science* **2009**, *323* (5921), 1590–1593.

(30) Lazarus, N.; Bedair, S. S.; Hawasli, S. H.; Kim, M. J.; Wiley, B. J.; Smith, G. L. Selective Electroplating for 3D-Printed Electronics. *Advanced Materials Technologies* **2019**, *4* (8), 1900126. https://doi.org/10.1002/admt.201900126.
(31) Kim, M. J.; Cruz, M. A.; Ye, S.; Gray, A. L.; Smith, G. L.; Lazarus, N.; Walker, C. J.; Sigmarsson, H. H.; Wiley, B. J. One-Step Electrodeposition of Copper on Conductive 3D Printed Objects. *Additive Manufacturing* **2019**, *27*, 318–326. https://doi.org/10.1016/j.addma.2019.03.016.
(32) Lee, S.; Wajahat, M.; Kim, J. H.; Pyo, J.; Chang, W. S.; Cho, S. H.; Kim, J. T.; Seol, S. K. Electroless Deposition-Assisted 3D Printing of Micro Circuitries for Structural Electronics. *ACS Appl. Mater. Interfaces* **2019**, *11* (7), 7123–7130. https://doi.org/10.1021/acsami.8b18199.
(33) Heikkinen, I. T. S.; Kauppinen, C.; Liu, Z.; Asikainen, S. M.; Spoljaric, S.; Seppälä, J. V.; Savin, H.; Pearce, J. M. Chemical Compatibility of Fused Filament Fabrication-Based 3-D Printed Components with Solutions Commonly Used in Semiconductor Wet Processing. *Additive Manufacturing* **2018**, *23*, 99–107. https://doi.org/10.1016/j.addma.2018.07.015.
(34) Kim, B. H.; Liu, F.; Yu, Y.; Jang, H.; Xie, Z.; Li, K.; Lee, J.; Jeong, J. Y.; Ryu, A.; Lee, Y.; Kim, D. H.; Wang, X.; Lee, K.; Lee, J. Y.; Won, S. M.; Oh, N.; Kim, J.; Kim, J. Y.; Jeong, S.-J.; Jang, K.-I.; Lee, S.; Huang, Y.; Zhang, Y.; Rogers, J. A. Mechanically Guided Post-Assembly of 3D Electronic Systems. *Advanced Functional Materials* **2018**, *28* (48), 1803149. https://doi.org/10.1002/adfm.201803149.
(35) Liu, Y.; Genzer, J.; Dickey, M. D. "2D or Not 2D": Shape-Programming Polymer Sheets. *Progress in Polymer Science* **2016**, *52*, 79–106. https://doi.org/10.1016/j.progpolymsci.2015.09.001.
(36) Lazarus, N.; Smith, G. L. Laser Forming for Complex 3D Folding. *Advanced Materials Technologies* **2017**, *2* (10), 1700109. https://doi.org/10.1002/admt.201700109.
(37) Lazarus, N.; Bedair, S. S.; Smith, G. L. Origami Inductors: Rapid Folding of 3-D Coils on a Laser Cutter. *IEEE Electron Device Letters* **2018**, *39* (7), 1046–1049. https://doi.org/10.1109/LED.2018.2841638.
(38) Geiger, M.; Vollertsen, F. The Mechanisms of Laser Forming. *CIRP Annals* **1993**, *42* (1), 301–304. https://doi.org/10.1016/S0007-8506(07)62448-2.
(39) Wu, C.-L.; Li, F.-C.; Pao, C.-W.; Srolovitz, D. J. Folding Sheets with Ion Beams. *Nano Lett.* **2017**, *17* (1), 249–254. https://doi.org/10.1021/acs.nanolett.6b03976.
(40) Leong, T. G.; Lester, P. A.; Koh, T. L.; Call, E. K.; Gracias, D. H. Surface Tension-Driven Self-Folding Polyhedra. *Langmuir* **2007**, *23* (17), 8747–8751. https://doi.org/10.1021/la700913m.
(41) Scully, Kevin. Laser Line Heating. *Journal of Ship Production* **1987**, *3* (4), 237–246.
(42) Yang, L.; Wang, M.; Wang, Y.; Chen, Y. Dynamic Analysis on Laser Forming of Square Metal Sheet to Spherical Dome. *Int J Adv Manuf Technol* **2010**, *51* (5), 519–539. https://doi.org/10.1007/s00170-010-2636-0.
(43) Seong, W.-J.; Jeon, Y.-C.; Na, S.-J. Ship-Hull Plate Forming of Saddle Shape by Geometrical Approach. *Journal of Materials Processing Technology* **2013**, *213* (11), 1885–1893. https://doi.org/10.1016/j.jmatprotec.2013.04.017.
(44) Cai, Z.-Y.; Lan, Y.-W.; Li, M.-Z.; Hu, Z.-Q.; Wang, M. Continuous Sheet Metal Forming for Doubly Curved Surface Parts. *Int. J. Precis. Eng. Manuf.* **2012**, *13* (11), 1997–2003. https://doi.org/10.1007/s12541-012-0263-4.

(45) Smith, G. L.; Lazarus, N.; McCormick, S. Laser Folded Antenna. In *2018 IEEE MTT-S International Microwave Workshop Series on Advanced Materials and Processes for RF and THz Applications (IMWS-AMP)*; 2018; pp 1–3. https://doi.org/10.1109/IMWS-AMP.2018.8457156.
(46) Walczyk, D. F.; Vittal, S. Bending of Titanium Sheet Using Laser Forming. *Journal of Manufacturing Processes* **2000**, *2* (4), 258–269. https://doi.org/10.1016/S1526-6125(00)70027-2.
(47) Watkins, K. G.; Edwardson, S. P.; Magee, J.; Dearden, G.; French, P.; Cooke, R. L.; Sidhu, J.; Calder, N. J. Laser Forming of Aerospace Alloys; 2001; pp 2001-01–2610. https://doi.org/10.4271/2001-01-2610.
(48) Guglielmotti, A.; Quadrini, F.; Squeo, E. A.; Tagliaferri, V. Laser Bending of Aluminum Foam Sandwich Panels. *Advanced Engineering Materials* **2009**, *11* (11), 902–906. https://doi.org/10.1002/adem.200900111.
(49) Gärtner, E.; Frühauf, J.; Löschner, U.; Exner, H. Laser Bending of Etched Silicon Microstructures. *Microsystem Technologies* **2001**, *7* (1), 23–26. https://doi.org/10.1007/s005420000065.
(50) Wu, D.; Zhang, Q.; Ma, G.; Guo, Y.; Guo, D. Laser Bending of Brittle Materials. *Optics and Lasers in Engineering* **2010**, *48* (4), 405–410. https://doi.org/10.1016/j.optlaseng.2009.09.009.
(51) Okamoto Y.; Uno Y.; Ohta K.; Shibata T.; Kubota S.; Namba Y. Study on Precision Laser Forming of Plastic with YAG Laser. *Journal of the Japan Society for Precision Engineering* **2000**, *66* (6), 891–895. https://doi.org/10.2493/jjspe.66.891.
(52) Arnet, H.; Vollertsen, F. Extending Laser Bending for the Generation of Convex Shapes. *Proceedings of the Institution of Mechanical Engineers, Part B: Journal of Engineering Manufacture* **1995**, *209* (6), 433–442. https://doi.org/10.1243/PIME_PROC_1995_209_107_02.
(53) Thomson, G.; Pridham, M. S. Controlled Laser Forming for Rapid Prototyping. *Rapid Prototyping Journal* **1997**, *3* (4), 137–143. https://doi.org/10.1108/13552549710191845.
(54) Bachmann, A. L.; Dickey, M. D.; Lazarus, N. Making Light Work of Metal Bending: Laser Forming in Rapid Prototyping. *Quantum Beam Science* **2020**, *4* (4), 44. https://doi.org/10.3390/qubs4040044.
(55) Umapathi, U.; Chen, H.-T.; Mueller, S.; Wall, L.; Seufert, A.; Baudisch, P. LaserStacker: Fabricating 3D Objects by Laser Cutting and Welding. In *Proceedings of the 28th Annual ACM Symposium on User Interface Software & Technology*; UIST '15; Association for Computing Machinery: New York, NY, USA, 2015; pp 575–582. https://doi.org/10.1145/2807442.2807512.
(56) Nisser, M.; Liao, C. C.; Chai, Y.; Adhikari, A.; Hodges, S.; Mueller, S. LaserFactory: A Laser Cutter-Based Electromechanical Assembly and Fabrication Platform to Make Functional Devices & Robots. In *Proceedings of the 2021 CHI Conference on Human Factors in Computing Systems*; CHI '21; Association for Computing Machinery: New York, NY, USA, 2021; pp 1–15. https://doi.org/10.1145/3411764.3445692.
(57) Lazarus, N.; Smith, G. L. Laser Folding in a Roll-to-Roll Manufacturing Process. *Lasers in Manufacturing and Materials Processing* **2018**, *5* (3), 237–247. https://doi.org/10.1007/s40516-018-0064-4.
(58) Shen, H.; Vollertsen, F. Modelling of Laser Forming – An Review. *Computational Materials Science* **2009**, *46* (4), 834–840. https://doi.org/10.1016/j.commatsci.2009.04.022.

(59) Lawrence, J. A Comparative Investigation of the Efficacy of CO 2 and High-Power Diode Lasers for the Forming of EN3 Mild Steel Sheets. *Proceedings of the Institution of Mechanical Engineers, Part B: Journal of Engineering Manufacture* **2002**, *216* (11), 1481–1491. https://doi.org/10.1243/095440502320783521.
(60) Optical Properties of Selected Elements. In *CRC Handbook of Chemistry and Physics*; CRC Press/Taylor & Francis.
(61) Gautam, S. S.; Singh, S. K.; Dixit, U. S. Laser Forming of Mild Steel Sheets Using Different Surface Coatings. In *Lasers Based Manufacturing: 5th International and 26th All India Manufacturing Technology, Design and Research Conference, AIMTDR 2014*; Joshi, S. N., Dixit, U. S., Eds.; Topics in Mining, Metallurgy and Materials Engineering; Springer India: New Delhi, 2015; pp 17–39. https://doi.org/10.1007/978-81-322-2352-8_2.
(62) Vásquez-Ojeda, C.; Ramos-Grez, J. Bending of Stainless Steel Thin Sheets by a Raster Scanned Low Power CO2 Laser. *Journal of Materials Processing Technology* **2009**, *209* (5), 2641–2647. https://doi.org/10.1016/j.jmatprotec.2008.06.026.
(63) Kitada, K.; Asahi, N. Laser Adjustment of Beryllium Copper Sheet Using Temperature Gradient Mechanism. In *Third International Symposium on Laser Precision Microfabrication*; International Society for Optics and Photonics, 2003; Vol. 4830, pp 30–35. https://doi.org/10.1117/12.486552.
(64) Chen, G.; Xu, X. Experimental and 3D Finite Element Studies of CW Laser Forming of Thin Stainless Steel Sheets. *Journal of Manufacturing Science and Engineering* **2000**, *123* (1), 66–73. https://doi.org/10.1115/1.1347036.
(65) Paeng, D.; Yoo, J.-H.; Yeo, J.; Lee, D.; Kim, E.; Ko, S. H.; Grigoropoulos, C. P. Low-Cost Facile Fabrication of Flexible Transparent Copper Electrodes by Nanosecond Laser Ablation. *Advanced Materials* **2015**, *27* (17), 2762–2767. https://doi.org/10.1002/adma.201500098.
(66) Zhang, W.; Yao, Y. L.; Chen, K. Modelling and Analysis of UV Laser Micromachining of Copper. *Int J Adv Manuf Technol* **2001**, *18* (5), 323–331. https://doi.org/10.1007/s001700170056.
(67) Tanaka, T. Optical Constants of Polycrystalline 3d Transition Metal Oxides in the Wavelength Region 350 to 1200 Nm. *Jpn. J. Appl. Phys.* **1979**, *18* (6), 1043. https://doi.org/10.1143/JJAP.18.1043.
(68) Lin, J.; Peng, Z.; Liu, Y.; Ruiz-Zepeda, F.; Ye, R.; Samuel, E. L. G.; Yacaman, M. J.; Yakobson, B. I.; Tour, J. M. Laser-Induced Porous Graphene Films from Commercial Polymers. *Nature Communications* **2014**, *5*, 5714. https://doi.org/10.1038/ncomms6714.
(69) Ang, L. K.; Lau, Y. Y.; Gilgenbach, R. M.; Spindler, H. L. Analysis of Laser Absorption on a Rough Metal Surface. *Appl. Phys. Lett.* **1997**, *70* (6), 696–698. https://doi.org/10.1063/1.118242.
(70) Kügler, H.; Vollertsen, F. Determining Absorptivity Variations of Multiple Laser Beam Treatments of Stainless Steel Sheets. *Journal of Manufacturing and Materials Processing* **2018**, *2* (4), 84. https://doi.org/10.3390/jmmp2040084.
(71) Ursu, I.; Nistor, L. C.; Teodorescu, V. S.; Mihailescu, I. N.; Apostol, I.; Nanu, L.; Prokhorov, A. M.; Chapliev, N. I.; Konov, V. I.; Tokarev, V. N. Continuous Wave Laser Oxidation Of Copper. In *Industrial Applications of Laser Technology*; International Society for Optics and Photonics, 1983; Vol. 0398, pp 398–402. https://doi.org/10.1117/12.935405.
(72) Lewis, J. A.; Ahn, B. Y. Three-Dimensional Printed Electronics. *Nature* **2015**, *518* (7537), 42–43. https://doi.org/10.1038/518042a.

(73) Hao, Y.; Lien, J.-M. Computational Laser Forming Origami of Convex Surfaces. In *Proceedings of the ACM Symposium on Computational Fabrication - SCF '19*; ACM Press: Pittsburgh, Pennsylvania, 2019; pp 1–11. https://doi.org/10.1145/3328939.3329006.
(74) Exner, H.; Loschner, U. Contactless Laser Bending of Silicon Microstructures; Chiao, J.-C., Varadan, V. K., Can, C., Eds.; Maspalomas, Gran Canaria, Canary Islands, Spain, 2003; p 383. https://doi.org/10.1117/12.498961.
(75) Khuje, S.; Sheng, A.; Yu, J.; Ren, S. Flexible Copper Nanowire Electronics for Wireless Dynamic Pressure Sensing. *ACS Appl. Electron. Mater.* **2021**, *3* (12), 5468–5474. https://doi.org/10.1021/acsaelm.1c00905.

Chapter 4: Laser Induced Graphene from SU-8 Photoresist: Toward Functional Micromolding

Adam L. Bachmann[a], Alan L. Ferris[a], Sooik Im[a] Michael D. Dickey[a], Nathan Lazarus[b]*

[a] Department of Chemical and Biomolecular Engineering, North Carolina State University, Raleigh, North Carolina, 27695

[b] Sensors and Electron Devices Directorate, US Army Research Laboratory, 2800 Powder Mill Road, Adelphi, Maryland 20783, United States

Abstract

Micromolding silicone elastomers has many uses in microfluidics, soft lithography and microfabrication but usually require further processing to integrate functional materials like electrodes. Herein, we report a simple method to pattern and integrate electrodes into micromolded elastomers in a single step by using laser-induced graphene (LIG) on SU-8, which is a popular photoresist. We characterized the role of laser power on the resulting graphitized SU-8, resulting in an unprecedented sheet resistance of 4 Ω sq^{-1}, an order of magnitude lower than anything reported to date. Raman spectroscopy confirms the porous carbon film is composed of large graphene domains, thereby demonstrating that SU-8 is an excellent LIG precursor. SU-8 is frequently used for molding silicones and laser graphitized SU-8 embeds conductive traces during the molding step. This process is used to produce a soft heater that can generate temperatures in excess of 40 °C with just 15 volts applied.

4.1 Introduction

Graphene is a 2D sheet of carbon that has many uses owing to its unique optical, mechanical, and electrical properties.[1,2] These properties make graphene useful in sensors,[3] thermal energy devices,[4] and in biomedical devices.[5] The first report of graphene involved mechanical exfoliation from bulk graphite,[6] but the flakes were small. Encouraged by this first report of graphene, researchers developed techniques to manufacture large area sheets using chemical vapor deposition.[7] Chemical vapor deposition produces high-quality graphene but is an expensive technology so cheaper alternatives were investigated. Improved exfoliation techniques were reported[8,9] that produced large flakes of few- and single-layer graphene. Graphene is hydrophobic which makes solution processing the flakes difficult, but graphene oxide is not owing to its many functional groups. This easy processing has lead others to produce graphene-based devices by reducing graphene oxide.[10,11]

Effective integration of graphene into electronic devices requires more than just high-quality, large area flakes; these flakes must be patterned. Numerous patterning techniques have been developed such as inkjet printing,[12] transfer methods,[13] and even screen printing.[14] A recent patterning technique is laser-induced graphene (LIG) in which a scanning laser locally converts a polymer substrate into a porous graphene foam, effectively writing circuity on the insulating layer.[15]

From the original report of laser-induced graphene using polyimide, researchers demonstrated that careful control of laser settings enables LIG to be generated from sulfonated polymers,[16,17] wood,[22] biomass-derived polymers,[19] and doped polymer films.[20] This wide substrate choice has led to LIG being used in catalysis,[21] flexible electronics,[22] and in sensors.[23] CO_2 lasers are often used for LIG owing to the strong absorption of organic materials at the 10.6

μm laser wavelength. This large wavelength limits the spot size of the focused laser beam so high-resolution patterns remain challenging. Based on older reports of laser-induced carbonization,[24–26] LIG has also been prepared using visible wavelength[27,28] and ultraviolet lasers[29] that would potentially enable higher resolutions.

Another method to limit the spot size is by scanning the CO_2 laser over a patterned polymer substrate with feature sizes smaller than the focused beam diameter. For example, S1818,[30] a positive photoresist (PR), is a viable substrate for LIG using a CO_2 laser. Another potential resist is SU-8, a negative PR that finds broad applications in microelectromechanical systems[31] and as molds for soft lithography[32] and soft microfluidics.[33,34] Prior studies report laser carbonization of SU-8 by adding an absorber to improve sensitivity to an 806 nm laser.[35] The addition of an absorbing modifier, however, limits the use of SU-8 in photolithography. The researchers also mention that a CO_2 laser can carbonize both modified and unmodified SU-8, but the conductivities were much lower than previous reported LIG, suggesting LIG was not formed. Owing to the broad use of SU-8, we investigated the LIG process on SU-8 using a CO_2 laser. LIG can be transferred to elastomers,[34,35] so successful conversion of SU-8 to LIG would enable single-step production of molded silicone with integrated electrodes.

Herein, we report the successful production of laser-induced graphene using SU-8 as a carbon source. These LIG films from SU-8 are, to our knowledge, more conductive than any previously reported LIG owing to the high thermal stability and high crosslink density of the SU-8 photoresist. Furthermore, the laser carbonized SU-8 patterns can be used to mold silicone elastomers. The LIG layer transfers to the elastomer during molding, thereby providing an easy method to fabricate compliant electrodes in molded silicone. We demonstrate an example in which the electrodes serve as heaters in silicone microfluidic channels.

4.2 Results and Discussion

We used a low-cost CO_2 (λ = 10.6 μm) to carbonize photolithographically patterned SU-8 that is then used as a template for PDMS soft lithography. The carbonized layer is loosely bound to the supporting SU-8 so when the PDMS peels off from the SU-8 mold, the carbonized layer transfers to the PDMS microchannel. This process is shown in **Figure 4.1a**. Care must be taken when designing asymmetric photomasks as the image of the carbonized SU-8 becomes inverted after the transfer process (**Figure 4.1b**).

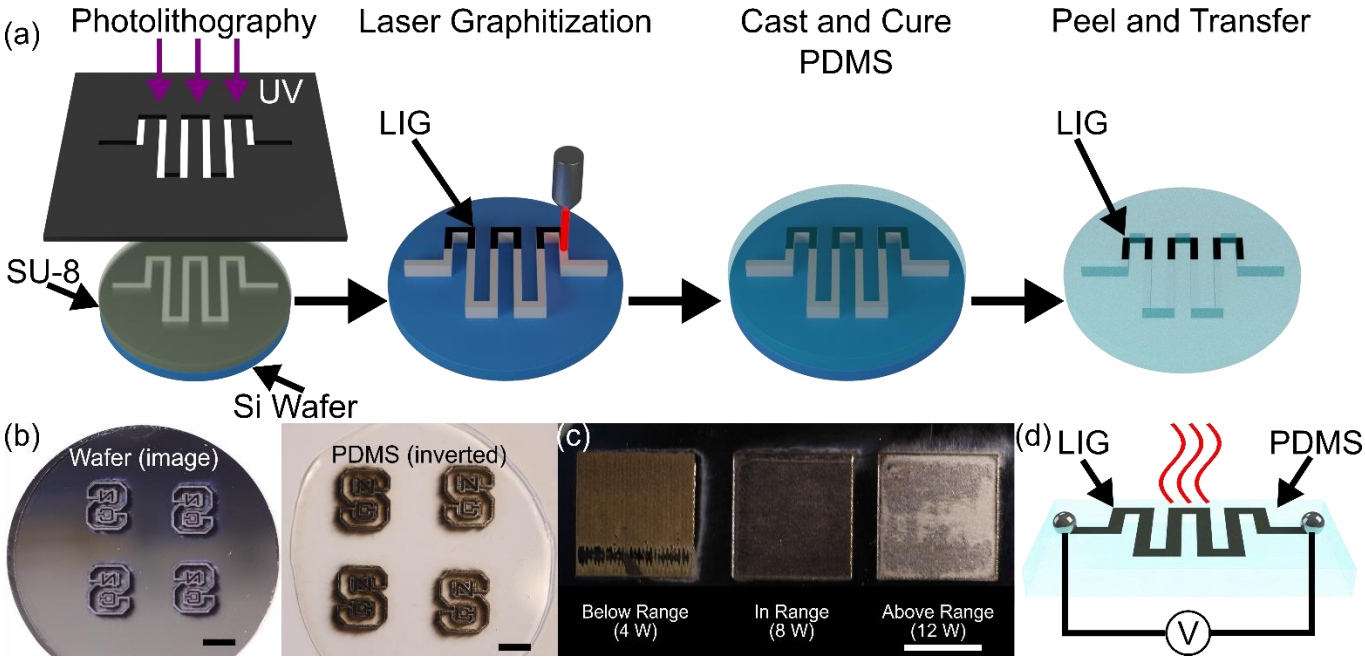

Figure 4.1. Schematic of the process (a) showing photolithographically patterned SU-8 carbonized by a CO2 laser. PDMS is cast and cured against the structures to mold the PDMS. Peeling the PDMS from the surface results in a molded silicone with embedded, conductive carbon features. (b) Photograph of photopatterned and carbonized SU-8 on a Si wafer. The carbon transfers to the PDMS, as shown on the image on the right, inverting the image. (c) LIG formed on SU-8 between 5 and 10 W of average power. At lower power, the laser caused incomplete carbonization and yellowing. At higher power, extensive ablation occurs. (d) Schematic of a soft heater. The carbonized film transfers to PDMS and can be used as a heating element by supplying a voltage difference. All scale bars are 1 cm.

To study the role of laser process parameters on SU-8 2050, we first exposed a 60 μm thick film of SU-8 to UV light and applied the post-exposure bake (following the directions from the manufacturer). We then laser carbonized these films under various laser power settings while

holding constant the laser scan speed and the pulses per inch (PPI). Below an average power of 5 W, we observed a slight discoloration in the PR film (**Figure 4.1c**), and it was not conductive. At P = 5 W, a black film was observed on the surface, which was conductive, indicating successful laser carbonization. Higher powers continued to produce dark films until P = 10 W, at which point ablation became dominant and a conductive layer was no longer observed. SU-8 is a common photoresist for micromolding so SU-8 LIG could enable functional micromolding to produce soft devices, such as a heater (**Figure 4.1d**). With this processing range established, we characterized the sheet resistance of the laser carbonized SU-8 films as a function of the average laser power.

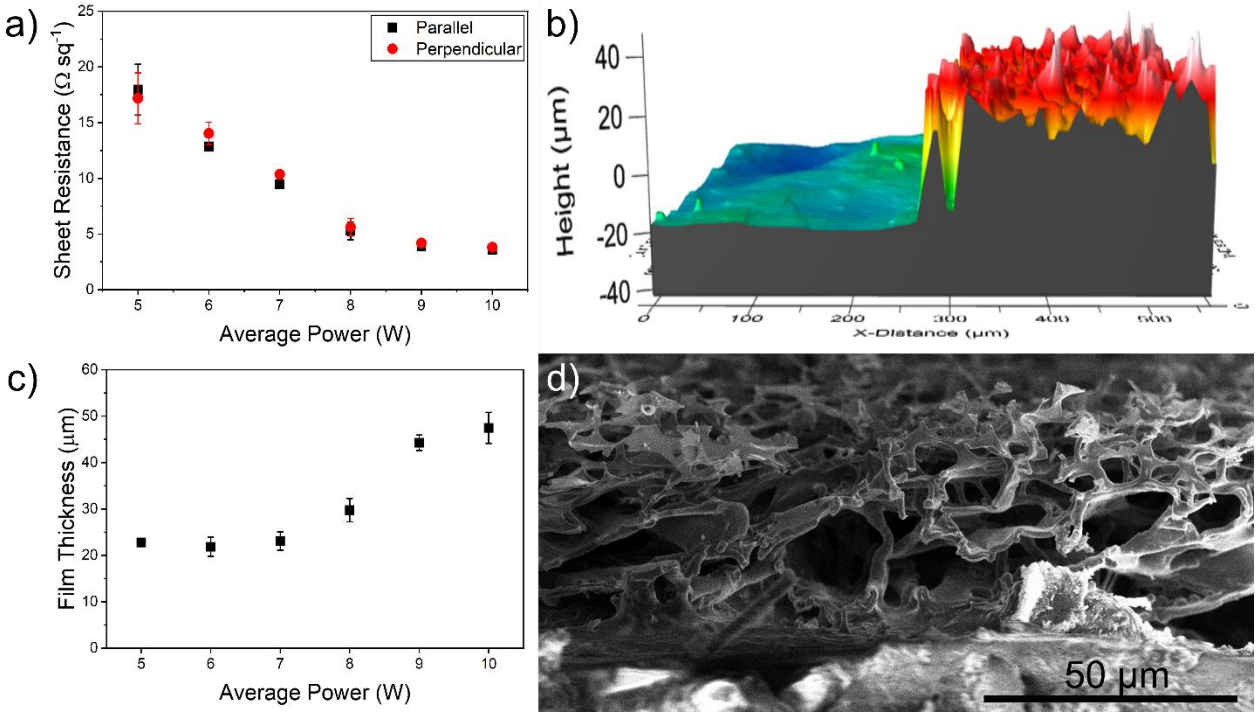

Figure 4.2. Sheet resistance (a) of the laser carbonized SU-8 as a function of average laser power measured using a linear four-point probe. Parallel refers to measuring the sheet resistance when the probes are parallel to the laser scan direction. Error bars are the standard deviation of measurements from 3 samples. Optical profilometry (b) of cross-sectioned samples of carbonized SU-8 films showing an average thickness ~40 µm. The bottom of the sample is SU-8 that was not carbonized by the laser. The film thickness was measured as a function of the average laser power (c). Cross-sectional electron micrograph (d) of a SU-8 film carbonized at 7W showing the porous graphene structure.

A previous report of laser-induced graphene on photoresist[30] measured sheet resistances of ~10 kΩ sq^{-1} using a focused laser and an optimized sheet resistance of ~120 Ω sq^{-1} by defocusing the laser by 2 mm. When lasing SU-8, we measured sheet resistances ~20 Ω sq^{-1} with an optimized sheet resistance of ~4 Ω sq^{-1}, all at the focal plane (**Figure 4.2a**). The LIG process involves the laser scanning across the surface one "row" at a time. We reasoned this could produce some anisotropy in the resulting film, so we measured the sheet resistance in the direction parallel to the laser scan direction and perpendicular to this direction and found minimal anisotropy in the films. Sheet resistance is not an intrinsic property of materials, so we cross-sectioned the sample and performed optical profilometry (**Figure 4.2b**) to evaluate the carbonized film thickness as a function of the average laser power (**Figure 4.2c**). We reasoned that the low sheet resistance of SU-8 derived LIG can be explained by the extensive crosslinking of the negative-tone photoresist that allows it to form a more ordered carbon when the laser converts it to a porous film (**Figure 4.2d**).

The previous report on LIG derived from a PR used a positive-tone resist, S1818,30 which is derived from novolak resins like SU-8. During photolithography, the positive resist, S1818, becomes more soluble while the negative resist, SU-8 becomes densely crosslinked and less soluble. Crosslinking has been shown to enable the formation of LIG16 in which polystyrene ablated and did not carbonize, but a highly crosslinked polystyrene, Rexolite®, did form LIG. We thus attribute the improved electrical properties of LIG derived from SU-8 to the extensive crosslinking during the photopatterning process. Having measured the electrical properties of LIG from SU-8, we sought to characterize the structure of the carbonized film. Raman spectroscopy is a non-destructive method to probe the vibrational modes of molecules

that works exceedingly well on carbonaceous materials as there are only three main peaks, but the peak intensities and shape provide extensive information on the structure.38–40

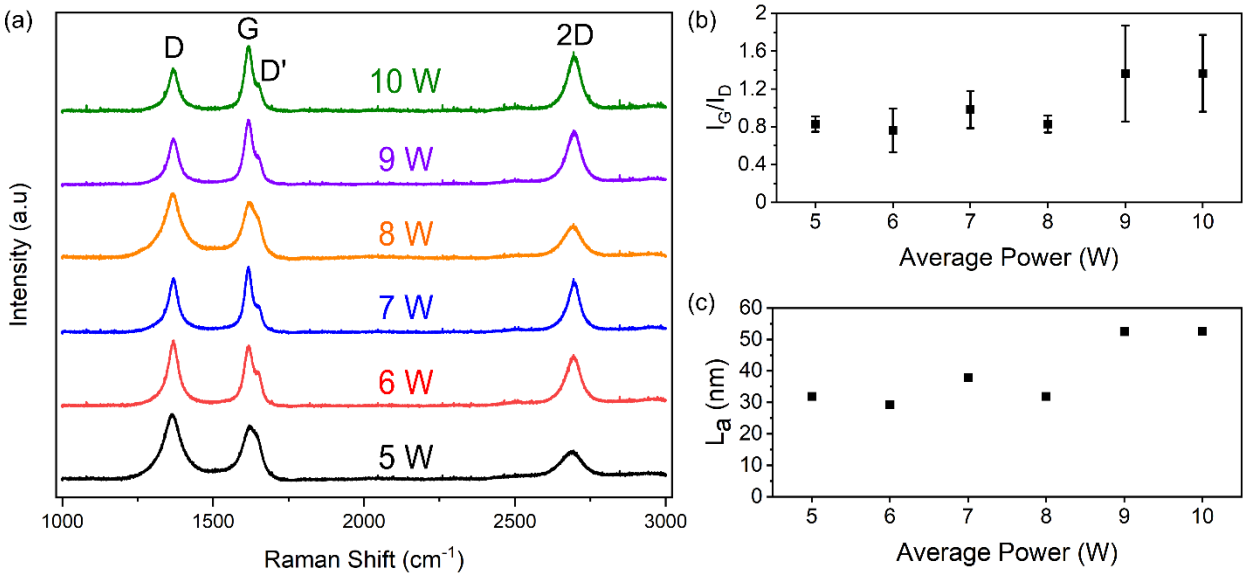

Figure 4.3. Normalized Raman spectra (a) of laser-carbonized SU-8 as a function of the average laser power used. The intensity of the D peak decreases as laser power increases, indicating formation of a more ordered graphene as the D peak results from a defect-activated process. The G peak is always present in graphitic carbons, so the ratio of the integrated intensities IG/ID (b) is used to characterize the quality of graphene. (c) From the intensity ratio, the crystallite size (La) of the graphene can be estimated.

Ideal graphene is a repeating lattice of sp^2-hybridized carbons which means the only vibrational mode permitted is the E_{2g} vibration mode that appears around 1580 cm^{-1} and is often called the G band and is found is almost any carbon material with sp^2 carbons.[40] Defect-free graphene also shows a band at ~2700 cm^{-1} that is often called the 2D band as it is the second order Raman scattering of the D band that appears ~1350 cm^{-1}. As a two-phonon process,[41] the 2D band is permitted even in defect-free graphene and is used to determine the number of layers in AB-stacked graphene.[41] The presence of defects permit another first-order Raman band to appear ~1350 cm^{-1} called the D band. Since this band requires defects to be observed, this band is highly correlated with the amount of disorder in the graphene sample.[38]

The normalized Raman spectra (**Figure 4.3a**) of LIG derived from SU-8 shows that all three of these bands are present suggesting that graphene with defects have been formed. As the average laser power increased, the D band intensity drops suggesting the LIG is more highly ordered from the increased energy entering the SU-8. A common metric is to compare the integrated intensity of the G band and the D band (**Figure 4.3b**) to determine the size of the graphene domains by assuming that most of the disorder is due to grain boundaries, so a large G/D band intensity would correspond to a large crystallite size,[42] but this logic ignores two key factors: the relationship between the band-intensity ratio and crystallite size is not a one-to-one function[43] and that the D band results from a resonant processes so it is dispersive—its position and intensity depends on the laser wavelength used to excite the Raman scattering.[41,44]

The problem of the D band being dispersive has been resolved by extending the conventional formula as a function of the excitation wavelength[45] which allows the average crystallite size to be estimated from the ratio of the band intensities (**Equation 1**):

$$L_a(nm) = (2.4 \times 10^{-10})\lambda_l^4 \left(\frac{I_G}{I_D}\right)$$

(**Equation 1**)

where λ_l is the excitation laser wavelength in nm (λ_l =632.8 nm). Using this formula, the calculated average crystallite sizes are plotted in **Figure 4.3c** as a function of laser power. Despite this formula accounting for the dispersive nature of the D band, it does not address the problem that the relationship between band intensity ratio and crystallite size is not a one-to-one function, but this can be solved by considering the 2D band. The relationship is one-to-one until the defect density is so high that the average crystallite size is only a couple of nanometers.[46] Nanocrystalline graphene, however, lacks a sharp 2D band ~2700 cm^{-1}.[43] The 2D bands in the Raman spectra confirm that the LIG produced from SU-8 is not nanocrystalline and the

crystallite size can be assigned unambiguously. The large crystallite size obtained from the Raman spectra is in good agreement with the low sheet resistance of LIG formed from SU-8.

Having characterized the electrical and structural properties of LIG produced from SU-8, we sought to fabricate a device that used the photopatternability of SU-8. SU-8 is a popular photoresist for soft lithography and microfluidics as the thick films produce robust molds that are used to shape soft elastomers.32,34,47 After patterning the SU-8, we selectively laser carbonized certain regions with 9 W average power and then cast PDMS (Sylgard-184, Dow) on top of these structures. After curing, the PDMS was peeled from the silicon wafer. The LIG transferred to the PDMS, as expected based on the ability of LIG to transfer from other polymers.36

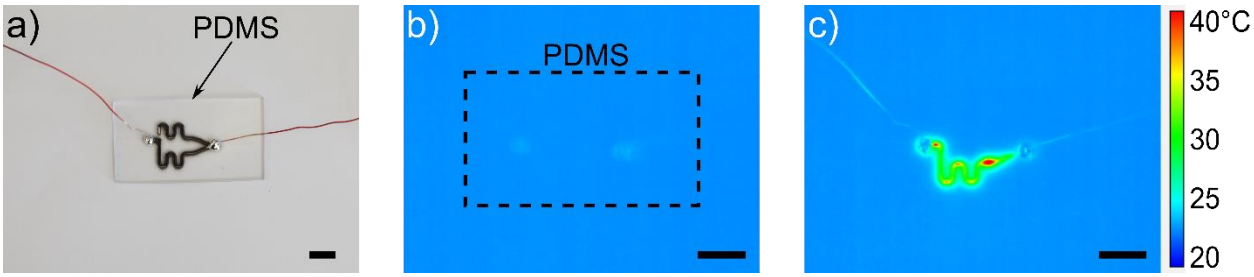

Figure 4.4. A photograph (a) showing the LIG transferred to the PDMS as well as the microchannels formed indicating the one-step production of microfluidic channel with an embedded electrode. The sample is at a uniform temperature (b) before voltage is applied to the LIG. When the power supply is turned on, the sample heats up (c) along the LIG pathway. Scale bars are 1 cm.

The transferred LIG was then connected to a power supply using copper wires and droplets of liquid metal (eutectic gallium-indium) to make good electrical contact (**Figure 4.4a**). When applying 15 V, the sample begins to heat up only in the carbonized areas, up to 40 °C at steady state. In principle, the transferred LIG could also be used for radio frequency heating[48] or as a surface to which proteins could attach.[23]

4.3 Conclusion

We have successfully demonstrated the use of SU-8 as a valuable substrate for producing laser-induced graphene (LIG). The graphene produced is substantially more conductive than any previous report of LIG. The conductivity is consistent with the unusually large graphitic crystallites as calculated from the integrated intensity ratio between the G and D peak measured via Raman spectroscopy. The laser-carbonized SU-8 can be used as a mold for imparting topography into silicone elastomers. When the elastomer is peeled from the SU-8 mold, the LIG also transfers to the elastomer, resulting in conductive features. We show that these features can be used for Joule heating, but in principle conductive molded silicone could have a wide range of applications.

4.4 Experimental Methods

4.4.1 Materials

SU-8 2050 (Kayuka), propylene glycol monomethyl ether acetate (PGMEA) developer (Sigma-Aldrich) and isopropyl alcohol (VWR) were used as received. Silicon wafers (76.2 mm) were purchased from University Wafer. Eutectic gallium-indium (EGaIn) was purchased from Indium Corporation.

4.4.2 Sample Preparation

Silicon wafers were O_2-plasma (Diener Electronic) cleaned (100 W, 30 s, 40 kHz) to remove any adsorbed species and to promote adhesion with the SU-8 2050. SU-8 was spin coated onto the wafers to an expected thickness of about 60 μm.

After spin coating, the wafers were soft baked to remove residual solvent before being patterned using contact lithography and illuminated by an IntelliRay 400 UV flood lamp

(Uvitron). The exposed samples were then baked again to allow full cross-linking to occur, after which the samples were allowed to cool to room temperature.

Once cooled, the samples were developed by submerging them in PGMEA to dissolve any uncrosslinked SU-8. After development, the samples were rinsed with isopropyl alcohol before being blown dry with air and stored in a cabinet.

Dry films were then laser carbonized with a ULS 3.50 laser writer equipped with a 40 W CO_2 laser tube. All laser scribing was done at the focal plane with an image density of 1000 DPI (dots per inch) and 1000 LPI (lines per inch) at a scan speed of 15 cm s^{-1} in raster mode. Power was controlled by adjusting the laser duty cycle from 5% up to 50%. Duty cycle refers to the fraction of time that a pulsed laser is "on."

The carbonized PR was transferred to polydimethylsiloxane (PDMS) by mixing Sylgard-184 (Dow) in a 10:1 ratio of prepolymer to crosslinker in a planetary centrifugal mixer (Thinky Mixer AR250). The mixture was then poured over the laser carbonized PR in a petri dish (Fischer) and placed under vacuum for 5 minutes. The sample was the removed from the vacuum and crosslinked at 80 °C for 2 hours at ambient pressure. The PDMS film was peeled from the silicon wafer and the carbonized layer transfers to the PDMS while producing molded features in the elastomer.

Soft heaters were fabricated by placing drops of eutectic gallium-indium (EGaIn) to make reliable electrical connection with the transferred graphene film. Copper wires were then used to connect the EGaIn droplets to the power supply (Keithly 2450 source meter).

4.4.3 Sample Characterization

Raman spectroscopy was conducted with a Horiba LabRAM HR equipped with a He-Ne laser (λ = 632.8 nm) to excite the Raman vibrations. Spectra were recorded with a 100x objective

lens, and five spectra were averaged for each sample. Sheet resistance was measured using a Jandel Model RM3-AR 4-point probe station with 1 mm pin spacing. Carbonized film thickness was characterized by optical profilometry (Filmetrics profilm3D) and cross-sectional SEM (FEI Verios 460L).

4.4.4 Device Characterization

Soft heaters were characterized by observing Joule heating using an IR camera (FLIR) and was processed with the accompanying software (ExaminIR).

4.5 Acknowledgements

We wish to thank Luke Cunningham for help when making and composing illustrations. We gratefully acknowledge the financial sponsorship from the Army Research Laboratory and research was accomplished under Cooperative Agreement Number W911NF-20-2-0243. The views and conclusions contained in this document are those of the authors and should not be interpreted as representing the official policies, either expressed or implied, of the Army Research Laboratory or the U.S. Government. The U.S. Government is authorized to reproduce and distribute reprints for Government purposes notwithstanding any copyright notation herein.

4.6 References

(1) Geim, A. K. Graphene: Status and Prospects. *Science* **2009**. https://doi.org/10.1126/science.1158877.

(2) Ren, W.; Cheng, H.-M. *The global growth of graphene*. https://www.nature.com/articles/nnano.2014.229 (accessed 2018-01-12). https://doi.org/10.1038/nnano.2014.229.

(3) Ushiba, S.; Ono, T.; Kanai, Y.; Inoue, K.; Kimura, M.; Matsumoto, K. Graphene as an Imaging Platform of Charged Molecules. *ACS Omega* **2018**, *3* (3), 3137–3142. https://doi.org/10.1021/acsomega.7b02008.

(4) Li, Y.-T.; Tian, Y.; Sun, M.-X.; Tu, T.; Ju, Z.-Y.; Gou, G.-Y.; Zhao, Y.-F.; Yan, Z.-Y.; Wu, F.; Xie, D.; Tian, H.; Yang, Y.; Ren, T.-L. Graphene-Based Devices for Thermal Energy Conversion and Utilization. *Advanced Functional Materials* **2020**, *30* (8), 1903888. https://doi.org/10.1002/adfm.201903888.

(5) Reina, G.; González-Domínguez, J. M.; Criado, A.; Vázquez, E.; Bianco, A.; Prato, M. Promises, Facts and Challenges for Graphene in Biomedical Applications. *Chem. Soc. Rev.* **2017**, *46* (15), 4400–4416. https://doi.org/10.1039/C7CS00363C.

(6) Novoselov, K. S.; Geim, A. K.; Morozov, S. V.; Jiang, D.; Zhang, Y.; Dubonos, S. V.; Grigorieva, I. V.; Firsov, A. A. Electric Field Effect in Atomically Thin Carbon Films. *Science* **2004**, *306* (5696), 666–669. https://doi.org/10.1126/science.1102896.

(7) Sun, Z.; Yan, Z.; Yao, J.; Beitler, E.; Zhu, Y.; Tour, J. M. Growth of Graphene from Solid Carbon Sources. *Nature* **2010**, *468* (7323), 549–552. https://doi.org/10.1038/nature09579.

(8) Huang, Y.; Sutter, E.; Shi, N. N.; Zheng, J.; Yang, T.; Englund, D.; Gao, H.-J.; Sutter, P. Reliable Exfoliation of Large-Area High-Quality Flakes of Graphene and Other Two-Dimensional Materials. *ACS Nano* **2015**, *9* (11), 10612–10620. https://doi.org/10.1021/acsnano.5b04258.

(9) Nicolosi, V.; Chhowalla, M.; Kanatzidis, M. G.; Strano, M. S.; Coleman, J. N. Liquid Exfoliation of Layered Materials. *Science* **2013**, *340* (6139), 1226419. https://doi.org/10.1126/science.1226419.

(10) Eda, G.; Fanchini, G.; Chhowalla, M. Large-Area Ultrathin Films of Reduced Graphene Oxide as a Transparent and Flexible Electronic Material. *Nat Nano* **2008**, *3* (5), 270–274. https://doi.org/10.1038/nnano.2008.83.

(11) Wang, Y.; Hao, J.; Huang, Z.; Zheng, G.; Dai, K.; Liu, C.; Shen, C. Flexible Electrically Resistive-Type Strain Sensors Based on Reduced Graphene Oxide-Decorated Electrospun Polymer Fibrous Mats for Human Motion Monitoring. *Carbon* **2018**, *126*, 360–371. https://doi.org/10.1016/j.carbon.2017.10.034.

(12) Torrisi, F.; Hasan, T.; Wu, W.; Sun, Z.; Lombardo, A.; Kulmala, T. S.; Hsieh, G.-W.; Jung, S.; Bonaccorso, F.; Paul, P. J.; Chu, D.; Ferrari, A. C. Inkjet-Printed Graphene Electronics. *ACS Nano* **2012**, *6* (4), 2992–3006. https://doi.org/10.1021/nn2044609.

(13) Yun, J.; Lim, Y.; Lee, H.; Lee, G.; Park, H.; Hong, S. Y.; Jin, S. W.; Lee, Y. H.; Lee, S.-S.; Ha, J. S. A Patterned Graphene/ZnO UV Sensor Driven by Integrated Asymmetric Micro-Supercapacitors on a Liquid Metal Patterned Foldable Paper. *Advanced Functional Materials* **2017**, *27* (30), 1700135. https://doi.org/10.1002/adfm.201700135.

(14) Hyun, W. J.; Secor, E. B.; Hersam, M. C.; Frisbie, C. D.; Francis, L. F. High-Resolution Patterning of Graphene by Screen Printing with a Silicon Stencil for Highly Flexible Printed Electronics. *Advanced Materials* **2015**, *27* (1), 109–115. https://doi.org/10.1002/adma.201404133.

(15) Lin, J.; Peng, Z.; Liu, Y.; Ruiz-Zepeda, F.; Ye, R.; Samuel, E. L. G.; Yacaman, M. J.; Yakobson, B. I.; Tour, J. M. Laser-Induced Porous Graphene Films from Commercial Polymers. *Nature Communications* **2014**, *5*, 5714. https://doi.org/10.1038/ncomms6714.

(16) Chyan, Y.; Ye, R.; Li, Y.; Singh, S. P.; Arnusch, C. J.; Tour, J. M. Laser-Induced Graphene by Multiple Lasing: Toward Electronics on Cloth, Paper, and Food. *ACS Nano* **2018**, *12* (3), 2176–2183. https://doi.org/10.1021/acsnano.7b08539.

(17) Singh, S. P.; Li, Y.; Zhang, J.; Tour, J. M.; Arnusch, C. J. Sulfur-Doped Laser-Induced Porous Graphene Derived from Polysulfone-Class Polymers and Membranes. *ACS Nano* **2018**, *12* (1), 289–297. https://doi.org/10.1021/acsnano.7b06263.

(18) Le, T.-S. D.; Park, S.; An, J.; Lee, P. S.; Kim, Y.-J. Ultrafast Laser Pulses Enable One-Step Graphene Patterning on Woods and Leaves for Green Electronics. *Advanced Functional Materials* **2019**, *0* (0), 1902771. https://doi.org/10.1002/adfm.201902771.

(19) Hawes, G. F.; Yilman, D.; Noremberg, B. S.; Pope, M. A. Supercapacitors Fabricated via Laser-Induced Carbonization of Biomass-Derived Poly(Furfuryl Alcohol)/Graphene Oxide Composites. *ACS Appl. Nano Mater.* **2019**, *2* (10), 6312–6324. https://doi.org/10.1021/acsanm.9b01284.

(20) Peng, Z.; Ye, R.; Mann, J. A.; Zakhidov, D.; Li, Y.; Smalley, P. R.; Lin, J.; Tour, J. M. Flexible Boron-Doped Laser-Induced Graphene Microsupercapacitors. *ACS Nano* **2015**, *9* (6), 5868–5875. https://doi.org/10.1021/acsnano.5b00436.

(21) Ren, M.; Zheng, H.; Lei, J.; Zhang, J.; Wang, X.; Yakobson, B. I.; Yao, Y.; Tour, J. M. CO2 to Formic Acid Using Cu–Sn on Laser-Induced Graphene. *ACS Appl. Mater. Interfaces* **2020**, *12* (37), 41223–41229. https://doi.org/10.1021/acsami.0c08964.

(22) Zang, X.; Shen, C.; Chu, Y.; Li, B.; Wei, M.; Zhong, J.; Sanghadasa, M.; Lin, L. Laser-Induced Molybdenum Carbide–Graphene Composites for 3D Foldable Paper Electronics. *Advanced Materials* **2018**, *30* (26), 1800062. https://doi.org/10.1002/adma.201800062.

(23) Mamleyev, E. R.; Heissler, S.; Nefedov, A.; Weidler, P. G.; Nordin, N.; Kudryashov, V. V.; Länge, K.; MacKinnon, N.; Sharma, S. Laser-Induced Hierarchical Carbon Patterns on

Polyimide Substrates for Flexible Urea Sensors. *npj Flex Electron* **2019**, *3* (1), 1–11. https://doi.org/10.1038/s41528-018-0047-8.

(24) Davenas, J. Laser and Ion Beam Processing of Conductive Polyimide. *Applied Surface Science* **1989**, *36* (1), 539–544. https://doi.org/10.1016/0169-4332(89)90948-3.

(25) Schumann, M.; Sauerbrey, R.; Smayling, M. C. Permanent Increase of the Electrical Conductivity of Polymers Induced by Ultraviolet Laser Radiation. *Appl. Phys. Lett.* **1991**, *58* (4), 428–430. https://doi.org/10.1063/1.104624.

(26) Srinivasan, R.; Hall, R. R.; Wilson, W. D.; Loehle, W. D.; Allbee, D. C. Formation of a Porous, Patternable, Electrically Conducting Carbon Network by the Ultraviolet Laser Irradiation of the Polyimide PMDA-ODA (Kapton). *Chem. Mater.* **1994**, *6* (7), 888–889. https://doi.org/10.1021/cm00043a005.

(27) Stanford, M. G.; Zhang, C.; Fowlkes, J. D.; Hoffman, A.; Ivanov, I. N.; Rack, P. D.; Tour, J. M. High-Resolution Laser-Induced Graphene. Flexible Electronics beyond the Visible Limit. *ACS Appl. Mater. Interfaces* **2020**, *12* (9), 10902–10907. https://doi.org/10.1021/acsami.0c01377.

(28) Zhang, Z.; Song, M.; Hao, J.; Wu, K.; Li, C.; Hu, C. Visible Light Laser-Induced Graphene from Phenolic Resin: A New Approach for Directly Writing Graphene-Based Electrochemical Devices on Various Substrates. *Carbon* **2018**, *127*, 287–296. https://doi.org/10.1016/j.carbon.2017.11.014.

(29) Carvalho, A. F.; Fernandes, A. J. S.; Leitão, C.; Deuermeier, J.; Marques, A. C.; Martins, R.; Fortunato, E.; Costa, F. M. Laser-Induced Graphene Strain Sensors Produced by Ultraviolet Irradiation of Polyimide. *Advanced Functional Materials* **2018**, *28* (52), 1805271. https://doi.org/10.1002/adfm.201805271.

(30) Beckham, J. L.; Li, J. T.; Stanford, M. G.; Chen, W.; McHugh, E. A.; Advincula, P. A.; Wyss, K. M.; Chyan, Y.; Boldman, W. L.; Rack, P. D.; Tour, J. M. High-Resolution Laser-Induced Graphene from Photoresist. *ACS Nano* **2021**, *15* (5), 8976–8983. https://doi.org/10.1021/acsnano.1c01843.

(31) Lorenz, H.; Despont, M.; Fahrni, N.; LaBianca, N.; Renaud, P.; Vettiger, P. SU-8: A Low-Cost Negative Resist for MEMS. *J. Micromech. Microeng.* **1997**, *7* (3), 121–124. https://doi.org/10.1088/0960-1317/7/3/010.

(32) Xia, Y.; Whitesides, G. M. Soft Lithography. *Annual Review of Materials Science* **1998**, *28* (1), 153–184. https://doi.org/10.1146/annurev.matsci.28.1.153.

(33) Zhang, J.; Tan, K. L.; Hong, G. D.; Yang, L. J.; Gong, H. Q. Polymerization Optimization of SU-8 Photoresist and Its Applications in Microfluidic Systems and MEMS. *J. Micromech. Microeng.* **2000**, *11* (1), 20–26. https://doi.org/10.1088/0960-1317/11/1/304.

(34) Saberi-Bosari, S.; Huayta, J.; San-Miguel, A. A Microfluidic Platform for Lifelong High-Resolution and High Throughput Imaging of Subtle Aging Phenotypes in C. Elegans. *Lab on a Chip* **2018**, *18* (20), 3090–3100. https://doi.org/10.1039/C8LC00655E.

(35) Ludvigsen, E.; Pedersen, N. R.; Zhu, X.; Marie, R.; Mackenzie, D. M. A.; Emnéus, J.; Petersen, D. H.; Kristensen, A.; Keller, S. S. Selective Direct Laser Writing of Pyrolytic Carbon Microelectrodes in Absorber-Modified SU-8. *Micromachines* **2021**, *12* (5), 564. https://doi.org/10.3390/mi12050564.

(36) Rahimi, R.; Ochoa, M.; Yu, W.; Ziaie, B. Highly Stretchable and Sensitive Unidirectional Strain Sensor via Laser Carbonization. *ACS Appl. Mater. Interfaces* **2015**, *7* (8), 4463–4470. https://doi.org/10.1021/am509087u.

(37) Lamberti, A.; Clerici, F.; Fontana, M.; Scaltrito, L. A Highly Stretchable Supercapacitor Using Laser-Induced Graphene Electrodes onto Elastomeric Substrate. *Advanced Energy Materials* **2016**, *6* (10), 1600050. https://doi.org/10.1002/aenm.201600050.

(38) Ferrari, A. C. Raman Spectroscopy of Graphene and Graphite: Disorder, Electron–Phonon Coupling, Doping and Nonadiabatic Effects. *Solid State Communications* **2007**, *143* (1), 47–57. https://doi.org/10.1016/j.ssc.2007.03.052.

(39) Ferrari, A. C.; Basko, D. M. Raman Spectroscopy as a Versatile Tool for Studying the Properties of Graphene. *Nature Nanotech* **2013**, *8* (4), 235–246. https://doi.org/10.1038/nnano.2013.46.

(40) Ferrari, A. C.; Robertson, J. Interpretation of Raman Spectra of Disordered and Amorphous Carbon. *Phys. Rev. B* **2000**, *61* (20), 14095–14107. https://doi.org/10.1103/PhysRevB.61.14095.

(41) Malard, L. M.; Pimenta, M. A.; Dresselhaus, G.; Dresselhaus, M. S. Raman Spectroscopy in Graphene. *Physics Reports* **2009**, *473* (5), 51–87. https://doi.org/10.1016/j.physrep.2009.02.003.

(42) Tuinstra, F.; Koenig, J. L. Raman Spectrum of Graphite. *J. Chem. Phys.* **1970**, *53* (3), 1126–1130. https://doi.org/10.1063/1.1674108.

(43) Cançado, L. G.; Jorio, A.; Ferreira, E. H. M.; Stavale, F.; Achete, C. A.; Capaz, R. B.; Moutinho, M. V. O.; Lombardo, A.; Kulmala, T. S.; Ferrari, A. C. Quantifying Defects in Graphene via Raman Spectroscopy at Different Excitation Energies. *Nano Lett.* **2011**, *11* (8), 3190–3196. https://doi.org/10.1021/nl201432g.

(44) Matthews, M. J.; Pimenta, M. A.; Dresselhaus, G.; Dresselhaus, M. S.; Endo, M. Origin of Dispersive Effects of the Raman ***D*** Band in Carbon Materials. *Phys. Rev. B* **1999**, *59* (10), R6585–R6588. https://doi.org/10.1103/PhysRevB.59.R6585.

(45) Cançado, L. G.; Takai, K.; Enoki, T.; Endo, M.; Kim, Y. A.; Mizusaki, H.; Jorio, A.; Coelho, L. N.; Magalhães-Paniago, R.; Pimenta, M. A. General Equation for the Determination of the Crystallite Size La of Nanographite by Raman Spectroscopy. *Appl. Phys. Lett.* **2006**, *88* (16), 163106. https://doi.org/10.1063/1.2196057.

(46) Ferrari, A. C.; Robertson, J. Resonant Raman Spectroscopy of Disordered, Amorphous, and Diamondlike Carbon. *Phys. Rev. B* **2001**, *64* (7), 075414. https://doi.org/10.1103/PhysRevB.64.075414.

(47) Kim, P.; Kwon, K. W.; Park, M. C.; Lee, S. H.; Kim, S. M.; Suh, K. Y. Soft Lithography for Microfluidics: A Review. **2008**.

(48) Gerringer, J. C.; Moran, A. G.; Habib, T.; Pospisil, M. J.; Oh, J. H.; Teipel, B. R.; Green, M. J. Radio Frequency Heating of Laser-Induced Graphene on Polymer Surfaces for Rapid Welding. *ACS Appl. Nano Mater.* **2019**. https://doi.org/10.1021/acsanm.9b01536.

Chapter 5: A Brief Future of Lasers: Outlook and Prospective Work

5.1 Introduction

This dissertation explored the role of lasers in manufacturing and rapid prototyping of electronic devices. Lasers are monochromatic beams of light that can be focused to small spot sizes allowing their effects to be highly localized. In these studies, the focused laser energy was converted to heat to locally drive physical and chemical transformations in numerous substrates.

Chapter 1 provided a brief historical overview of the development of laser technology, from the first reported laser in 1960[1] to modern analytical,[2] medical,[3] and manufacturing[4–6] methods that rely on the unique properties of lasers. Most, but not all, rely on the conversion of the laser energy to heat meaning lasers can be used as directed heat sources.

Chapter 2 reviewed the technique called laser forming and its applications in rapid prototyping. Laser forming is the use of laser to generate thermal stresses in materials causing them to fold. In sufficiently thick materials, the bending moment is large enough that the substrate shortens instead of folding. This shortening means laser forming can be used to produce non-developable surfaces[7] such as saddle shapes.[8] Laser forming is conventionally done on thick (> 1 mm) metal plates, but the use of light to make mechanical adjustments has been embraced as a quality-control technique for electronics.[9–11]

Chapter 3 reported the use of laser forming as a *manufacturing* technique for 3D electronic devices. Photolithography produces high-quality patterns but is limited to use on 2D substrates such as printed circuit boards. A two-step lasing process was developed that transforms flexible printed circuit boards (PCBs), a copper/polymer bilayer, into 3D structures while retaining electrical functionality. A single pass of a high-power (16 W) laser (λ = 1064 nm) drives surface oxidation of the copper. The copper oxides produced are strong absorbers at

the laser wavelength which enables folding to be done with lower laser powers (6 W), minimizing cutting in the thin bilayers. This laser forming technique was found to be compatible with conventional flexible PCB manufacturing with a commercial nickel/gold coating as an absorbing layer instead of laser-induced oxidation.

Chapter 4 explored the use of SU-8, a popular photoresist,[12,13] as a substrate for laser-induced graphene (LIG). LIG is a porous graphene film produced by localized pyrolysis from a laser beam.[14,15] SU-8 was investigated as a LIG precursor because it had similar thermal characteristics to previously reported LIG precursors[16,17] and its use as a mold for elastomers.[18,19] LIG produced from SU-8 had the lowest reported sheet resistance of any LIG previously reported which was attributed to the high crosslink density that enabled the formation of a highly ordered carbon during the laser pyrolysis. The enhanced ordering was confirmed by calculating the average crystallite size from Raman spectroscopy. Photopatterned SU-8 was then laser carbonized and used to mold a silicone elastomer. When the elastomer was peeled from the SU-8 mold, the LIG layer transferred to the elastomer, producing microchannels with an embedded electrode.

5.2 Further Research

Many laser technologies have seen industrial adoption,[20] but new techniques are constantly being developed, but often lack strong predictive models for the processing windows for new materials. The modelling of laser forming is a striking example of this problem. Despite using advanced finite-element models, computational predictions of the fold angle routinely deviates from the experimental values of multi-scan laser forming by more than 30%.[21]

Many factors contribute to the discrepancy between numerical and experimental results. The first source of error is the lack of thermophysical data for most systems. During laser

forming, the substrate is rapidly heated to just below melting. The thermal expansion coefficient, Young's modulus, and absorptivity are all functions of temperature so a lack of data means these important parameters need to be regressed from conditions far from the process conditions. Supposing careful experimental data was gathered, there remain assumptions on boundary conditions that could generate systematic errors. First, the samples are usually modeled as well defined, atomically smooth sheets of metal while most metals are rough and have surface oxides. These oxides can drastically modify the coupling of the laser to the substrate. Second, the laser is usually modelled as a moving gaussian heat flux, which is accurate in the limit of continuous-wave lasers, but many lasers are pulsed systems. The importance of laser pulse duration has been demonstrated in other laser processing technologies.[22–24] More accurate modelling would thus benefit from careful characterization of the lasers used, even for commercial systems.

During the investigation of low-power laser forming of flexible PCBs, laser-induced oxidation was observed. Laser-induced oxidation is well known,[25–27] but has been used to introduce various colors on metals when laser marking.[28,29] Recently, laser-induced oxidation was used to locally convert molybdenum sulfide into various oxide and sulfide phases to directly write conductors, insulators, and semiconductors from a single precursor.[30] Similarly, low-power lasers were used to enhance the photoluminescence of molybdenum sulfide by passivating sulfur vacancies with ambient water.[31] Taken together, lasers could be used to tune the electronic and opto-electronics properties of numerous materials. Laser-oxidation/passivation may find use in manufacturing perovskite solar cells,[32] or quantum dots[33] where surface defects in these materials can lead to pronounced losses from inhibited charge transfer.

While not as mature at photolithography, 3D printing is a rapid prototyping technology that has become very popular in recent years.[34] 3D printing encompasses numerous process with

fused filament fabrication (FFF) being the most popular. The FFF process builds up a 3D object layer by layer, but the poor interaction between layers often leads to diminished mechanical properties. Lasers could be used for microannealing between the printed layers[35] to strengthen these 3D printed parts by promoting sintering[36] or polymer interpenetration.[37] Many of the polymers used in FFF have a low glass-transition temperature which makes them poor candidates for laser-induced graphene (LIG).[16] There exist thermally robust filaments that can be used for LIG[38] but these filaments tend to be expensive. Based on previous reports[16] and the study of LIG using SU-8, extensive crosslinking can minimize ablation and promote graphitization. Thus, highly crosslinked structures from vat polymerization or two-photon lithography are promising candidates for 3D electronic structures using LIG.

Last, laser forming and LIG are not mutually exclusive processes. Flexible printed circuit boards use a polymer layer for support and as a dielectric. One of the most common polymers is polyimide which was the first reported substrate to form LIG.[14] A resistive element can be laser scribed into the polymer as LIG that can then connect with a lithographically patterned circuit. The entire structure could then be laser formed to produce 3D electronics. For certain applications, the polymer might be sufficient for both LIG and bending as laser forming is nearly material agnostic and has been demonstrated in polymer films.[39,40]

Lasers have rapidly transitioned from physical curiosity[41] to valuable tools in the manufacturing,[42] modification,[43] and measurement[2,44] of materials. Modern lasers span all the way from low-powered continuous-wave laser pointers[45] to petawatt pulsed lasers delivering hundreds of joules of energy in femtosecond pulses.[46] With a wide range of powers and pulse durations, the future of laser manufacturing looks bright.

5.3 References

(1) Maiman, T. H. Stimulated Optical Radiation in Ruby. *Nature* **1960**, *187* (4736), 493–494. https://doi.org/10.1038/187493a0.

(2) Charvat, A.; Abel, B. How to Make Big Molecules Fly out of Liquid Water: Applications, Features and Physics of Laser Assisted Liquid Phase Dispersion Mass Spectrometry. *Phys. Chem. Chem. Phys.* **2007**, *9* (26), 3335–3360. https://doi.org/10.1039/B615114K.

(3) Peng, Q.; Juzeniene, A.; Chen, J.; Svaasand, L. O.; Warloe, T.; Giercksky, K.-E.; Moan, J. Lasers in Medicine. *Rep. Prog. Phys.* **2008**, *71* (5), 056701. https://doi.org/10.1088/0034-4885/71/5/056701.

(4) Farsari, M.; Chichkov, B. N. Two-Photon Fabrication. *Nature Photon* **2009**, *3* (8), 450–452. https://doi.org/10.1038/nphoton.2009.131.

(5) Wagner, C.; Harned, N. Lithography Gets Extreme. *Nature Photon* **2010**, *4* (1), 24–26. https://doi.org/10.1038/nphoton.2009.251.

(6) Aboulkhair, N. T.; Simonelli, M.; Parry, L.; Ashcroft, I.; Tuck, C.; Hague, R. 3D Printing of Aluminium Alloys: Additive Manufacturing of Aluminium Alloys Using Selective Laser Melting. *Progress in Materials Science* **2019**, *106*, 100578. https://doi.org/10.1016/j.pmatsci.2019.100578.

(7) Lawrence, S. Developable Surfaces: Their History and Application. *Nexus Netw J* **2011**, *13* (3), 701–714. https://doi.org/10.1007/s00004-011-0087-z.

(8) Liu, C.; Yao, Y. L.; Srinivasan, V. Optimal Process Planning for Laser Forming of Doubly Curved Shapes. *J. Manuf. Sci. Eng* **2004**, *126* (1), 1–9. https://doi.org/10.1115/1.1643077.

(9) Schmidt, M.; Dirscherl, M.; Rank, M.; Zimmermann, M. Laser Micro Adjustment—from New Basic Process Knowledge to the Application. *J. Laser Appl.* **2007**, *19* (2), 10.

(10) Zhang, X. R.; Xu, X. Laser Bending for High-Precision Curvature Adjustment of Microcantilevers. *Appl. Phys. Lett.* **2005**, *86* (2), 021114. https://doi.org/10.1063/1.1851617.

(11) Folkersma, K. G. P.; Römer, G. R. B. E.; Brouwer, D. M.; Herder, J. L. High Precision Optical Fiber Alignment Using Tube Laser Bending. *Int J Adv Manuf Technol* **2016**, *86* (1), 953–961. https://doi.org/10.1007/s00170-015-8143-6.

(12) Lorenz, H.; Despont, M.; Fahrni, N.; LaBianca, N.; Renaud, P.; Vettiger, P. SU-8: A Low-Cost Negative Resist for MEMS. *J. Micromech. Microeng.* **1997**, *7* (3), 121–124. https://doi.org/10.1088/0960-1317/7/3/010.

(13) Campo, A. del; Greiner, C. SU-8: A Photoresist for High-Aspect-Ratio and 3D Submicron Lithography. *J. Micromech. Microeng.* **2007**, *17* (6), R81–R95. https://doi.org/10.1088/0960-1317/17/6/R01.

(14) Lin, J.; Peng, Z.; Liu, Y.; Ruiz-Zepeda, F.; Ye, R.; Samuel, E. L. G.; Yacaman, M. J.; Yakobson, B. I.; Tour, J. M. Laser-Induced Porous Graphene Films from Commercial Polymers. *Nature Communications* **2014**, *5*, 5714. https://doi.org/10.1038/ncomms6714.

(15) Stanford, M. G.; Zhang, C.; Fowlkes, J. D.; Hoffman, A.; Ivanov, I. N.; Rack, P. D.; Tour, J. M. High-Resolution Laser-Induced Graphene. Flexible Electronics beyond the Visible Limit. *ACS Appl. Mater. Interfaces* **2020**, *12* (9), 10902–10907. https://doi.org/10.1021/acsami.0c01377.

(16) Chyan, Y.; Ye, R.; Li, Y.; Singh, S. P.; Arnusch, C. J.; Tour, J. M. Laser-Induced Graphene by Multiple Lasing: Toward Electronics on Cloth, Paper, and Food. *ACS Nano* **2018**, *12* (3), 2176–2183. https://doi.org/10.1021/acsnano.7b08539.

(17) Beckham, J. L.; Li, J. T.; Stanford, M. G.; Chen, W.; McHugh, E. A.; Advincula, P. A.; Wyss, K. M.; Chyan, Y.; Boldman, W. L.; Rack, P. D.; Tour, J. M. High-Resolution Laser-Induced Graphene from Photoresist. *ACS Nano* **2021**, *15* (5), 8976–8983. https://doi.org/10.1021/acsnano.1c01843.
(18) Xia, Y.; Whitesides, G. M. Soft Lithography. *Annual Review of Materials Science* **1998**, *28* (1), 153–184. https://doi.org/10.1146/annurev.matsci.28.1.153.
(19) Kim, P.; Kwon, K. W.; Park, M. C.; Lee, S. H.; Kim, S. M.; Suh, K. Y. Soft Lithography for Microfluidics: A Review. **2008**.
(20) Kaplan, A. F. H.; Zimmermann, J. W.; Schuöcker, D. Combined Laser Welding, Cutting and Scribing; 1997.
(21) Shen, H.; Vollertsen, F. Modelling of Laser Forming – An Review. *Computational Materials Science* **2009**, *46* (4), 834–840. https://doi.org/10.1016/j.commatsci.2009.04.022.
(22) Olsen, F. O.; Alting, L. Pulsed Laser Materials Processing, ND-YAG versus CO2 Lasers. *CIRP Annals* **1995**, *44* (1), 141–145. https://doi.org/10.1016/S0007-8506(07)62293-8.
(23) Forsythe, R. C.; Cox, C. P.; Wilsey, M. K.; Müller, A. M. Pulsed Laser in Liquids Made Nanomaterials for Catalysis. *Chem. Rev.* **2021**, *121* (13), 7568–7637. https://doi.org/10.1021/acs.chemrev.0c01069.
(24) Phillips, K. C.; Gandhi, H. H.; Mazur, E.; Sundaram, S. K. Ultrafast Laser Processing of Materials: A Review. *Adv. Opt. Photon., AOP* **2015**, *7* (4), 684–712. https://doi.org/10.1364/AOP.7.000684.
(25) Baufay, L.; Houle, F. A.; Wilson, R. J. Optical Self-regulation during Laser-induced Oxidation of Copper. *Journal of Applied Physics* **1987**, *61* (9), 4640–4651. https://doi.org/10.1063/1.338375.
(26) Ursu, I.; Nistor, L. C.; Teodorescu, V. S.; Mihailescu, I. N.; Apostol, I.; Nanu, L.; Prokhorov, A. M.; Chapliev, N. I.; Konov, V. I.; Tokarev, V. N. Continuous Wave Laser Oxidation Of Copper. In *Industrial Applications of Laser Technology*; International Society for Optics and Photonics, 1983; Vol. 0398, pp 398–402. https://doi.org/10.1117/12.935405.
(27) Wautelet, M.; Baufay, L. Laser-Induced Oxidation of Thin Cadmium and Copper Films. *Thin Solid Films* **1983**, *100* (1), L9–L12. https://doi.org/10.1016/0040-6090(83)90233-X.
(28) Amara, E. H.; Haïd, F.; Noukaz, A. Experimental Investigations on Fiber Laser Color Marking of Steels. *Applied Surface Science* **2015**, *351*, 1–12. https://doi.org/10.1016/j.apsusc.2015.05.095.
(29) Antończak, A. J.; Stępak, B.; Kozioł, P. E.; Abramski, K. M. The Influence of Process Parameters on the Laser-Induced Coloring of Titanium. *Appl. Phys. A* **2014**, *115* (3), 1003–1013. https://doi.org/10.1007/s00339-013-7932-8.
(30) Austin, D.; Gliebe, K.; Muratore, C.; Boyer, B.; Fisher, T. S.; Beagle, L. K.; Benton, A.; Look, P.; Moore, D.; Ringe, E.; Treml, B.; Jawaid, A.; Vaia, R.; Joshua Kennedy, W.; Buskohl, P.; Glavin, N. R. Laser Writing of Electronic Circuitry in Thin Film Molybdenum Disulfide: A Transformative Manufacturing Approach. *Materials Today* **2021**, *43*, 17–26. https://doi.org/10.1016/j.mattod.2020.09.036.
(31) Sivaram, S. V.; Hanbicki, A. T.; Rosenberger, M. R.; Jernigan, G. G.; Chuang, H.-J.; McCreary, K. M.; Jonker, B. T. Spatially Selective Enhancement of Photoluminescence in MoS2 by Exciton-Mediated Adsorption and Defect Passivation. *ACS Appl. Mater. Interfaces* **2019**, *11* (17), 16147–16155. https://doi.org/10.1021/acsami.9b00390.

(32) Zhao, P.; Kim, B. J.; Jung, H. S. Passivation in Perovskite Solar Cells: A Review. *Materials Today Energy* **2018**, *7*, 267–286. https://doi.org/10.1016/j.mtener.2018.01.004.
(33) Brawand, N. P.; Goldey, M. B.; Vörös, M.; Galli, G. Defect States and Charge Transport in Quantum Dot Solids. *Chem. Mater.* **2017**, *29* (3), 1255–1262. https://doi.org/10.1021/acs.chemmater.6b04631.
(34) Ligon, S. C.; Liska, R.; Stampfl, J.; Gurr, M.; Mülhaupt, R. Polymers for 3D Printing and Customized Additive Manufacturing. *Chem. Rev.* **2017**, *117* (15), 10212–10290. https://doi.org/10.1021/acs.chemrev.7b00074.
(35) Pflug, T.; Anand, A.; Busse, S.; Olbrich, M.; Schubert, U. S.; Hoppe, H.; Horn, A. Spatial Conductivity Distribution in Thin PEDOT:PSS Films after Laser Microannealing. *ACS Appl. Electron. Mater.* **2021**, *3* (6), 2825–2831. https://doi.org/10.1021/acsaelm.1c00403.
(36) Kruth, J. P.; Wang, X.; Laoui, T.; Froyen, L. Lasers and Materials in Selective Laser Sintering. *Assembly Automation* **2003**, *23* (4), 357–371. https://doi.org/10.1108/01445150310698652.
(37) Gerringer, J. C.; Moran, A. G.; Habib, T.; Pospisil, M. J.; Oh, J. H.; Teipel, B. R.; Green, M. J. Radio Frequency Heating of Laser-Induced Graphene on Polymer Surfaces for Rapid Welding. *ACS Appl. Nano Mater.* **2019**. https://doi.org/10.1021/acsanm.9b01536.
(38) Jiao, L.; Chua, Z. Y.; Moon, S. K.; Song, J.; Bi, G.; Zheng, H.; Lee, B.; Koo, J. Laser-Induced Graphene on Additive Manufacturing Parts. *Nanomaterials* **2019**, *9* (1), 90. https://doi.org/10.3390/nano9010090.
(39) Okamoto Y.; Uno Y.; Ohta K.; Shibata T.; Kubota S.; Namba Y. Study on Precision Laser Forming of Plastic with YAG Laser. *Journal of the Japan Society for Precision Engineering* **2000**, *66* (6), 891–895. https://doi.org/10.2493/jjspe.66.891.
(40) Okamoto, Y.; Miyamoto, I.; Uno, Y.; Takenaka, T. Deformation Characteristics of Plastics in YAG Laser Forming. In *Fifth International Symposium on Laser Precision Microfabrication*; International Society for Optics and Photonics, 2004; Vol. 5662, pp 576–581. https://doi.org/10.1117/12.596567.
(41) Hecht, J. Short History of Laser Development. *OE* **2010**, *49* (9), 091002. https://doi.org/10.1117/1.3483597.
(42) Akinlabi, S. A.; Shukla, M.; Akinlabi, E. T.; Marwala, T. Lasers in Metal Forming Applications. In *Lasers in Manufacturing*; John Wiley & Sons, Ltd, 2013; pp 69–108. https://doi.org/10.1002/9781118562857.ch2.
(43) Comita, P. B. Surface Modification with Lasers. *Advanced Materials* **1990**, *2* (2), 82–90. https://doi.org/10.1002/adma.19900020204.
(44) Rusak, D. A.; Castle, B. C.; Smith, B. W.; Winefordner, J. D. Fundamentals and Applications of Laser-Induced Breakdown Spectroscopy. *Critical Reviews in Analytical Chemistry* **1997**, *27* (4), 257–290. https://doi.org/10.1080/10408349708050587.
(45) Galang, J.; Restelli, A.; Hagley, E. W.; Clark, C. W. A Green Laser Pointer Hazard. **2010**.
(46) Danson, C.; Hillier, D.; Hopps, N.; Neely, D. Petawatt Class Lasers Worldwide. *High Power Laser Science and Engineering* **2015**, *3*. https://doi.org/10.1017/hpl.2014.52.

APPENDIX

Appendix A – Supplementary Information for Chapter 3

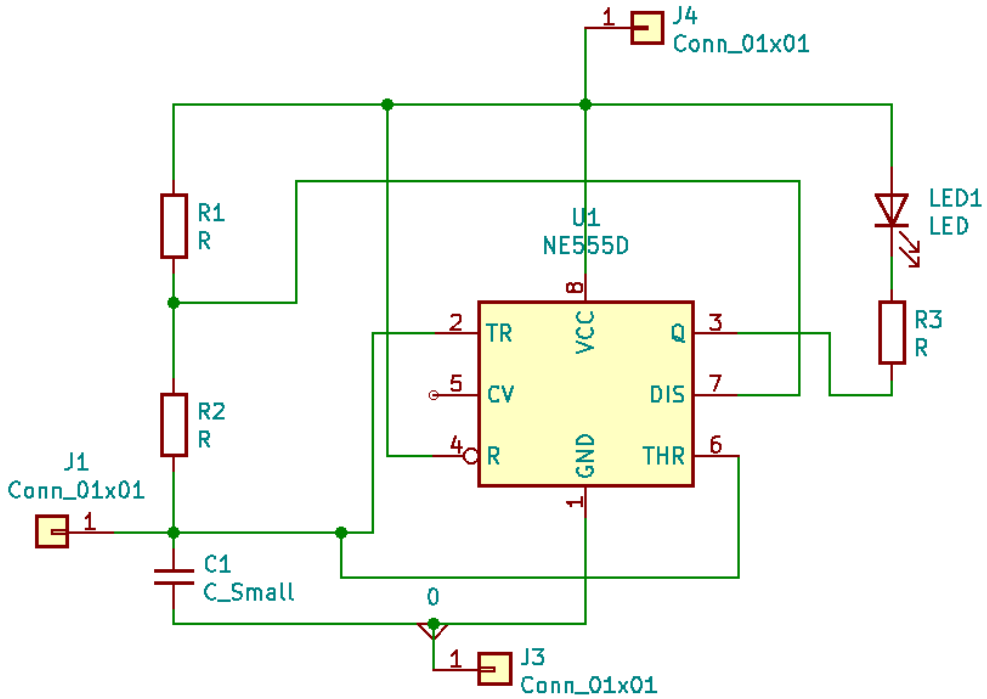

Figure A.1. The schematic for the astable 555 timer circuit. The following values were chosen to generate a blinking frequency of 2 Hz.
C1: 680 nF
R2: 91 kΩ
R3: 160 kΩ

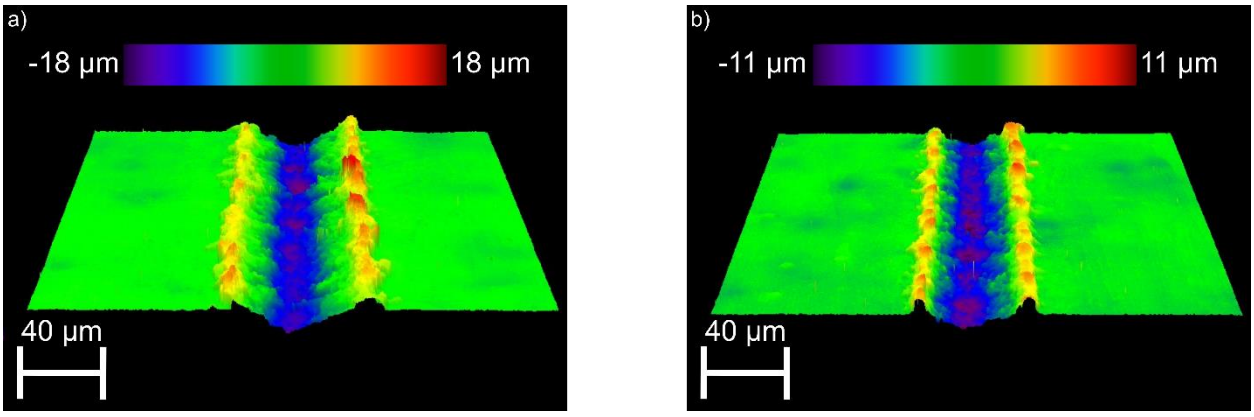

Figure A.2. Commercial boards cover exposed copper with ENIG, electroless nickel immersion gold, which is 3-6 µm nickel covered by a layer ~100 nm gold. The nickel layer absorbs the laser strongly causing deep cutting (a) in the sample when exposed to the HPM. This causes problems when trying to laser form the sample as usual. The normal bending settings (b) do results in some cutting but is like that observed by the HPM for bare copper.